

EARTH SCIENCE B ESSAY PLANS

DISCLAIMER This guide is based on the syllabus written in the 2024/25 Earth Sciences Course Guide, and the 2018-2024 past papers. Course content and syllabus styles may change with time. We have included ‘model’ answers to most questions on the theory exam. Please use this for reference only – academic dishonesty is a serious breach of conduct.

The materials in this document will certainly be sufficient for a 2:1, and if combined with your own study beyond the syllabus, should get you a 1st. However, while written to the best of our ability, this has not been proofread and will almost certainly contain errors. We are not liable for any consequences that may arise from using this as your only source of reference material. You should always cross-reference any doubts with academic materials or ask your supervisor.

Answers in red and blue are complete. Answers in green are incomplete. That is the unavoidable consequence of having to study a vast syllabus in a month’s time. We welcome any suggestions or alternative answers to tripos questions and will add them to this document if appropriate. We can be reached by the email addresses given above.

Credits

Terry Lam (All topics relating to Physics, e.g. thermodynamics, geophysics; Metamorphic rocks; Phase diagrams; Isotopes)

Raphael Lin (Mineralogy; Solar System; Igneous rocks; Mantle science; Miscellaneous)

Earth Sciences Dept., Cambridge

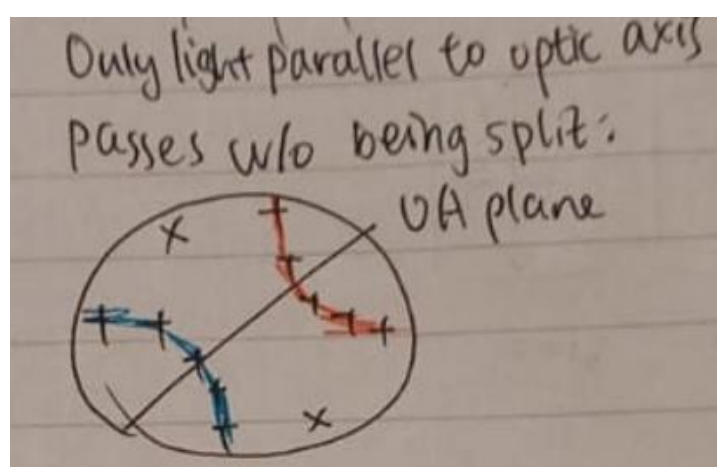
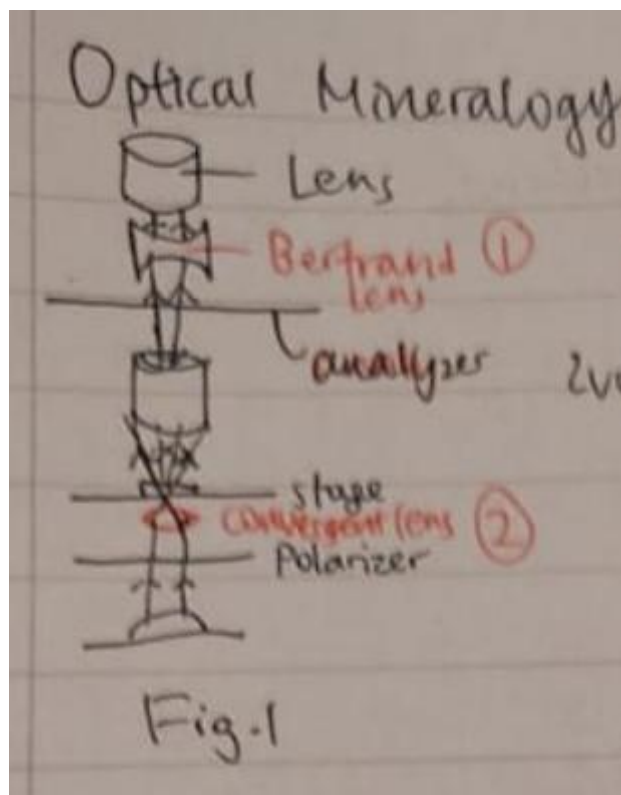
Mineralogy

Optical Mineralogy – NOT TESTED ANYMORE unfortunately

2018

1. Explain briefly how convergent beam interference figures are formed in the optical microscope and what information about the optical properties of a mineral can be determined using them.

Observe mineral grain through convergent cross polarized light under a Bertrand lens (fig. 1).

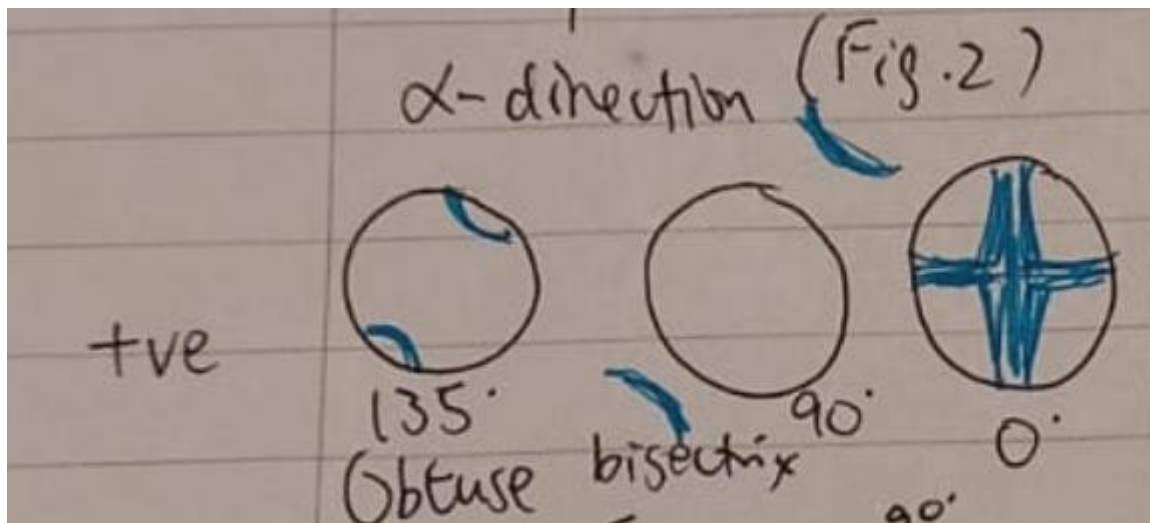


Under convergent light, light enters the crystal in many different orientations, creating a ‘map’ of light travelling directions, which is the interference figure. Isogyes are formed from isotropic sections of the indicatrix, i.e. when light travels parallel to the optic axis.

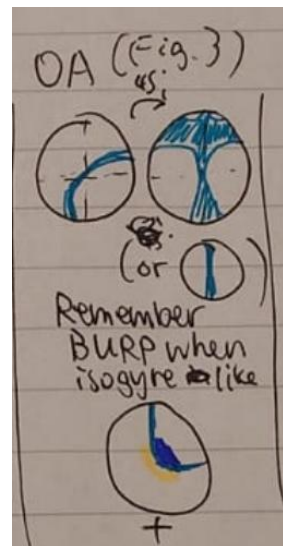
Obtain: i) Optic sign (symmetry of interference figure) ii) Orientation of grain iii) 2V angle (biaxial) iv) Refractive indices

Sketch and label the expected form of the interference figures for:

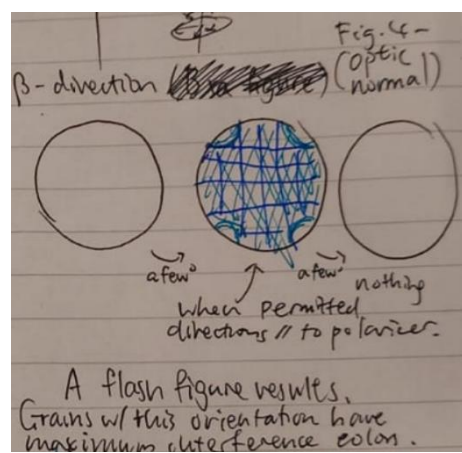
a biaxial positive mineral viewed along the α direction (Fig 2)



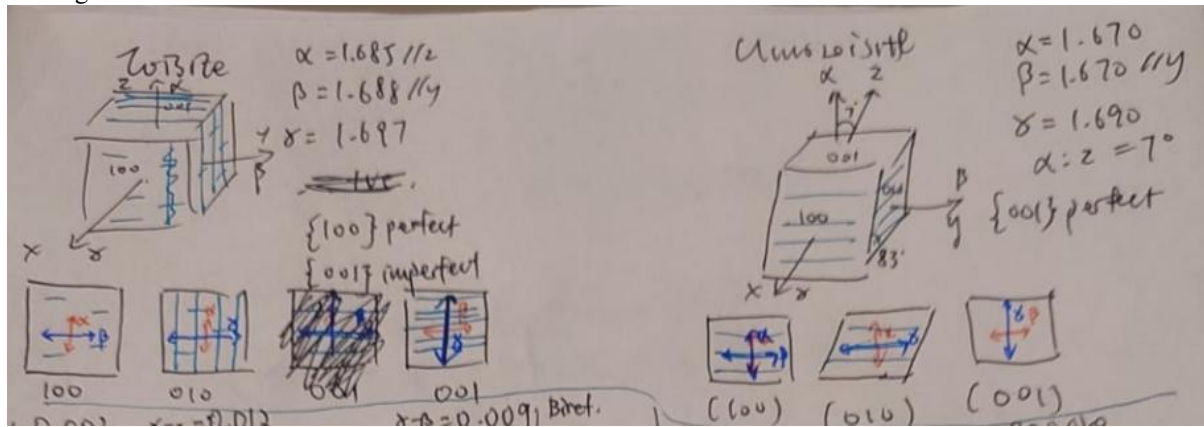
a biaxial positive mineral viewed along an optic axis (Fig 3)



a biaxial positive mineral viewed along the β direction (Fig 4)

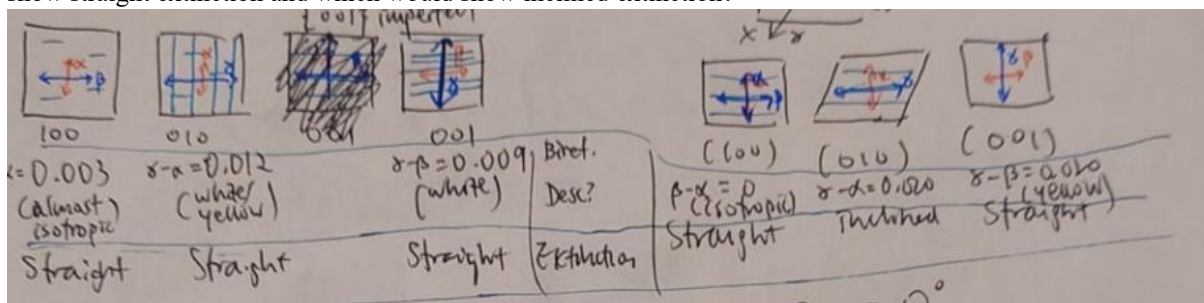


Zoisite and clinozoisite are minerals with similar compositions and structure, but zoisite is orthorhombic and clinozoisite is monoclinic. Both form elongate crystals, with the long direction parallel to the crystallographic y-axis. For zoisite $n\alpha = 1.685$, $n\beta = 1.688$, $n\gamma = 1.697$, $\alpha \parallel z$ and $\beta \parallel y$. Zoisite shows perfect $\{100\}$ cleavage and imperfect $\{001\}$ cleavage. Clinozoisite has $n\alpha = 1.670$, $n\beta = 1.670$, $n\gamma = 1.690$, $\alpha : z = 7^\circ$, $\beta \parallel y$, and perfect $\{001\}$ cleavage.

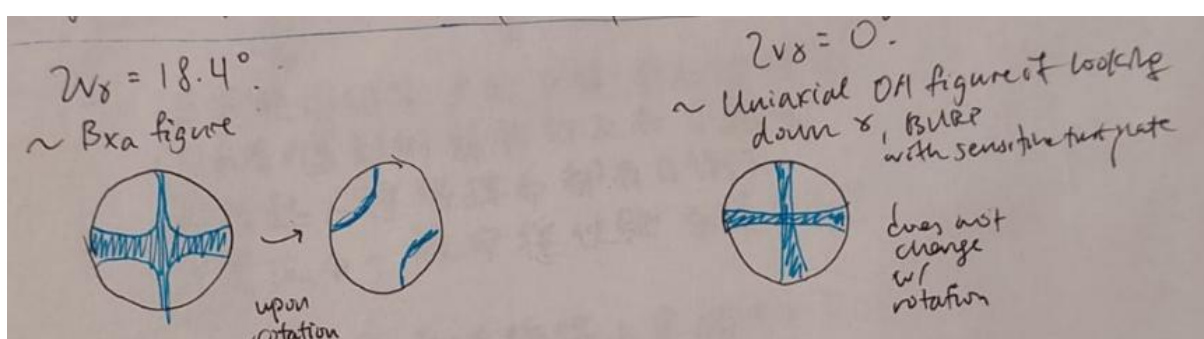


(for own reference)

(iv) Draw sketches of (100), (010) and (001) sections of zoisite and clinozoisite. Show the orientations of crystallographic axes, cleavage planes and, where possible, the directions of α , β and γ . (v) Describe the birefringence which would be expected for each orientation in a normal thin section. Which sections would show straight extinction and which would show inclined extinction?



(vi) Calculate $2V$ and determine the optic sign of zoisite and clinozoisite. Describe the interference figure which would be observed from a thin section cut parallel to (100) of each mineral. [$\tan 2V = (n\beta - n\alpha)/(n\gamma - n\beta)$]



(vii) Suggest three features which would help to distinguish between zoisite and clinozoisite in thin section.

Birefringence: clinozoisite has a section with higher
2 sets of cleavage planes in zoisite (010 section) but 1 in clinozoisite
Inclined extinction in 010 section of clinozoisite

2021

1. (a) Explain, with appropriate examples, how the pleochroic colours associated with the ordinary and extraordinary rays in a uniaxial mineral, and α , β and γ in a biaxial mineral, can be determined using a petrographic microscope.

Omega section (0 birefringence), epsilon – omega section (max birefringence) to determine pleochroic scheme

Optic axis section (0 birefringence) – beta & beta' section, which should show two colours. Beta' is in the middle between alpha and gamma...

Beta – gamma section: isolate beta so we know gamma

Alpha – gamma section (max birefringence) so we know alpha

[15 minutes]

- (b) A monoclinic pyroxene has a prismatic habit and is elongate along the crystallographic c-axis with refractive indices $n\alpha = 1.776$, $n\beta = 1.820$, $n\gamma = 1.836$. Cleavage is well-developed in the {110} planes. A maximum birefringent section has one cleavage with an extinction angle between the cleavage and the **fast ray** of 20° . The pleochroic colours of this section are emerald green and yellowish green. Another section with one cleavage has straight extinction and pleochroic colours of emerald-green and green.

- (i) Assign, giving reasons, the pleochroic colours to the α , β and γ vibration directions. [5 minutes]

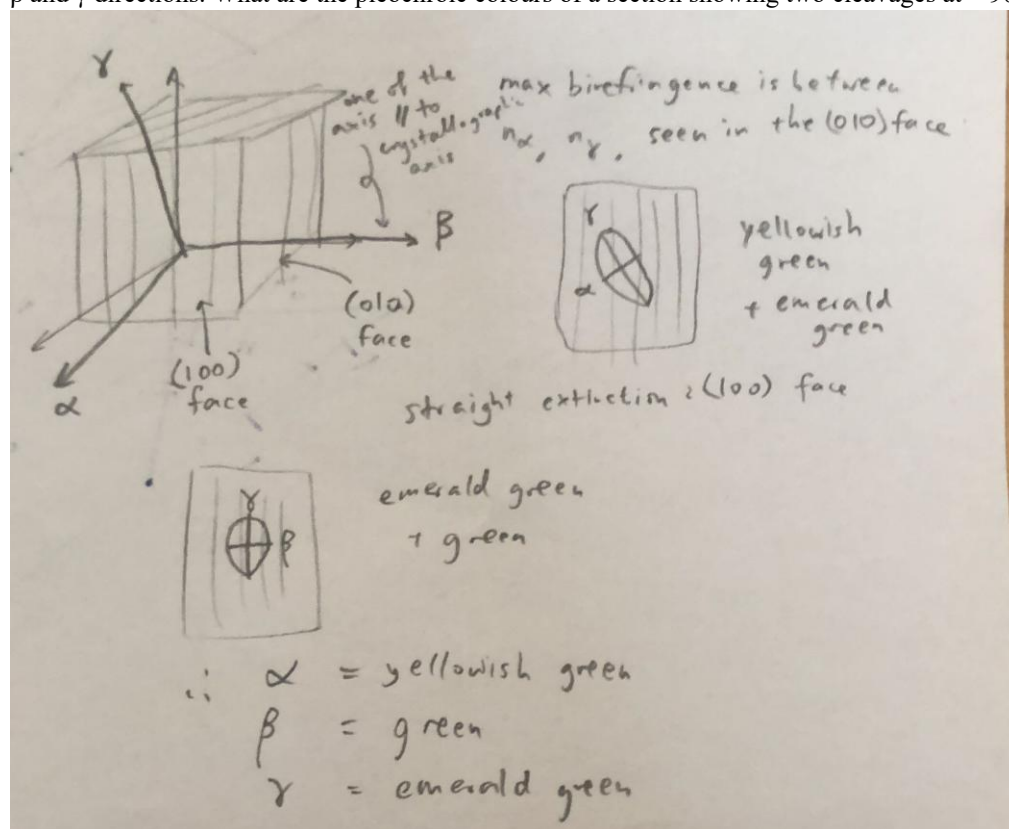
both maximum birefringence section and straight extinction section have gamma, common colour is emerald green, so

gamma = emerald green

alpha = yellowish green (maximum birefringence section)

beta = green

- (ii) Draw sketches of the (001), (010) and (010) sections to show the two cleavages and the orientations of the α , β and γ directions. What are the pleochroic colours of a section showing two cleavages at $\sim 90^\circ$? [10 minutes]



(iii) Add the optic axis directions to your sketches [recall that $\tan 2V\gamma = (\beta-\alpha)/(\gamma-\beta)$] and sketch the interference figure that would be obtained from a section showing two cleavages at $\sim 90^\circ$. [15 minutes]

Xy section

OA figure

Curvature fixed by 2V,
10 degrees off center.

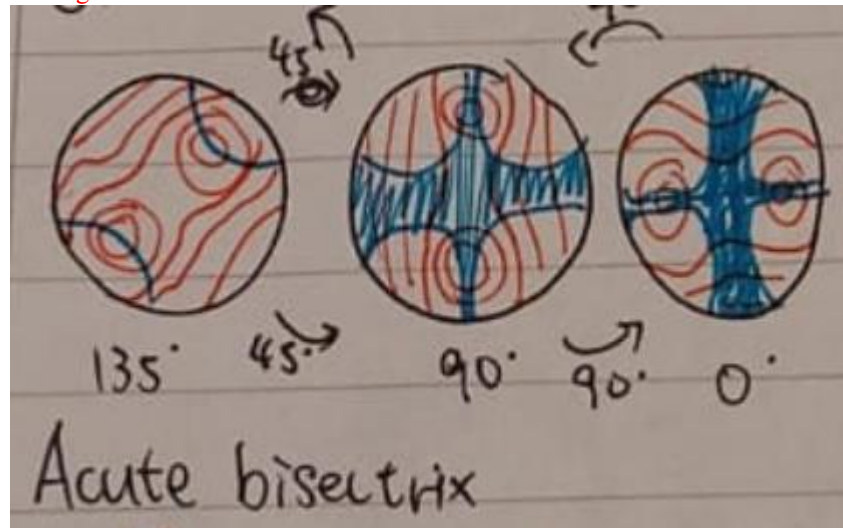
2022

1. (a) Explain briefly how convergent beam interference figures are formed in the optical microscope and what information about the optical properties of a mineral can be determined using them. [15 minutes]

Sketch and label the expected form of the interference figures for:

- (i) a biaxial negative mineral viewed along the α direction

Bxa figure



- (ii) a biaxial negative mineral viewed along an optic axis

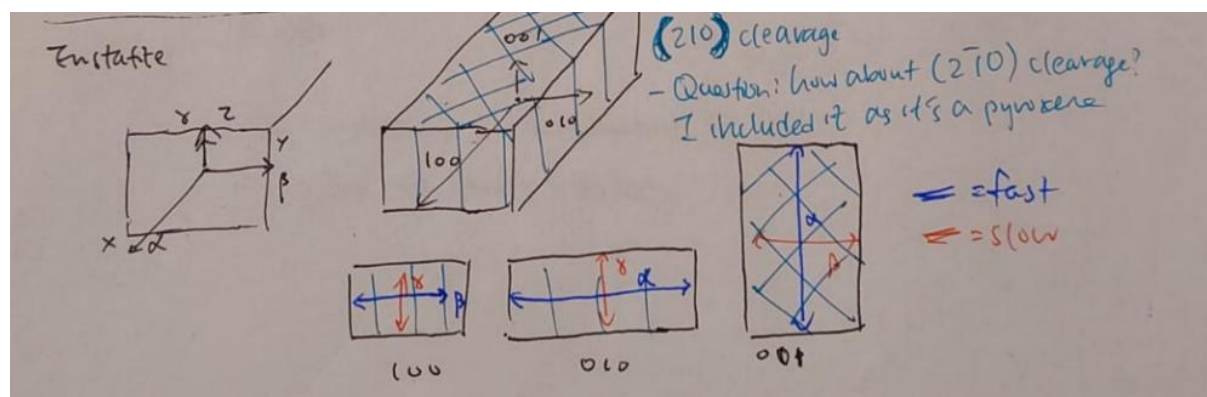
OA figure – see the first question

- (iii) a biaxial negative mineral viewed along the β direction [9 minutes]

flash figure – see the first question

Enstatite is orthorhombic, with refractive indices $n_{\alpha} (\parallel x) = 1.669$, $n_{\beta} (\parallel y) = 1.674$, $n_{\gamma} (\parallel z) = 1.680$ and unit cell parameters $a = 18.2 \text{ \AA}$, $b = 8.83 \text{ \AA}$, $c = 5.2 \text{ \AA}$. Enstatite shows cleavage parallel to (210).

- (b) Sketch the appearance of thin sections of enstatite parallel to (001), (010) and (100) in parallel light, indicating the fast and slow directions in each case. [12 minutes]



- (c) Sketch the optical interference figure when viewed down [001] and label important features. Recall that $\tan^2[\frac{\pi}{2}][V_{\gamma}] = (n_{\beta} - n_{\alpha}) / (n_{\gamma} - n_{\beta})$. [9 minutes] **Acute bisectrix figure, as viewing down γ , and enstatite is +ve. So the answer would be the same as part ai).**

Solid Solutions

2018 3. Explain the concept of an ideal solid solution and describe how the regular solution model of mineral equilibria can be derived from a discussion of ideal mixing. Include in your answer a discussion of the regular solution parameter, W. Hence explain the temperature-dependent behaviour of the forsterite-fayalite system.

Outline the principal factors that determine the limits of solid solution in minerals. Hence, explain the range of compositions observed for pyroxenes in igneous and metamorphic rocks.

Ideal solid solution: Chemically means when $\Delta H_{\text{mix}} = 0$ (and non-ideal when $\Delta H_{\text{mix}} \neq 0$). Physically means there is **no preference** for AA, BB over AB pairs in a lattice composed of A, B cations. → Solid solution remains stable at all temperatures regardless of concentration.

Mineral equilibria regular solution model: Assumes E_{ss} arises only from interaction between nearest neighbour pairs. As $G = H - TS$, find expression of H & TS in terms of x_A & x_B (mole fractions)

H: Let energy associated with A-A, B-B, A-B be W_{AA} , W_{BB} , W_{AB} ; strong bonds have large negative W . If cations are mixed randomly, probability of pairs A-A, B-B, A-B are x_A^2 , x_B^2 , $2x_Ax_B$. Note $x_A = 1 - x_B$.

Let z be coordination number of lattice sites on which mixing occurs, and N be the number of sites. The TOTAL number of nearest neighbour bonds = $Nz/2$ (factor of 2 is to avoid counting twice)

$$\begin{aligned} H_{\text{tot}} &= \frac{1}{2} Nz(W_{AA}x_A^2 + W_{BB}x_B^2 + 2W_{AB}x_Ax_B) = \frac{1}{2} Nz(W_{AA}x_A(1-x_B) + W_{BB}x_B(1-x_A) + 2W_{AB}x_Ax_B) \\ H_{\text{mm}} &= \frac{1}{2} Nz(W_{AA}x_A + W_{BB}x_B) \\ \Delta H_{\text{mix}} &= H_{\text{tot}} - H_{\text{mm}} = \frac{1}{2} Nz x_A x_B (-W_{AA} - W_{BB} + 2W_{AB}) = w x_A x_B \end{aligned}$$

w is the **regular solution parameter**, and its sign determines sign of ΔH_{mix} . Physically, a positive w means it is more energetically favourable to have A-A and B-B neighbours than A-B neighbours.

S: Number of microstates of a system, $S = k_B \ln \Omega = k_B \ln \frac{N!}{N x_A! N x_B!}$ where $N x_A$ is the number of A atoms, etc.

Using Stirling's approximation $\ln N! = N(\ln N - 1)$, you get $\Delta S = R(x_A \ln x_A + x_B \ln x_B)$. Purely configurational.

Hence, we get $G = G_A^0 x_A + G_B^0 x_B + w x_A x_B + RT(x_A \ln x_A + x_B \ln x_B)$.

Temperature dependent behaviour:

High-energy configurations are more probable at high temperatures, due to Boltzmann distribution $p_i = e^{\frac{-E_i}{k_B T}}$.

Hence, at high temperatures, system adopts disordered configuration regardless of the sign of w.

When w is +ve; exsolution occurs at low temperatures. This is when $TS < H$, meaning it is preferred to maximise the number of A-A and B-B pairs rather than A-B pairs, forming unmixed A-rich and B-rich regions. E.g. Ca-rich and Ca-poor regions in pyroxene forming exsolution lamellae.

When w is -ve: order-disorder phase transition occurs at a critical temperature during cooling. As the system maximizes number of A-B bonds and there are *two equivalent arrangements of ordered cations – ordered / antiphase*, domains containing alternating arrangements of A & B ions in either ordered / antiphase state grow

Forsterite-fayalite system has +ve w and exsolves at low temperatures. There is a miscibility gap.

Factors that limit solid solution:

- Cation size. If sizes very similar (~15% difference) then extensive solid solution is observed.
- Cation charge. Extensive solid solution only possible if cations differ by ±1

- Structural flexibility. Ions have shallow curvature interatomic potentials, e.g. large polarizable cations (K^+ , Cs^+ , Ba^{2+} etc), or ions with more covalent bonding (e.g. Pb^{2+}). They are more easily displaced to **accommodate differently sized atoms** (because displacement comes with less energy cost).

Cation size mismatch increases H, disfavouring solid solution at low T.

Increase in equivalent ways of distributing atoms in disordered SS = high S & favouring solid solution at high T.

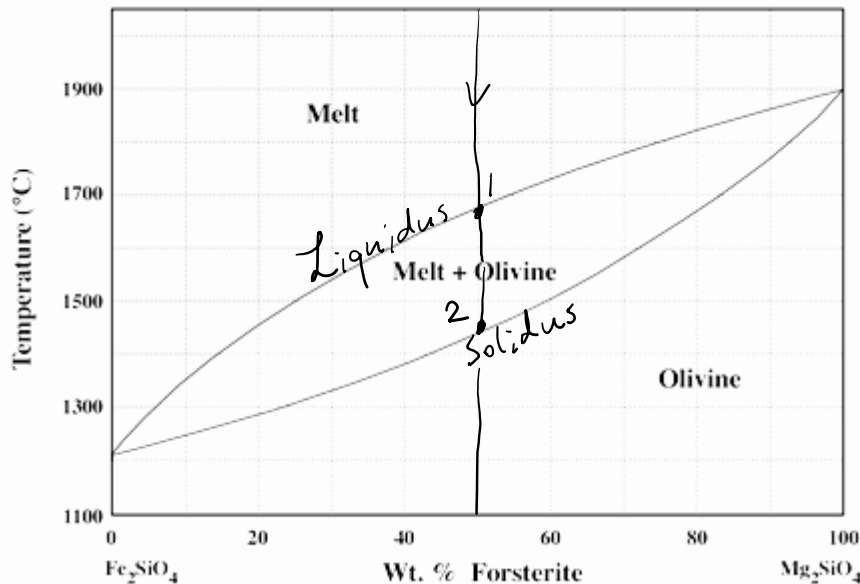
Pyroxene case study: XYZ_2O_6 . Most common form – $(Ca, Mg, Fe)_2Si_2O_6$.

- Cation size: Mg^{2+} and Fe^{2+} have similar ionic radii, so form extensive substitution. However, Mg^{2+} & Fe^{2+} and Ca^{2+} have very different ionic radii, so Ca^{2+} substitution is limited.
- Charge balance: Tschermak's substitution of Na^+ and Al^{3+} in jadeite. Tolerated as $\Delta \pm 1$

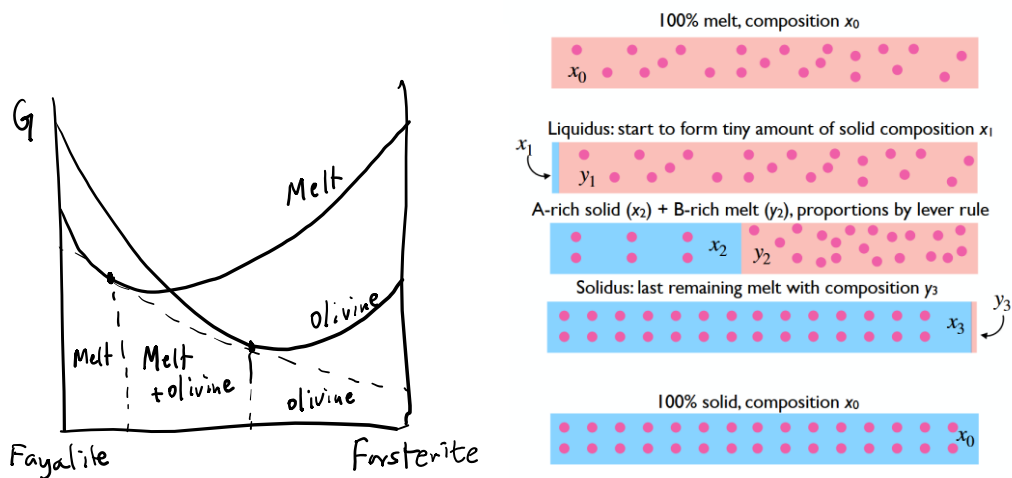
2020

3. (i) Explain the concept of an ideal solid solution. Thus, describe how the regular solution model of mineral equilibria can be derived from a discussion of ideal mixing. Include in your answer a discussion of the regular solution parameter, W . [20 minutes] [Answer given above](#)

(ii) Sketch the phase diagram for the forsterite-fayalite solid solution. On your sketch, label the liquidus and solidus and hence describe how a 50:50 melt will behave on slow cooling through the liquidus to the solid state. Indicate the approximate compositions of any phases that form and sketch the free energy curves for any two-phase regions. [15 minutes]



As the melt goes to point 1 (intersects with liquidus), Olivine will start to crystallise with an initially forsterite-rich domain. As cooling goes between 1 and 2, more and more olivine will crystallise, but the composition of the solid will be increasingly Fayalite-rich. At point 2, the bulk composition intersects the solidus, and at that point all melt has been crystallised, giving a pure olivine with 50 wt% Forsterite still.



(iii) Describe the behaviour of the 50:50 mixture upon rapid cooling and any microstructure that might develop. [10 minutes]

- Upon rapid cooling, there is insufficient time for diffusion $x \sim \sqrt{Dt}$ to occur. If no diffusion occurs it is practically the same as fractional crystallization
 - ➔ as olivine is being crystallised it is being ‘locked up’ in the crystal, and hence the remaining liquid composition becomes more Fayalite-rich. (This is very similar to fractional crystallisation).
- The liquid composition moves along the liquidus until it reaches the Fayalite endmember, at which Fayalite is crystallised.

Microstructure:

- Zoning in the olivine (the core of the olivine is more Forsterite-rich than the outer regions)
- Olivine crystals are finer (rapid cooling)

2022

2. (a) To what extent can the process of cation ordering be considered the ‘opposite’ of exsolution in a simple binary solid solution? [15 minutes]

(b) Give an example of a binary solid solution where both cation ordering and exsolution processes occur. Explain how this behaviour can be reconciled thermodynamically. [30 minutes]

2023

4. (a) Explain the atomistic origins of the **regular solution model** for a binary solid solution, and outline how the “Monte Carlo” simulation method can be used to explore its behaviour as function of temperature and composition. [20 minutes]

Monte Carlo method: Consider square lattice with alternating sites labelled α and β , and place A and B atoms on the squares with defined proportions. Colour A atom on α site blue, A atom on β site yellow, and B atoms black.

Swap two atoms at random and calculate ΔE by counting *change in A-A bonds after the swap and multiplying by -w*. If ΔE is -ve, swap is accepted. If ΔE is +ve, swap is accepted with probability $e^{(-E/RT)}$. This is then iterated until the solution approaches equilibrium.

(Repeat the temperature dependent point in the essay outline above, but draw Monte Carlo diagrams.)

Ordered phase will have A atoms in α sites and B atoms in β sites, resulting in yellow/black lattice. Antiphase will have B atoms in α sites and A atoms in β sites, resulting in blue/black lattice.)

(b) To what extent can the process of cation ordering in a non-ideal binary solid solution be considered the ‘opposite’ of the process of exsolution? Give an example of a binary solid solution where both cation ordering and exsolution processes occur and suggest how this behaviour might be accounted for by modifying the atomistic model in a Monte Carlo simulation. [25 minutes]

2024

4. The diagram below represents the variation of Gibbs free energy (G) as a function of bulk composition (x_B) for a binary mineral solid solution between end members A and B, drawn for a fixed temperature, T .

(a) Explain why the G - x curve has this form. How would you expect it to change as a function of temperature? [10 mins]

Above a certain temperature will have one minimum

At high temperature, the entropy of mixing dominates and the curves look similar to those for ideal solutions.

At intermediate temperature, the curves flatten in the central portion.

At lower temperature, the curves develop two distinct minima and an intermediate maximum.

(b) What is the equilibrium state of the system for a solid solution with bulk composition X at temperature T? How does this compare to the equilibrium state of the system for a solid solution with bulk composition Y at temperature T? [5 mins]

Ratio according to lever rule will differ.

(c) Explain the potential mechanism(s) available for solid solutions with bulk compositions X and Y to reach their equilibrium states. [10 mins]

Spinodal decomposition, X only

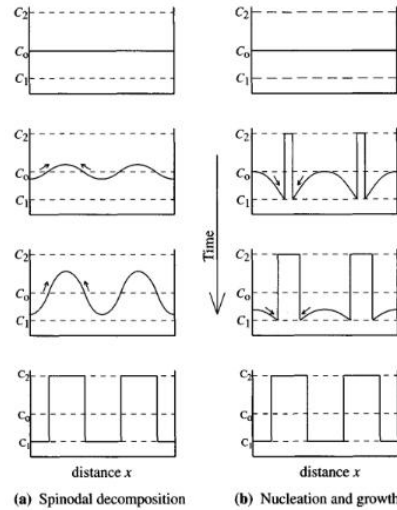
nucleation & growth X and Y

(d) Compare and contrast the long-term microstructural evolution of solid solutions with bulk compositions X and Y during isothermal annealing at temperature T. What differences, if any, would you expect to observe in the final microstructural state of sample X compared to sample Y? [10 mins]

Note that the starting and ending states are the same for each, so it can be hard to prove which mechanism operated once the breakdown is completed.

In many cases, however, textural evolution stops before complete equilibrium is achieved, leaving evidence of stranded diffusion profiles and/or compositional fluctuations

Spinodal vs Nucleation and growth

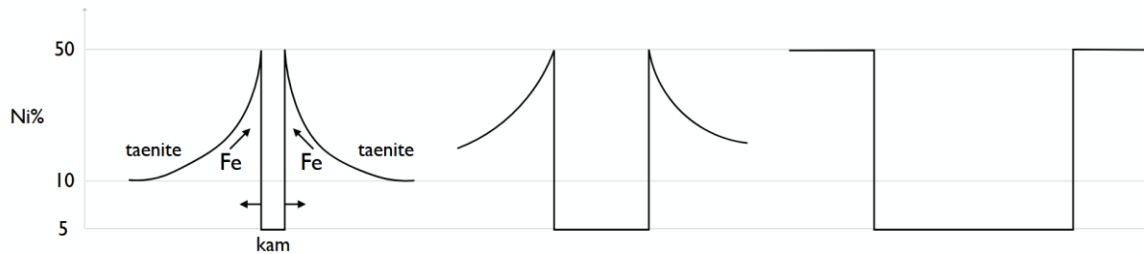


If frozen at any stage, spinodal will show gradual boundaries between phases, while nucleation will see hard boundaries with depleted halos.

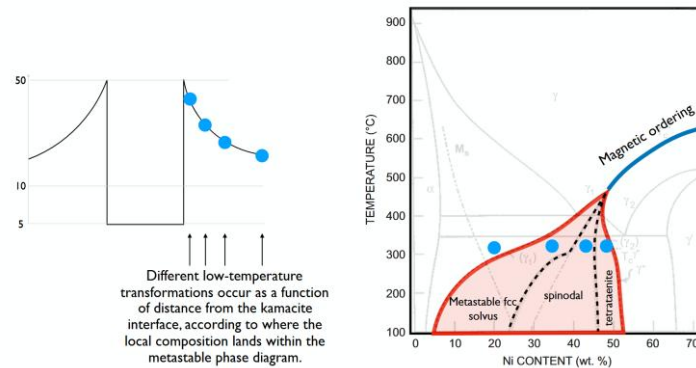
(e) Using a suitable natural example, describe how the concepts discussed in the previous four sections are useful in revealing the thermal history of natural solid solutions. [10 mins]

Fe-Ni meteorite:

Two phases between Kamacite (Fe-rich) and Taenite (Ni-rich). For a typical bulk composition of 10% Ni, at high T usually start as Taenite, and then as temperature drops Kamacite is exsolved by nucleation and growth, forming lamellae of Kamacite and Taenite. (showing Widmanstatten textures, {111} on the fcc taenite host)



However, for most cooling rates, growth is incomplete (as diffusion length $x \sim \sqrt{Dt}$ but $D \propto D_0 e^{-E_a/kT}$) and so leaves stranded diffusion profiles (M-shaped taenite profile). The M-shaped profile can be fitted to determine cooling rate (\rightarrow size of planetary body / impact history of meteorite).



As diffusion length is very short, each part of the stranded profile can be treated as their own bulk composition and evolves independently. Some compositions fall within the spinodal so fluctuations grow spontaneously into ‘cloudy’ regions, which are intergrowths of Ni-rich tetrataenite and Fe-rich taenite.

Silicate Mineral Case Studies

2018

2. Explain what is meant by the “aluminium avoidance principle”, sometimes known as “Loewenstein’s Rule”. Discuss how this principle influences the development of the microstructures seen in feldspars during slow cooling in (a) alkali feldspars and (b) plagioclase feldspars. Discuss the relationship between aluminium avoidance, displacive transformations, and exsolution in these feldspars, and how these phenomena are reflected in their microstructures.

2020

2. (i) Describe the structure of the equilibrium phase of SiO_2 in the Earth’s crust. [5 minutes]

α -quartz (low quartz), stable under ambient P,T. Trigonal, with enantiomorphous forms $P3_121$ or $P3_221$ (depending on chirality). Framework silicate with corner-sharing SiO_4 tetrahedra in a helix spiraling along the c axis.

(ii) Explain with the aid of diagrams, the reason why this phase has a propensity to form twins. [15 minutes]

(iii) What happens to these twins as temperature is increased? [10 minutes]

(iv) What other forms of SiO_2 exist in the earth’s crust while not being the most stable phase? [5 minutes]

Other forms also include high quartz (hexagonal), tridymite, cristobalite...

Tridymite and cristobalite are found principally in **felsic** volcanic rocks; requires high T, low P, just like in a magma chamber. For example, cristobalite composes the ‘snowflakes’ in snowflake obsidian.

(v) Describe the fundamental difference in the nature of the thermodynamic transitions between these phases of SiO_2 and the twin transitions described earlier. [10 minutes]

See 2023 3b)

4. Upon cooling from just below 1000°C, a sodium-rich feldspar will undergo a series of phase and microstructural transitions. Describe the driving force for these transitions and the origin of the microstructure in the space groups of the phases. Explain why more potassium-rich phases have lower transition temperatures and the reasons for the ordering of aluminium and silicon in lower temperature phases. [45 minutes]

DRIVING FORCES

Minimize G to adopt a lower-energy state, which results in exsolution, cation ordering, and loss of symmetry.

Feldspar – formula $(K,Na)(Si,Al)4O_8$. Two sets of solid solutions available. Albite = $NaSiAl_3O_8$

High-energy configurations are more probable at high temperatures, due to Boltzmann distribution $p(i) = e^{\frac{-E_i}{k_B T}}$. Hence, at high temperatures, system adopts disordered configuration: Monalbite (Na) and high sanidine (K)

Na endmember: Monalbite ($C2/m$) \rightarrow High albite ($C-1$ with disordered Al/Si) \rightarrow Low albite ($C-1$ ordered Al/Si); Displacive phase transition creates a **loss of symmetry**, then Al-Si ordering follows.

(K endmember: High sanidine ($C2/m$ with disordered Al/Si) \rightarrow Microcline ($C-1$ with ordered Al/Si))
Al-Si ordering creates a loss of symmetry from monoclinic ($C2/m$) to triclinic ($C-1$).

Mixing of K-Na non-ideal: K^+ larger than Na^+ , introducing **lattice strain**. K^+ holds the framework apart; transition temperature decreases with K-content, stabilizes **monoclinic** phase ($C2/m$) at lower temperatures as the unit cell has a **larger volume** (However, difference in cation size causes +ve ΔH , leads to a **solvus** at low T.)

(Mixing of Ca-Na non-ideal: Ca^{2+} smaller than Na^+ causing tetrahedral framework to distort and adopt a smaller volume, so transition temperature increases with Ca^{2+} content.)

Mixing of Al-Si is non-ideal: as Al-O bonds and Si-O bonds have very different bond lengths (and strengths), Al tetrahedra have different size from Si tetrahedra. Al-O-Al bonds thus introduce **lattice strain**. From above, Al-O-Al linkages are thermodynamically disfavoured; creates the **alumina avoidance principle**. Al-Si interactions are preferred over Al-Al / Si-Si ; w is -ve, driving **ordering** at low T.

When w is -ve: order-disorder phase transition occurs at a critical temperature during cooling. As the system maximizes number of A-B bonds and there are *two equivalent arrangements of ordered cations – ordered / antiphase*, domains containing alternating arrangements of A & B ions in *either ordered / antiphase state grow*

MICROSTRUCTURE – TWINNING AND ORDERING WRT TEMPERATURE

'Albite' twins: reflection twins, twin plane // (010)

'Pericline' twins: rotation twins, twin axis // [010]

Correspond to the **symmetry elements** which are lost from **C2/m** to **C-1**: two equivalent triclinic distortions which differ in orientation but not in energy. Sets of twins **intersect at 90°** and may **occur at the same time**, creating cross-hatched transformation twins

Cooling rate affects diffusion-controlled processes:

Rapid: no time for exsolution / cation ordering to take place. Only displacive phase transition takes place, creating cross-hatched transformation twins.

Result: Big crystal of anorthoclase with cross-hatched twins

INTERMEDIATE: crystals exsolve into Na-rich and K-rich monoclinic phases ~650C parallel to (100); is the orientation which **minimises strain energy** to keep lattices of exsolved phases **in congruence w/ each other**
Further cooling: displacive phase transition of **Na lamellae in K host**. Hence, lamellae shape are constrained by the host. To distort structure while maintaining overall shape, **periodic albite twins develop**.

Periodicity of twins proportional to **thickness** of lamellae; able to determine whether **coarsening of exsolution lamellae occurred (prolonged cooling at x temperature)**.

Al/Si ordering rate very slow; hence high albite and sanidine are metastable.

Result: Lamellae of **high albite in sanidine**.

SLOW: Sanidine host has time to convert to microcline. Transformations defined by phase diagram.

Result: Intergrowth of low albite and microcline.

5. Explain the structure of pyroxenes. Describe how interpretation of this structure can be used to determine the temperature and cooling rates in igneous rocks. [45 minutes]

Pyroxene: single chain silicate mineral, $XY(Si, Al)_2O_6$. X,Y can be a lot of things, but most commonly Mg^{2+} , Fe^{2+} , Ca^{2+} . Pyroxenes show open structures at high temperature and collapsed ones at low temperature

2021

2. (a) Silicon and oxygen are important mineral-forming elements. Describe the bonding and their mutual coordination under different temperature and pressure conditions in the Earth. Describe the importance to mineral structures of the variability of the Si-O bond and the Si-O-Si bonds. [20 minutes]

Si: period 3, group 4. Small ion; thus steric considerations prefer 4-fold over 6-fold coordination at low pressure. Orbitals more diffuse than carbon (sideways overlap of p orbitals are poor); π bonds are disfavoured as a result, and Si prefers to use head-on overlap of sp^3 hybridized orbitals to form σ bonds with O.

Si-O bonds: strong, highly polar bonds. O may coordinate to another Si atom, forming interconnected tetrahedra. The bond length of Si-O may vary with temperature. Si-O-Si bonds are rotationally flexible. Quartz is used as an example to demonstrate this:

Crustal conditions (low P low T) – 4-fold Si coordination (tetrahedra). Long bond lengths, e.g. low quartz ($P3_21$)

Volcanic conditions: (high P high T): Si-O-Si angles become more flexible, forming polymorphs with more open structures like tridymite ($P6_3/mmc$)

For example tridymite crystallizes from an acid lava at 1000 °C and low quartz from a low temperature hydrothermal vein at 350 °C. High PT quartz phases are found in nature only when the cooling rate is too rapid to allow reconstructive transitions to quartz to occur.

Mantle conditions (high P high T) – 6-fold Si coordination (octahedra), e.g. stishovite. Short bond lengths, hence high-energy, high-density form (and favoured under high P)

Note that Stishovite has been found on the crust, specifically in K/T boundary clays, due to high pressures generated by meteorite impacts. This has been used as evidence for a meteorite as the cause of K/T extinction.

Although Si centres are all tetrahedral, the flexible Si-O-Si bond allows a variety of structures to be formed. e.g. isolated tetrahedra, single chain, double chain, tectosilicates, etc.

(b) How are displacive and reconstructive phase transitions in silica polymorphs controlled by the nature of silicon oxygen bonding? [25 minutes]

Si-O-Si bonds being rotationally flexible means adjustment of Si-O-Si angles require little energy, making such displacive transitions rapid and reversible.

3. (a) Describe the exsolution textures that are observed in natural pyroxenes and explain how they develop. [20 minutes]

Exsolution: when w is +ve, A-A & B-B interactions favoured over A-B. With decreasing T, pigeonite ss:

- 1) Exsolves augite (C2/c) – calcium rich clinopyroxene.
- 2) Pigeonite host transforms to Opx at **eutectoid**: reconstructive phase transition.

Two possible mechanisms of exsolution development:

Nucleation and growth: when random fluctuations in local concentration of atoms become sufficiently high (when ΔG of precipitation > surface energy + strain energy of interface), creating **stable nuclei** of a phase. They grow larger via diffusion of the same atom down the concentration gradient.

Spinodal decomposition: in compositions where curvature of free energy curve is negative, $\frac{d^2G}{dx^2} < 0$, chemical potential of a phase in phase-rich region is lower than that in phase-poor region, which drives diffusion up the concentration gradient. In other words, the **amplification of compositional fluctuations** are spontaneous.

(b) How can these textures be used in: (i) thermobarometry of granulites, and (ii) determining the cooling histories of igneous rocks? [25 minutes]

Thermobarometry: quantitative determination of the temperature and pressure at which a metamorphic or igneous rock **reached chemical equilibrium**

Exsolution lamellae "freeze in" when diffusion ceases at a closure temperature

Cooling speed is reflected in pyroxene texture:

Rapid: No time for diffusion or reconstructive phase transition; pigeonite remains homogeneous and in Cpx form. Displacive phase transition high -> low pigeonite still occurs.

Medium: Augite exsolution lamellae develop // (001) of pigeonite host. No reconstructive phase transition, but displacive phase transition high -> low pigeonite still occurs.

Slow: Augite exsolution // (001) of pigeonite host, THEN reconstructive phase transition Cpx -> Opx (C2/c -> Pbca), and further augite exsolution // (100) of opx host, forming inverted pigeonite.

Spacing of exsolution lamellae gives **duration** rocks spend at specific temperatures during cooling:

Spacing of exsolution lamellae \propto time^{1/3} during isothermal annealing: where pyroxene crystals are held at **constant temperature** for an extended period, allowing for ionic diffusion throughout the crystal lattice.

Crystal with coarse lamellae -> prolonged residence at high temperature (e.g. slow-cooling granites)

Crystal with fine lamellae -> rapid quenching (e.g. basalt)

During transition from high to low pigeonite, antiphase domains may develop due to loss of translational symmetry (from C lattice to P lattice), can only be viewed using TEM

4. (a) Discuss the factors governing how aluminium can substitute for silicon in a tectosilicate. Include a discussion of the energetics and temperature dependence of the distribution of aluminium. [15 minutes]

Tectosilicate: Minerals with Si:O ratio of 1:2. Includes feldspars, zeolites and quartz (!)

(b) Using your answer to (a), explain the microstructural development of the alkali and plagioclase feldspars during slow cooling. Why is the typical scale of exsolution microstructures in the alkali feldspars so different from the scale of exsolution in plagioclase feldspars? [30 minutes]

Plagioclase feldspars: As Ca^{2+} takes up very little volume, in compositions with high Ca, one extra displacive phase transition from C-1 to P-1 (with a smaller unit cell) occurs to stabilize structure at low temperatures.

Ultra-fine-scale lamellae: create optical **iridescence** when periodicity of lamellae = wavelength of light. See labradorite

- Exsolution in plagioclases requires **COUPLED DIFFUSION OF Al / Si** in conjunction with Ca / Na. Al / Si diffusion is **VERY SLOW** and diffusion lengths are very small

2022

3. Compare and contrast the crystal structures and sub-solidus phase behaviours of pyroxenes and amphiboles. How does the crystal structure of amphibole influence the chemical substitutions observed in different metamorphic facies? [45 minutes]

4. (a) Aluminium is an important constituent of many crustal minerals on Earth. Using appropriate examples from at least two different mineral groups, describe the different ways in which aluminium may be coordinated by oxygen in silicates, and explain the substitutional mechanisms by which aluminium is incorporated into silicate solid solutions. [30 minutes]

(b) Why do we not find aluminium-rich olivines in nature? [15 minutes]

Phase Transitions

2023

3. (a) Describe briefly how knowledge of crystal symmetry can be used to simplify the description of complex mineral structures and facilitate the determination of those crystal structures using diffraction techniques. [15 minutes]

Knowledge of crystal symmetry greatly reduces the amount of information needed to define the entire crystal: Instead of storing coordinates of every atom in the infinite crystal lattice, we only need to:

1. Specify **unique atomic positions** which compose the **asymmetric unit** – the part of the unit cell which can be used to generate the complete unit cell via symmetry operations
2. Specify **space group** which gives the set of symmetry operations to generate the complete unit cell, and the type of lattice to generate the entire crystal via translation.

Reciprocal lattice formally same as diffraction pattern of lattice; this pattern is dependent on translational symmetry (determined by lattice type) and site symmetry (all the other operations)

Systematic absences in diffraction patterns can be predicted by the structure factor:

$$F(\mathbf{hkl}) = f(\sum_j e^{-2\pi i(hx_j + ky_j + lz_j)})$$

i) non-primitive unit cells. E.g. BCC lattice introduces extra point at $(\frac{1}{2}, \frac{1}{2}, \frac{1}{2})$ alongside basic point $(0, 0, 0)$. Plugging this into the formula given above gives the general reflection condition $\mathbf{h+k+l=0}$ if $\mathbf{h+k+l}$ is odd, so those points are not formally allowed.

ii) presence of screw axes and glide planes in the space group, which introduces fractional translations which cause phase cancellations. Similarly by using the formula, the general reflection conditions can be predicted for a particular symmetry element. (They can be found on the International Tables for Crystallography.)

(b) Minerals can change their crystal symmetry as a function of changing temperature and/or pressure due to phase transitions. Describe an example of a mineral that undergoes a displacive phase transition and an example of a mineral that undergoes a reconstructive phase transition. In each case, compare the thermodynamic and kinetic factors that control the phase transition and the resulting microstructures that may develop due to the phase transition. What information about the **geological history** of the mineral might be gleaned from the study of the resulting microstructures? [30 minutes]

Mineral polymorphs: Different crystal structures of the same chemical compound that form under different T, P. The polymorph with lowest G at any T, P is the **thermodynamically stable** one; when T, P changes, most stable polymorph may also change.

The occurrence of any particular silica polymorph has the potential to provide information about the physical conditions in the rock at the time this mineral crystallized.

Reconstructive transition: When **free energy curves** of two polymorphs intersect, (i.e. 1st order discontinuity in the preferred G curve) polymorph spontaneously transforms to another polymorph with **completely unrelated structure**. As bonds are **broken and reformed**, a **high energy barrier** needs to be overcome, the process requires nucleation, is **diffusion dependent**, and it is **slow**

- **High quartz to high tridymite** reconstructive transition: from P6₂22 (hexagonal) to P6₃/mmc (hexagonal)
- Due to slow nature of reconstructive transition, possible to **quench** high-temperature polymorphs such that they do not have time to transform at low T; study of metastable phases allows study of high-T, high-P assemblages of rocks, giving us insight into the hidden mineralogy of Earth's depths.
- No transformation twins possible, as polymorphs are not related by twin law (the symmetry operation)
- Complete tridymite formation requires **prolonged high-T low-P events** (e.g. in magma chamber)
- If conditions long enough for nucleation to start but not long enough for complete formation, microstructures (dendritic crystals) of tridymite in quartz occur.
- Note that high tridymite undergoes displacive transition back to low tridymite (orthorhombic) which is what we observe at room temperature (as displacive transitions can't be quenched). Gives characteristic arrow head crystal shapes.

Displacive transition: When **2nd** order discontinuity in G curve exists, polymorph spontaneously transforms to polymorph with **related structure** (low symmetry group is a subgroup of high symmetry group). Rapid, reversible. Only involves rotations and no bond breaking; activation energy is low. While crystal may retain external shape of previous polymorph, internal structure is different. (**Pseudomorph**)

- **Low-high** quartz displacive transition: when heated, from low P3₂1 (trigonal) symmetry to high P6₂22 (hexagonal) symmetry. Causes **small rotations of tetrahedra about <100>**
- Note that this rotation can occur in two senses; leads to chemically identical but differently oriented twins, which are related to each other by the symmetry operation that was lost (2 along z)
- Dauphine twins (only visible via TEM)
- Not possible to quench high quartz. All high quartz in collections represent **pseudomorphs** of quartz after high quartz, but as high quartz has a different (hexagonal) habit, it is trivial to show that the mineral has crystallized under high temperature conditions for a while.

2024

3. The mineral CaCO₃ can exist in two unrelated structures – one with a trigonal symmetry (calcite), and one with orthorhombic symmetry (aragonite). A simplified phase diagram is shown below.

(a) Discuss how a knowledge of both thermodynamics and kinetics can be used to predict the stability and behaviour of minerals under changing conditions of temperature and pressure. [15 mins]

Thermodynamics: describes theoretical stability of phases under different conditions. Because natural systems tend to **minimize energy** the polymorph with least energy will be the stable one.

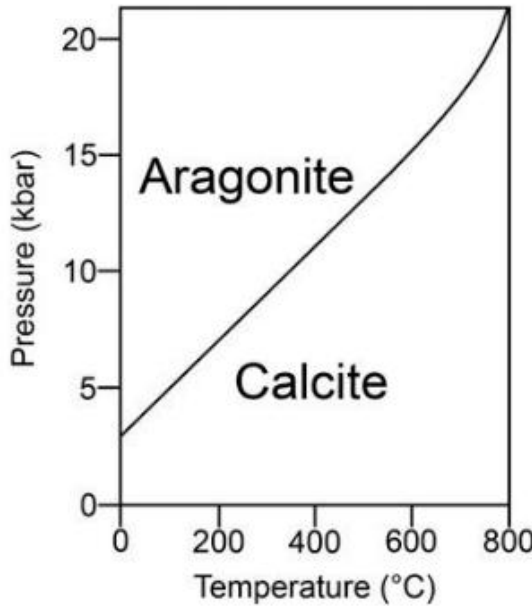
Gibbs free energy: ΔG = the energy released / consumed when a pure phase is created from other phases. It is a **relative value** so this allows us to compare energies and stabilities of phases in a reaction under different P, T.

$\Delta G = VdP - SdT$. From this, we deduce that at high T, phases with high entropy are stable, and at high P, phases with low volume are stable.

At equilibrium, $\Delta G = 0$ so this rearranges to $\frac{dP}{dT} = \frac{\Delta S}{\Delta V}$ which is the Clapeyron equation; it shows how T and P covary for two phases to exist in equilibrium. Knowledge of ΔS & ΔV gives the slope of phase boundaries which can be used to predict stability fields (which phase exists at different T and P)

Thermodynamics only applies to systems at equilibrium, and lower temperature rocks often do not reach equilibrium, as the activation energy is too high:

Kinetics: describes observed mineral preservation; activation energy and reaction rates, diffusion. If activation energy is high, may prevent spontaneous reactions from happening and re-equilibration from occurring. E.g. reconstructive phase transitions. However, if activation energy is low, minerals may transform / react spontaneously, like in displacive phase transitions.



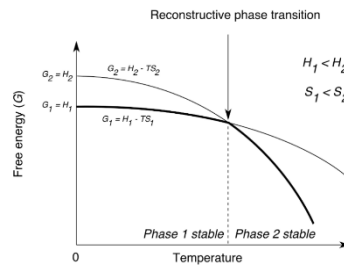
(b) Make a schematic sketch of Gibbs free energy (G) as a function of temperature (T) for the CaCO_3 system for a fixed pressure of 10 kbar. Label any key features of your sketch. What kind of transformation between calcite and aragonite would you expect to occur on slow cooling from 800°C at 10 kbar pressure, and at what temperature would the transformation occur? [5 mins]

Given the structures of calcite and aragonite are **unrelated** we expect a **reconstructive phase transition** (first order phase transformation), where the free energy curves would cross at $\sim 673^\circ\text{C}$. This requires large amounts of bonds to be broken and reformed.

Phase 1 = aragonite

Phase 2 = calcite

The first derivative of G (dG/dT) is discontinuous at the transition temperature.



(c) Explain why the phase boundary between aragonite and calcite is expected to be a straight line in P-T space, giving details of the factors that determine the slope of that line. Suggest possible reasons for the departure from linearity observed for temperatures above 600°C . [10 mins]

Clausius Clapeyron equation: $\frac{dP}{dT} = \frac{\Delta S}{\Delta V}$ where $\Delta S = L/T$ is the entropy change in transformation (L is the latent heat) and ΔV is the volume change in the phase transformation.

- This is a straight line because ΔS and ΔV are assumed to be constant with temperature / pressure. Although high T increases S and V (greater disorder, thermal expansion), and high P decreases S and V (less room to vibrate, contraction under stress), these two effects roughly cancel out.
- **Departure from straight line:** The phases may undergo other reactions at high temperature that may alter the Clapeyron slope. For example, the decomposition of aragonite introduces CO_2 gas into the mixture, which causes non-linearity. → fluids and gases increase the entropy of the system significantly
(It is known that aragonite decomposes at ~ 1000 K.)

(d) A range of different experiments are performed to explore the transformation from calcite to aragonite. Explain briefly how and why the rates of transformation would differ in the following experiments:

Reconstructive phase transitions rely on **diffusion** to create the new crystal structure. The rate of diffusion is dependent on Fick's law $\text{diffusion flux} = D * \frac{dc}{dx}$ where D = diffusion coefficient and dc/dx = concentration gradient. At grain boundaries, the concentration gradient is greatest

i. A single crystal of calcite is cooled slowly from 800°C to 0°C at 10 kbar pressure;

The driving force for nucleation is the negative change in free energy due to undercooling.

$G = -RT\ln K$. At high pressure, aragonite is favoured, so G is more negative, and K is large.

However, no grain boundaries, so must go through **homogeneous nucleation**: there is a high positive change in free energy associated with the creation of a strained interface. Hence, it has a high activation energy, so rate is slow.

ii. A fine-grained polycrystalline sample of calcite is cooled slowly from 800°C to 0°C at 10 kbar;

Polycrystalline samples have a lot of grain boundaries. **Heterogeneous nucleation** may occur on grain boundaries where the **energy barrier** to nucleation (surface energy) is **reduced** (e.g. triple junctions). This means that there are a lot of boundaries for diffusion to occur; as the reaction surface area has increased, a fast rate results.

iii. A fine-grained polycrystalline sample of calcite is slowly cooled from 800°C to 0°C at 5 kbar;

At low pressure, calcite is favoured; using logic from i), it should have a slower rate than ii)

iv. A single crystal of calcite is cooled from 800°C to 0°C at 5 kbar in the presence of water.

Water has a **catalytic** effect as it can weaken mineral structure. As a very small molecule, water can insert itself into the crystal structure and (1) **hydrolyze bonds (hydrolytic weakening)** and (2) enhance diffusion rates. This has by far the largest rate out of all the factors, despite being a single crystal at 5 kbar. Fastest rate expected.

Hence rate from fast to slow: iv > ii > iii > i

[15 mins]

Geophysics

Seismology

2020

6. Figure 2(A) shows the distribution of six tectonic regions with distinguishing seismic profiles in the top 350 km across the Earth. Figure 2(B) shows a tomographic model for the six areas shown in (A); and 2(C) the mean radial anisotropy, ξ , for the top 350 km beneath these six tectonic regions. The profile that is fastest on average (green) represents the cratons in continental regions. The profile that is slowest on average (red) represents young oceanic plates and some back-arc basins.

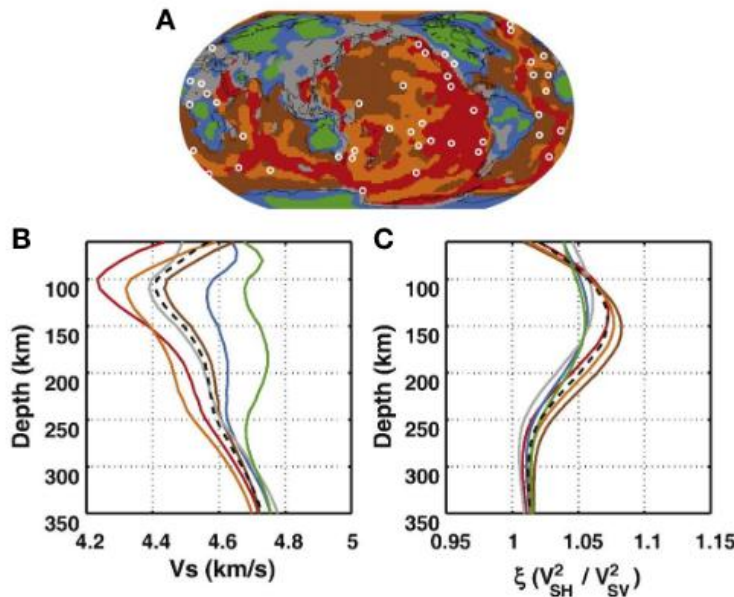


Figure 2. Seismic variations in the top 350 km of the Earth. Note that V_s = isotropic shear wave velocity (km/s); V_{SH} = horizontally polarised shear wave velocity (km/s); V_{SV} = vertically polarised shear wave velocity (km/s)

(i) Consider a shear wave propagating vertically from a depth of 350 km to the surface. Using Figure 2(B) estimate the travel time difference for such a wave between the fastest (green) and slowest (red) tectonic regions. [5 minutes]

Time is distance travelled d divided by V_s . Estimate this by taking the average velocity every 50 km (except for the top 100 km) and calculating the travel time for each 50 km:

$$t_{Slow/Red} \approx \frac{50}{4.7} + \frac{50}{4.6} + \frac{50}{4.55} + \frac{50}{4.45} + \frac{50}{4.3} + \frac{100}{4.3} = 78.6 \text{ s}$$

For fast (Green), the velocities are all roughly 4.7 km/s, so it is easier to just estimate it as $t_{Fast/Green} \approx 350/4.7 = 74.4$ s. So, the time difference is roughly $\Delta t = t_{Slow/Red} - t_{Fast/Green} \approx 4.2$ s.

(ii) Explain why an observation of the travel time difference calculated in question (i) above provides poor vertical resolution on the velocity profile. How can surface waves observations help to resolve the vertical velocity variations? [5 minutes]

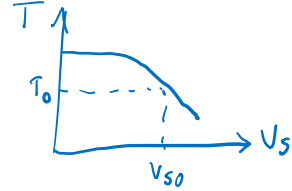
- Data coverage: If we only have this one data, then we cannot infer much about the variation of velocities in the 350 km depth regions; all we get is an ‘average’ velocity difference. Since total travel time is an integral $t = \int ds/v$, the data from all vertical depths are all mixed together, we need more data to unravel this integral.
- Generally, resolution (i.e. sensitivity) is of the order of wavelength $\lambda = v/f$. Shear waves have a higher frequency than surface waves (of the period 30 - 100 s), so they have a shorter wavelength and

thus provide a poorer resolution. Surface waves on the other hand have better resolution (can be much more than 100 km).

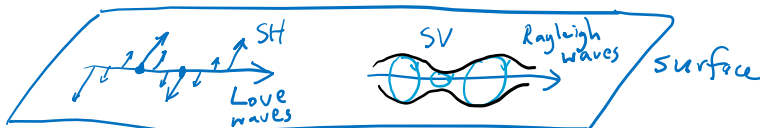
- Also, surface waves are travelling horizontally, so give a good vertical resolution. (They don't integrate up the velocity variations vertically)

(iii) Describe two approaches to convert models of seismic velocities in the **lithosphere** into models of temperature. Explain the underlying assumptions made. [10 minutes]

- Deduce T based on **mineral physical** models. From experiments determine V_s for certain compositions under various P and T conditions, then map V_s to T correspondingly.
Results can be tested against surface heat flow observations / mantle potential temperatures from MORB and OIB.
 - Assumption 1: Composition of the lithosphere is known (roughly pyrolytic) and that does not vary with depth. Justified because V_s is much more sensitive to T than composition.
 - Assumption 2: Lab results (10^6 Hz) can effectively predict seismic scale ($\sim 10^0$ to 10^2 Hz), and also can extrapolate from low P, T to high P, T.
- Deduce T based on a **pre-existing tomographic model**, i.e. oceanic lithosphere. Map between V_s and T based on **oceanic plate cooling model** and apply this also to continental lithosphere as well. Deeper depths require geothermobarometer constraints.
 - Assumption: Compositional variation within the continental lithosphere is ignored, and that the V_s -T map works equally well in the oceans as well as land.



(iv) Explain the types of seismic data used to determine the radial anisotropy profiles shown in Figure 2(C). [5 minutes]



- We use **surface wave** travel time differences. **Love waves** (sensitive to V_{SH}) and **Rayleigh waves** (sensitive to V_{SV}) travel at different speeds and the time difference gives the radial anisotropy.
- Different frequencies of these waves are sensitive to different depths, and so a range of frequencies of these waves can give us a map of $\xi = (V_{SH}/V_{SV})^2$ against depth.

(v) Within each radially anisotropic profile in Figure 2(C), the condition $V_{SH} > V_{SV}$ holds within the portion of the upper mantle that is shown. How can this property be interpreted in terms of the mantle's composition and dynamics? [6 minutes]

- Mantle composition:** (Lattice Preferred Orientation (LPO)) The upper mantle is primarily composed of olivine, which is highly anisotropic due to its crystal structure. When olivine crystals deform under strain (to accommodate dislocation creep), they tend to align their fast axes in the direction of flow, so $V_{SH} > V_{SV}$.
- Mantle dynamics:** (Shape Preferred Orientation (SPO)) Since $\xi > 1$, we imply a horizontal flow in the upper mantle as the weak, ductile asthenosphere deforms, consistent with large-scale tectonic plate motion. Alignment in features of a scale $< \lambda$. Also means the vertical flows in the mantle (such as downgoing slabs / upwelling plumes) are not dominant

(vi) An SKS wave recorded at a seismic station on a craton has an incidence angle of 12.0° . What is the incidence angle of this seismic wave at 150 km depth (i.e. the depth at which the observed radial anisotropy is strongest)? [7 minutes]

Snell's law implies that the ray parameter $p = r \sin \theta / v$ is constant, $v_1 = 4.6 \text{ km/s}$, $r_1 = 6300 \text{ km}$ at the surface and $v_2 = 4.5 \text{ km/s}$ and $r_2 = 6150 \text{ km}$ at the 150 km depth, as we read from the graph:

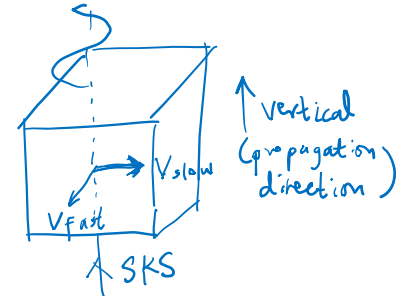
$$\frac{6150 \sin \theta_2}{4.5} = \frac{6300 \sin 12.0^\circ}{4.6} \Rightarrow \theta_2 \approx 12.02^\circ$$

Assume that we ignore the radial anisotropy, since the wave is travelling almost vertically anyways.

(vii) Explain what complimentary information SKS waves can provide about lithospheric anisotropy beyond the radial anisotropy shown in Figure 2(C). [7 minutes]

SKS waves usually travel almost vertically up the lithosphere, so it is highly sensitive to **azimuthal anisotropy** (V_s differences in the horizontal plane). It splits into two polarised components which travel at different speeds and hence have a travel time difference δt . (Similar to crystal birefringence)

This informs us about the horizontal motion (or ‘palaeo-motion’) of the lithosphere, as V_s is faster in directions aligned with the plate motion rather than those orthogonal to them. (E.g. Edge-driven flow around cratons)



SKS waves are the best waves for this application as they are simply polarized, so quite strong

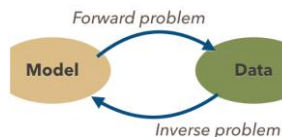
2021

5. (a) Describe the main factors limiting the accuracy of global tomographic models, and outline steps that can be taken to ensure geodynamic interpretations derived from such models are robust. [30 minutes]

Introduction

Global tomographic models: 3D plots of the seismic velocities as a function of location and depth (does not include interpretations of temperature).

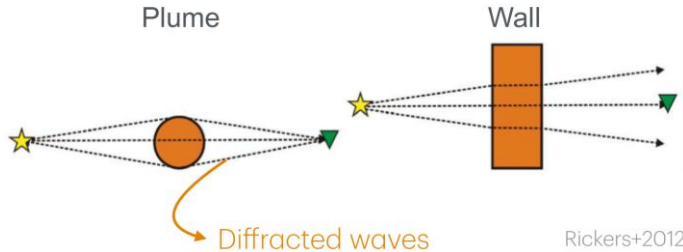
Use data such as travel times curves, amplitude, waveforms, ... to infer the model → seismic inversion.



Factors limiting accuracy:

- **Noise in data:** Data obtained from seismometers are often noisy. At times, interference from another earthquake can also mess up the signal. Noises could lead to uncertainty in inversion
 - Small timescales (<0.5 s): Anthropogenic noise, weather
 - Medium timescales (1 – 10 s): Microseism noise, water waves in oceans and lakes
 - Longer timescales (50 – 300 s): Earth’s ‘hum’
- **Data availability:** Not all places have seismic stations and seismic sources (especially in oceans, and in the S hemisphere).
 - Some places have earthquakes very often (at the same locations, like the Circum-pacific Belt), but some don’t at all (null-space) so some earthquake ray paths are over-sampled and some vastly under-sampled (lack of crossing rays)
 - Overall a mixed-determined problem, and under-determined parts will give rise to non-unique solutions to seismic inversion problem. (This means you can change the model without changing the fit)
- **Resolution of waves:** The smallest scale measurable. Why is it important? Plate movements are of the scale of mm/year, so to track small changes in mantle over the years need good model.
 - Surface waves: longer λ penetrate deeper, but can only be used to resolve large features. They cannot be used in models deeper than the crust and upper mantle. If wavelength and feature scale are not same → anomalies to appear of reduced magnitude and size in the resulting model.
 - Waves travel faster as we get deeper, but as a result the wavelength gets larger λ → poorer resolution in deep mantle. However, smaller λ waves also get attenuated more.

- Also have the problem of wavefront healing → diffraction from mantle plumes gives rise to interference and blurs out the plume anomaly



Rickers+2012

- P and S wave models respond differently to the types of anomalies. Models based solely on the wave that arrives first naturally prefer faster pathways, causing models based on these data to have lower resolution of slow (often hot) features (e.g. volcanoes, partial melts).
- Computational cost and trade-offs:** Seismic inversion is in its core a non-linear problem i.e. the observations do not linearly depend on the model parameters., and hence computationally expensive (the most accurate way is to get the correct velocity profile by reiteration).
Make assumptions that lead to potential second-order errors:
 - We often assume velocity variations are weak and ray path changes are a secondary effect and ignore those (using just the ray paths in a 1D background model).

Ways to ensure seismic interpretations are robust

- Filter and clean seismic data from the seismometer using Fourier transform, remove instrument response, highlight some frequencies, etc.
- Find simplest solution to model:** Occam's razor: simpler models are better. Over-parametrised models are bad because errors are also fitted into the model!!
 - Dampen** model: mellows out model (average it with reference) such that new model is closer to reference model, makes it more simple
 - Smoothen** model: decrease roughness (the gradient between points) – reduces effect of outliers
- Testing of sensitivity of models:** Carry out a ‘checkerboard test’, which is a synthetic input with alternating fast and slow anomalies at a specific wavelength. Ensures that anomalies can be recovered smoothly without losing information about their amplitudes.
- Compare between seismological approaches:**
 - e.g. normal modes of the Earth give an independent measurement of the density profile of the outer core, compare with those obtained by body P waves.
- Compare with multidisciplinary approaches:**
 - e.g. thermal convection in the mantle revealed by temperature anomalies recorded by seismology, link to convection studied in the laboratory, as well as in computer calculations.
 - Temperature profiles interpreted from seismology tested against observations of geothermobarometers (cratonic xenoliths), surface heat flow observations (combined with knowledge of radiogenic elements), and constraints on mantle potential temperatures from basalts at MORBs and OIBs.
- Multiscale approaches:** Improvements can also be made by making regional models. Because the model is smaller, it is computationally feasible to use higher frequency observations and thus improve the resolution, used to complement global seismology models.

(b) Describe how the internal structure of the deep Earth can be inferred from a knowledge of the seismic responses and the physical properties of mantle minerals. [15 minutes]

Seismic responses and physical properties complement each other well to form a picture of the inner Earth.

Internal structure of the deep Earth: from inner mantle to inner core.

Inner mantle, outer core, inner core.

Many ScS waves at different angles can constrain shape of LLSVPs.

We know the core is a ferromagnetic alloy due to our magnetic field. S waves can't travel through outer core -> liquid. We know from P wave data that the outer core is isotropic which supports it being a liquid.

Comparison of PKIKP vs PKPbc gives velocity of inner core vs outer core;

Body-wave evidence for inner-core anisotropy comes from PKIKP(or PKPdc) - PKPbc travel-time observations as a function of the angle, ζ , between Earth's rotation axis and the direction of the PKIKP ray in the inner core. N-S (polar path) & E-W (equatorial path) waveforms may be plotted on a seismogram; the anisotropy in the inner core corresponds to the travel time difference.

Inner core anisotropy corresponds with our knowledge of the inner core experiencing thermal convection / lattice preferred orientation from deformation stress caused by the magnetic field.

Can confirm observations using lab experiments: using high pressure devices like diamond anvil cells may simulate deep Earth conditions to measure the bulk/shear moduli of minerals at high P, T. May also help to understand phase transitions, which are the cause of discontinuities in seismic velocity.

2022

6. P wave to S wave converted phases, or *receiver functions*, are used to map the depths of the seismic discontinuities in the mantle caused by phase transitions. Figure 1, below, shows a P wave arriving at the seismic discontinuity around 410 km depth (referred to as the ‘410’ in this question). Here, the discontinuity is perturbed 20 km deeper by a mantle plume. The P wave has an incidence angle, i , of 37.0° .

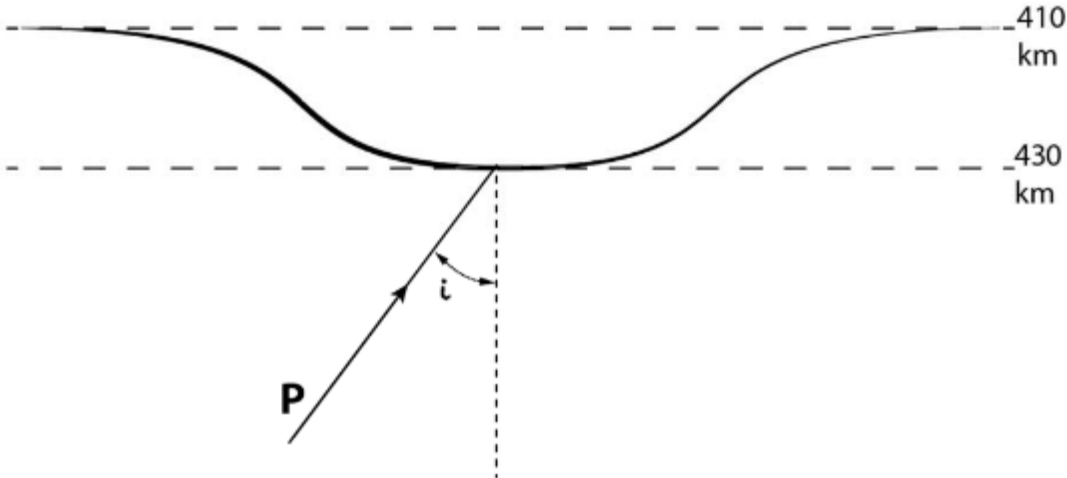


Figure 1: Diagram of a P wave incident on a perturbed ‘410’ discontinuity, not to scale.

Depth (km)	Vp (km/s)	Vs (km/s)	Density (kg/m³)
0.00	5.80	3.20	2600
15.00	5.80	3.20	2600
15.00	6.80	3.90	2900
24.40a	6.80	3.90	2900
24.40b	8.11	4.49	3381
40.00	8.10	4.48	3380
60.00	8.09	4.48	3377
80.00	8.08	4.47	3374
115.00	8.06	4.46	3371
150.00	8.03	4.44	3367
185.00	8.01	4.43	3363
220.00	8.56	4.64	3360

265.00	8.65	4.68	3462
310.00	8.73	4.71	3489
355.00	8.82	4.74	3516
410.00a	8.91	4.77	3543
410.00b	9.13	4.93	3723
450.00	9.39	5.08	3787
500.00	9.65	5.22	3899
550.00	9.90	5.37	3913
600.00	10.16	5.51	3976
635.00	10.21	5.54	3984
660.00a	10.27	5.57	3992
660.00b	10.75	5.95	4381
721.00	10.91	6.09	4412

Table 1 Vp, Vs velocities and density as a function of depth across the upper mantle. Depths labelled with ‘a’ refer to values above a discontinuity and ‘b’ below.

$$p = \frac{r \sin i}{v},$$

(a) What is the outgoing angle of the converted S wave above the discontinuity? Use the velocity values given for 410 km depth, not 430 km. [5 minutes]

At a single depth, use the ordinary Snell’s law $v_2 \sin \theta_1 = v_1 \sin \theta_2$ with $v_1 = 9.13 \text{ km/s}$ and $v_2 = 4.77 \text{ km/s}$ and $\sin \theta_1 = 37.0^\circ$, so

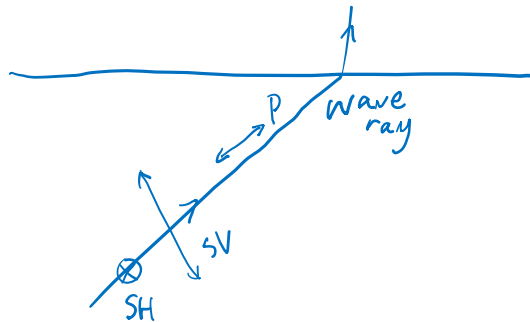
$$\sin \theta_2 = \frac{v_2}{v_1} \sin \theta_1 = \frac{4.77}{9.13} \sin 37.0^\circ \Rightarrow \theta_2 = 18.3^\circ$$

(b) Compute the incidence angle of the phase converted by the discontinuity when it arrives at the seismic station on the surface. [6 minutes]

As it moves up, due to the spherical geometry, the ray parameter p is constant:

$$\frac{(6300 - 430) \sin 18.3^\circ}{4.77} = \frac{6300 \sin \theta_s}{3.20} \Rightarrow \theta_s = 11.3^\circ$$

(c) On what seismic component(s) do we expect to mainly observe the converted phase? Explain why we expect little to no energy on the other component(s) [6 minutes]

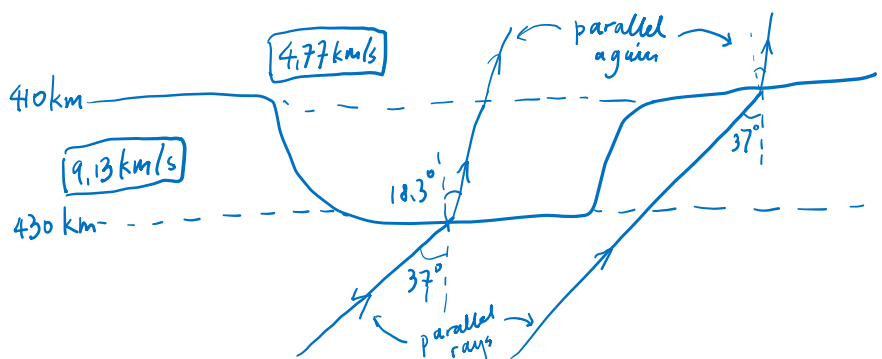


We expect mostly energy in the shear waves polarised in the vertical direction S_V , so on a seismogram this is the vertical and radial directions.

For a P-S conversion at a horizontal boundary, the energy conversion takes place in the **vertical-radial plane** which is **orthogonal** to the horizontal direction. SH has no common component of displacement with P or S_V (it requires horizontal motion perpendicular to propagation direction), so most of the seismic energy is converted to S_V .

(d) Estimate the time delay of the converted phase coming from the perturbed '410' compared to one that would come from an unperturbed '410' based on the 1D model given in the table. [5 minutes]

Assume that the time delay is only due to the region in the vicinity of the 410 km boundary, as shown below, which occurs between the 410 km and 430 km depths:



$$\Delta t = \frac{20}{\cos 18.3^\circ} \div 4.77 - \frac{20}{\cos 37^\circ} \div 9.13 \approx 1.7 \text{ s}$$

(e) Given that the seismic velocities across the upper mantle and crust will also be perturbed by the mantle plume, explain how this can affect the observed depth of the perturbed '410'. [4 minutes]

- Assume that the plume is perturbing the upper mantle and crust downwards, then throughout the rest of the sub-surface layers the velocities of seismic waves should be smaller than the surroundings.
- This would **exaggerate** the time difference observed, making us believe that the plume is **deeper than we think**.

(f) Which mineral phase transition do we relate to the ‘410’ seismic discontinuity? [2 minutes]

Olivine \rightarrow wadsleyite

(g) Calculate the temperature of the plume based on the perturbation of the ‘410’. Use a Clapeyron slope of 2.5 MPa/K and a value of $g = 10 \text{ m/s}^2$. [7 minutes]

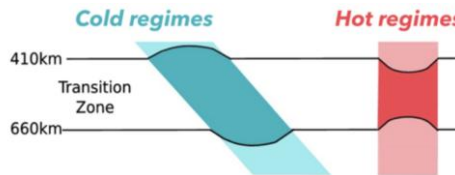
For the density, we use the value just above the 410 km boundary (technically using that below the boundary is also fine).

$$\frac{dP}{dT} \approx \frac{\Delta P}{\Delta T} = 2.5 \frac{\text{MPa}}{\text{K}} \Rightarrow \frac{\rho g \Delta h}{\Delta T} = \frac{(3543)(10)(20 \times 10^3)}{\Delta T} = 2.5 \times 10^6 \Rightarrow \Delta T \approx 280 \text{ K}$$

This means that the plume is 280 K hotter than its surroundings. Note that the question didn’t give us how hot the surroundings is, and also where we are supposed to calculate the temperature of the plume (right at this point? or at the surface of the plume?). If we say the surroundings is $\sim 1500 \text{ K}$, then we can approximately say the plume is about $\sim 1780 \text{ K}$ at this depth.

(h) How do we expect the seismic discontinuity around 660 km depth to be perturbed by the mantle plume in an olivine dominated mantle? Based on what mineral reaction? [4 minutes]

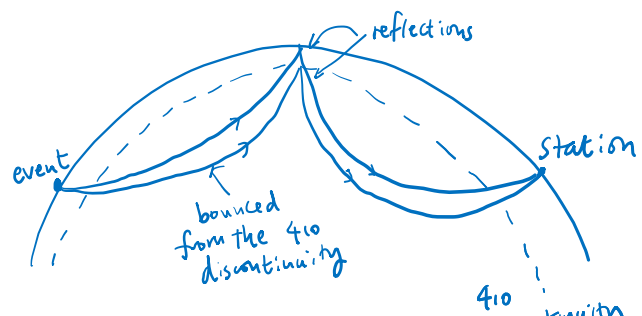
- Note that the reaction at 660 km is Ringwoodite \rightarrow Bridgmanite + Periclase (Ringwoodite is converted from Wadsleyite at $\sim 520 \text{ km}$), which has a **negative** Clapeyron slope.
- Hence, as this perturbation increases the temperature at the 660 km depth, this decreases the pressure required to for this transition, and hence the 660 km discontinuity is **moved up**. (see diagram below)



(i) Sketch a diagram showing the ray paths from event to station of two other seismic phases with different geometries that could be used to map the perturbed ‘410’. [6 minutes]

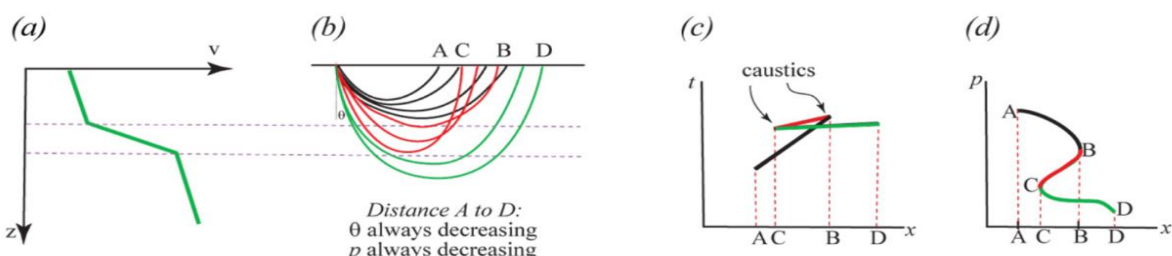
1. Precursors (Underside reflection of PP / SS reflections)

Reflections from the ‘410’ boundary arrive faster than the main P wave, so the time difference infers the ‘410’ depth



2. Triplications (Topside reflection of Direct body waves)

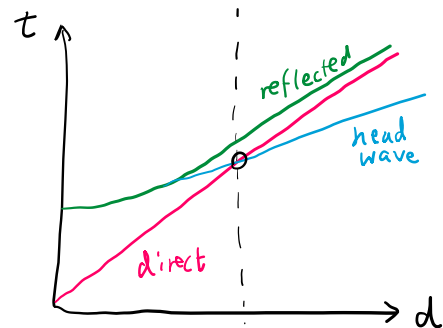
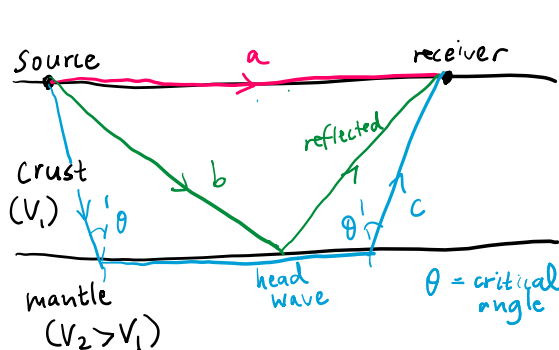
Triplications occur when seismic waves split into three arrivals due to a velocity gradient at a discontinuity. Waves may be reflected, refracted by the discontinuity, or travel directly through. This complicates seismic signals but gives structural constraints on velocity vs depth.



2023

6. (a) With the aid of schematic ray-path diagrams and traveltimes curves, describe how Andrija Mohorovičić was able to detect the presence of the Moho using recordings of the Kupa Valley earthquake of October 8 th, 1909. [15 minutes]
- (b) Inge Lehmann discovered the presence of the inner core in 1936. Explain, with the help of a schematic ray-path diagram, how this was achieved. How does the P-wave velocity of the inner core compare to the outer core and lower mantle? [15 minutes]
- (c) Describe how the Earth's radial velocity and density structure can be estimated from measurements of seismic waves. Which body-wave phases are most sensitive to inner-core velocity structure? [15 minutes]

(a) Discovery of Moho



D = distance between source and receiver. No head wave possible until a certain distance where the critical angle can be reached

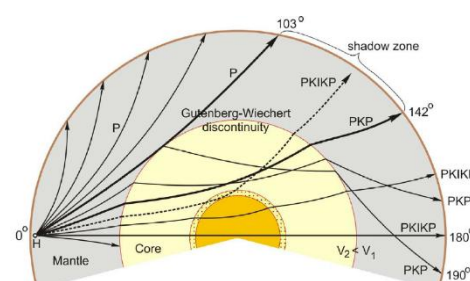
- His observation: by marking the time t required for the first wave (P-wave) to reach a seismic station at a distance d away, the slope of the curve ($1/v$) has a discontinuity at a certain distance.
- Three waves: (a) direct, (b) reflected and (c) head wave (arrive at the crust-mantle boundary at the critical angle and then travel in the mantle).
- The head wave becomes faster than the direct wave at a certain distance, meaning that the seismic velocity of the crust has a discontinuous jump. → from ~6.5 km/s in the crust to about ~8.0 km/s in the mantle.

(b) Lehmann's discovery of inner core

- Previously, scientists thought that the whole core was a homogeneous ball of liquid, with a radius derived from the extent of the P-wave shadow zone, 103 to 142 degrees from the source.
- However, weak P wave phases were found in the shadow zone. Lehmann interpreted this as wave phases that get reflected from the inner core (the PKiKP phase), which were notably found in the **P-wave shadow zone**. Which implies a **seismic velocity contrast** within the core, so thus established the boundary between the inner core and the outer core.
- The P-wave velocity in the inner core > outer core as the inner core is solid but the outer core is liquid ($\mu = 0$)

$$v_p = \sqrt{\frac{\kappa + \frac{4}{3}\mu}{\rho}}$$

- However, P wave velocity in the inner core < lower mantle, as the inner core is much denser than the lower mantle.



(c)(i) Radial velocity structure

- Seismic waves from different global stations can be measured by travel times (of S-waves and P-waves), which reveals the integral of the seismic velocity along the path: $t = \int ds/v$. With many data, these together can be used to solve the inverse problem – the radial velocity as a function of the depth. Sometimes ray paths are also sensitive to velocities off the ray path, so also have to take into account.

(c)(ii) Density structure

- Then, apply the Adams-Williamson Equation:

$$\kappa = -V \frac{dP}{dV} = \rho \frac{dP}{d\rho} \Rightarrow \frac{dp}{dr} = \frac{d\rho}{dP} \frac{dP}{dr} = \frac{\rho(r)}{\kappa} \frac{dP}{dr} = -\frac{g(r)\rho(r)}{\Phi}$$

- here Φ is the seismic parameter, which can be solved by $V_s = \sqrt{\mu/\rho}$ and $V_p = \sqrt{(4\mu/3 + \kappa)/\rho}$, to give

$$\Phi \equiv \frac{\kappa}{\rho} = V_p^2 - \frac{4}{3}V_s^2$$

- Hence, we can integrate this equation below from the surface to get the density distribution with depth. Note that gravity needs to be updated, where $g(r) = GM/r^2$, where M is the total mass of the earth subtracted by the mass which is outside of the radius r .

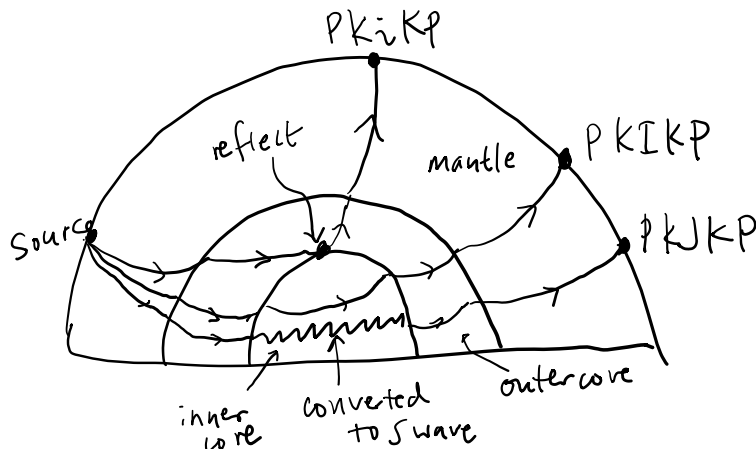
- The above assumes no jumps in the density, but this is untrue. The seismic discontinuities can be shown through waveforms (amplitudes) analysis:

- When a wave encounters a boundary (e.g., sediment-bedrock), part reflects (RR) and part transmits. These reflections appear as "peaks" or "troughs" in seismograms.
- the reflection coefficient quantifies the fraction of a seismic wave's energy **reflected** at a boundary between two materials with different physical properties. The coefficient of amplitude at normal coincidence is

$$r = \frac{Z_2 - Z_1}{Z_1 + Z_2} = \frac{\rho_2 v_2 - \rho_1 v_1}{\rho_2 v_2 + \rho_1 v_1}$$

- Hence, this informs us of density jumps, such as the base of the crust (Moho) and the core-mantle boundary, and at phase boundaries at the 410 km (Olivine \rightarrow wadsleyite), 660 km (Ringwoodite \rightarrow Bridgmanite + periclase), and inner-core boundary.
- Finally, normal modes of the earth (<10 mHz) (especially spheroidal modes) at strong earthquakes also constrain the density variations within the earth.

(c)(iii) Wave phases that are sensitive to inner core velocity variations



- PKIKP: P-wave refracted through the inner core (most direct probe). Compare with PKPBC to see the difference with the outer core. Can be used to detect the anisotropies of the inner core through
- PKJJP: S-wave converted in the inner core (rare, confirms solidity).
- PKiKP: P-wave reflected off the ICB (constrains ICB sharpness).

7. Receiver-function observations show the arrivals of P410s and P660s waves, converted from up-going P waves to up-going S waves at the 410 and 660 km discontinuities. The global-average arrival times of P410s and P660s, relative to the first P wave, are $t(P410s) = 44.0$ s and $t(P660s) = 68.0$ s.

(a) What causes the 410 and 660 km discontinuities? What minerals are involved? [5 minutes]

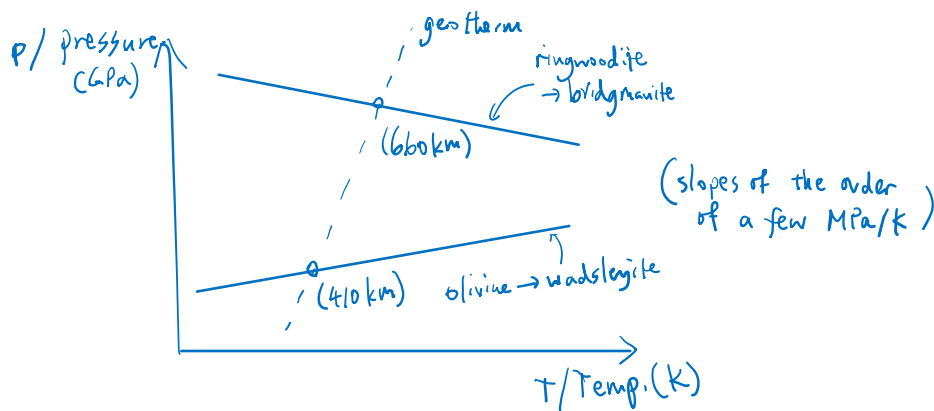
410 km: Olivine \rightarrow Wadsleyite

660 km: Ringwoodite \rightarrow Bridgemanite + Periclase

Discontinuous changes in the seismic velocities V_S , V_P .

(b) What are the signs of the Clapeyron slopes associated with the 410 km and 660 km discontinuities? Draw a pressure-temperature sketch. [10 minutes]

Clapeyron slope is given by the Clausius-Clapeyron equation: $\frac{dP}{dT} = \frac{\Delta S}{\Delta V}$. The signs are positive (at 410 km) and negative (at 660 km) respectively.



(c) The table gives receiver-function observations at three seismic stations. For each of the stations, what are the signs (i.e., positive or negative) of the probable temperature anomalies within the transition zone (410–660 km) and in the mantle above 410 km depth? We can assume that V_P and V_S vary such that the V_P/V_S ratio remains unchanged. Illustrate using a schematic diagram of the deflections of the 410-km and 660-km discontinuities, the signs of the temperature anomalies within the transition zone, and the signs of the seismic-velocity and temperature anomalies above the transition zone beneath each of the 3 stations.

	$t(P410s)$, seconds	$t(P660s)$, seconds
Station 1	47	69
Station 2	41	67
Station 3	46	72
Global average	44	68

[20 minutes]

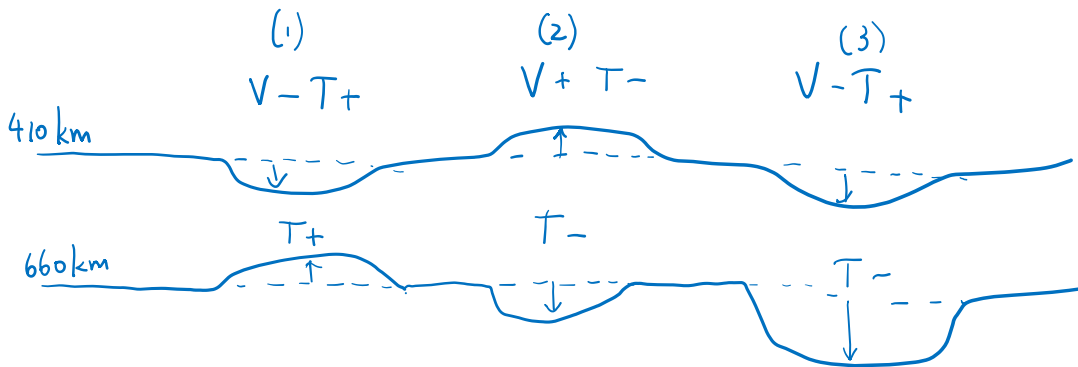
The seismic velocity decreases with increasing temperature, at about $\sim 0.5\%$ per 100 K. $V_S = \sqrt{\mu/\rho}$ and $V_P = \sqrt{(K + 4\mu/3)/\rho}$, although ρ decreases with temperature, μ and K is more sensitive to temperature. Ignore changes in the refraction angle with temperature as V_P/V_S ratio is unchanged.

- The $t(P410s)$ reflects the distance from the 410 km discontinuity to the surface and also the seismic velocity. If the temperature anomaly above the 410 km discontinuity is positive, this results in
 - a slower seismic velocity
 - downward perturbation of the boundary as $dP/dT > 0$.

These effects both add up to give a longer travel time.

→ the three stations have temperature perturbations (1) + (2) – (3) + respectively.

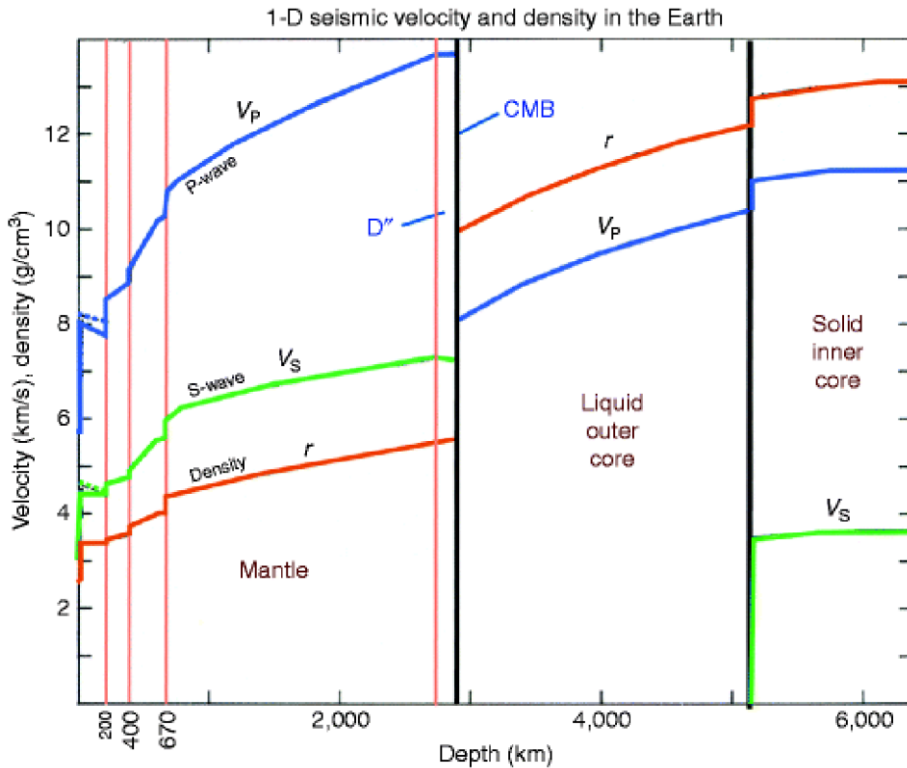
- The time difference $\Delta t = t(P660s) - t(P410s)$ reflects the time required for an S-wave to move between the two discontinuities. On average this is 24 s, but it is 22 s, 26 s and 26 s here (difference of about 8%).
- If the temperature anomaly in the transition zone is positive, this results in a slower wave speed, BUT at the same time the 660 km boundary is displaced upwards since $dP/dT < 0$.
 - However, I would suspect that the perturbation of the zone boundary is the dominating effect, since for e.g. a temperature difference of 300 K, this results in ~1.5% change in wave speed but the width of the transition zone would change by ~20 km (let's assume a Clapeyron slope of 2 MPa/K), which is ~8% change.
 - So if the temp. anomaly is +ve, then I would expect Δt to be smaller than average.
- With this assumption, I would conclude the temperature anomalies are (1) + (2) - (3) -



(d) Which station(s) is/are most likely to be near active volcanoes? Discuss how deep the origin of the volcanism may be. [10 minutes]

Stations (1) and (3) are most likely to be near active volcanoes, as they have positive temperature anomalies. The depth of melt seems to be deeper in station (1), estimated to be $d > 660$ km as the +ve anomaly reaches that far; the depth of melt seems to be shallower in station (2), estimated to be $410 \text{ km} < d < 660$ km because temperature anomaly changes to -ve in the transition zone.

8. A stable Phanerozoic platform comprises two regions, A and B. Beneath Region A, there is one layer of azimuthal seismic anisotropy in the upper mantle, extending from 80 to 280 km depth and with 2% azimuthal S-wave anisotropy. Beneath Region B, there are two layers of anisotropy in the upper mantle with a different fast propagation direction within each. One layer spans from 30–100 km depth and the other from 100–250 km depth.



(a) For SKS waves arriving to a station in Region A approximately vertically, estimate the amplitude of the shear-wave splitting (the delay time, δt). The PREM reference model is plotted below for reference.

[15 minutes]

At 200 km depth, the S-wave speed is around $V_S = 4.5$ km/s (assume this is constant throughout the 80 to 280 km depth). We have $t = d/V_S$, so

$$\delta t = \frac{d}{V_S} \left(\frac{\delta V_S}{V_S} \right) = \frac{280 - 80}{4.5} \times 2\% = 0.89 \text{ s}$$

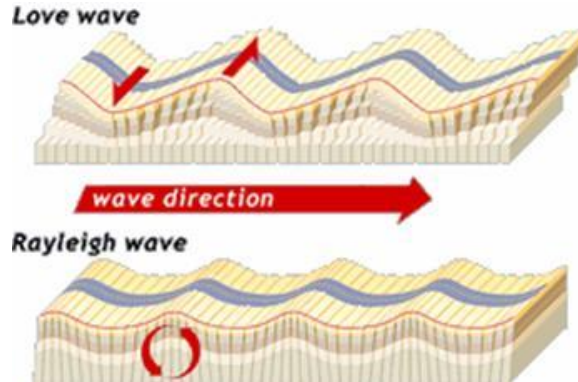
(b) For Region B, discuss which of the two layers is likely to have older anisotropic fabric. [10 minutes]

- The deeper layer (100–250 km) is likely to contain older anisotropic fabric:
 - The upper mantle undergoes deformation and fabric alignment over time (shape/lattice preferred orientation)
 - Deeper layers being subject to longer-term tectonic processes.
 - Shallow layers influenced by more recent tectonic activities or processes such as magmatism, which can create more recent fabric alignments.

(c) Discuss how we could determine radial S-wave anisotropy. What waves do we need to use for that? [10 minutes]

Radial S-waves anisotropy describes differences in the wave speed V_S along the vertical and horizontal direction, i.e. the ratio V_{SV}/V_{SH} , which is mainly due to horizontal layering.

To detect this, seismologists use **surface waves** (wavelength of $\lambda \sim 100$ km). **Rayleigh waves** are sensitive to V_{SV} and **Love waves** are sensitive to V_{SH} . By looking at their arrival times in earthquakes, we can see the difference in these velocities in the upper mantle (resolution of the order λ).



(d) The absolute plate motion of the platform is east-west. What is the likely azimuth of the fast-propagation direction at 150 km depth? Explain why. [10 minutes]

- The fast direction of S-wave anisotropy typically aligns with the direction of maximum horizontal stress or strain, as the main composition of mantle (olivine is the most abundant mineral and has ~18% intrinsic anisotropy) at this depth aligns its fast axis along the direction of max stress. Therefore, would expect it to be E-W alignment.
- Although, slight deviations could happen with local geological factors and any pre-existing frozen-in anisotropic fabric.

2024

6. Describe the seismological data and techniques used to map the lateral extent of:

- (a) a craton; [15 minutes]
- (b) a mantle plume crossing the mantle transition zone; [15 minutes]
- (c) an LLSVP in the lower mantle. [15 minutes]

Cratons

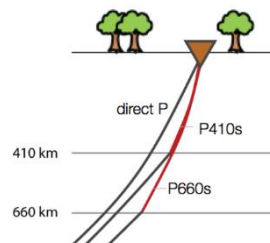
Cratons are fast regions in the continental lithosphere with roots extending to up to 200 km in depth (often deeper than most continental crust). They are old, cool parts of the continental lithosphere → high V_S , V_P .

- **Seismic tomography of body waves (V_S , V_P)**
 - Collect a lot of data from natural earthquakes. Each one is an integration through the subsurface but we get a lot of crossing paths → deconvolution gives a 3D map of the seismic velocities underneath the Earth's surface.
 - V_S to T can be done through either mineral physics calibration (extrapolation from lab experiments of pyrolite-like compositions) or a calibration from the known oceanic cooling plate model. Obtain a temperature map → Identify cratons as low temp. regions to see lateral extent.
 - Errors comes from uncertainty in the V_S -T curve, as in labs (MHz waves) we cannot get the low frequency required in earthquakes.
- **Dispersion of Surface waves**
 - Rayleigh waves are sensitive to S_V energy and Love waves to S_H energy. From earthquake travel times, usually after P and S waves.
 - They too can give a better resolution to the upper mantle with wavelengths of about $\lambda \sim 200$ km, also the base of the lithosphere. Therefore, detect lithospheric base of cratons which are thicker than usual.
- **SKS wave splitting**
 - SKS waves leaves the CMB with a S_V polarisation, and S_H polarisation detected on the surface is due to the interaction with anisotropy in the path. These waves are near vertical, so get azimuthal anisotropy (fast axis ϕ and time difference δt). We can infer any strong deformations which may be ‘fossilised’ in these oldest parts of the continental lithosphere.

Mantle Plume across Transition Zone

Plumes are hot parts of the mantle which are buoyant and rising, so slow regions of V_S , V_P . (~100 km wide) Transition zones are at 410 km and 660 km resp. and are due to olivine → wadsleyite and ringwoodite → bridgemanite + periclase, and so discontinuities in V . These are perturbed by plumes because T changes the P of phase transition (Clausius-Clapeyron equation). Therefore 410 km perturbed **down** and 660 km perturbed **up**.

- **Seismic Tomography:**
 - Similar method as before. Low-velocity anomalies detected in the mantle. Lateral extent is delineated by the size of the low-velocity anomaly.
 - V_P/V_S ratio also reflects on the degree of melting.
- **Receiver Function Analysis:**
 - Converted phases at 410 km and 660 km discontinuities (e.g. P to S at 410 called P410S). Travel times infer the depths of these discontinuity.
 - Tracking of these depths, see the perturbations of these boundaries as well as the degree of perturbation (infer temp. of mantle plume) → thermodynamic constraints on width of plume.
 - Alternatives include bounced PP phases (precursors) which reflect from these discontinuities but require on a very precise velocity model over a very lengthy wave path.

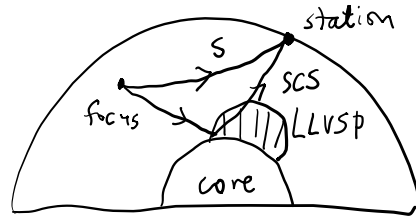


- **Surface waves**

- Similar technique as before. Focus on the V_{SH} : V_{SV} ratio obtained from the two types of surface waves. As we have a distinct vertical flow in the plume, this could potentially give a $V_{SV} > V_{SH}$ value as minerals align their fast axis with the direction of flow (Lattice Preferred Orientation LPO, induced anisotropy)
- Surface waves have better depth resolution as their wavelength is long. Use surface waves of different periods. Many crossing surface waves are required to observe azimuthal anisotropy

LLVSP

Low velocity (both shear and pressure waves) region underneath Pacific and Africa. Size scale \sim 1000s km.



- **Seismic Tomography / waveform analysis:**

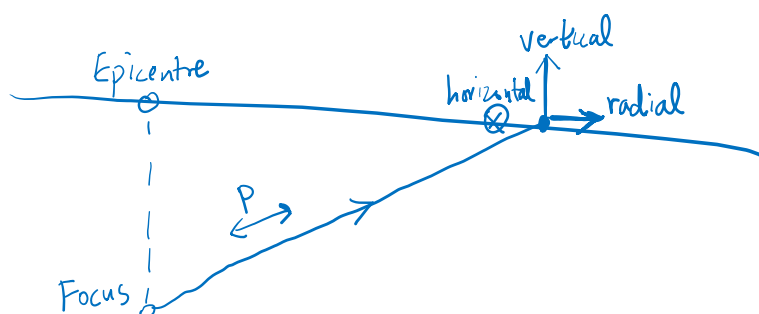
- LLVSPs appear 2-4% slower than the surroundings
- Specific waves, e.g. higher frequency body waves (like ScS that reflects off the core) with specific geometries that skirt the LLVSP boundaries → reveals sharp boundaries of the LLVSP (high contrast is seen in the waveform analysis)

- **Normal modes of the Earth**

- Earth's oscillations after a strong earthquake (e.g. Dec 2004 Sumatra earthquake) can inform us the interior structure.
- Frequency splitting and also the shifts in frequency from a homogeneous interior informs us the lateral extent and density anomaly of the LLVSPs.

8. Body-wave evidence for inner-core anisotropy comes from PKIKP(or PKPdf) - PKPbc travel-time observations as a function of the angle, ζ , between Earth's rotation axis and the direction of the PKIKP ray in the inner core. The figure below shows seismograms of these phases that sample the Earth's core at different ζ values.

(a) State which of the vertical, radial or transverse component of the seismogram is plotted, and explain why. [5 minutes]



The waves are **almost vertical** (to Earth's surface) when coming directly from the core, so the P waves (oscillating longitudinally) has energy in the vertical direction, and hence the seismogram should show the **vertical** component.

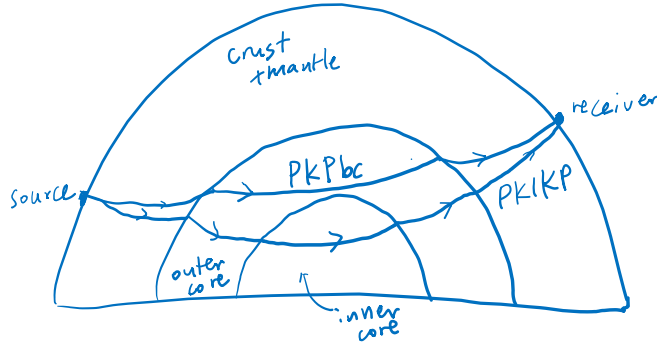
(b) What processing steps do you expect have been applied to the data in the plot? [5 minutes]

The data has probably been processed to remove the instrument response (the correspondence between ground motion and instrument recording) and the noise.

$$s(t) = v(t) * I(t) + n(t) \Leftrightarrow \tilde{s}(\omega) = \tilde{v}(\omega)\tilde{I}(\omega) + \tilde{n}(\omega)$$

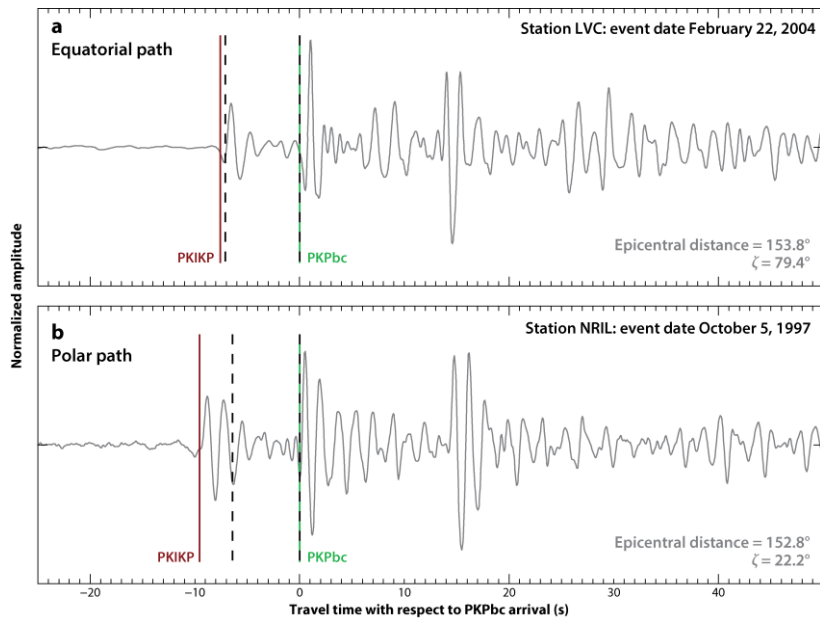
The filtering could probably be done in the Fourier domain, where noise can also be removed by applying a filter to select specific frequencies for the body wave, so diffuse, harmonic, or transient noise can be removed. Examples include anthropogenic noise (traffic).

- (c) Explain why PKIKP(PKPdf)-PKPbc differential travel times are useful to constrain the velocity variations in the inner core. Illustrate your answer with ray diagrams. [5 minutes]



The PKPbc travels only in the outer core but PKIKP travels in the inner core. The difference in time gives the difference in seismic velocities in the inner core vs the outer core, and since the outer core is known to be basically isotropic in seismic velocities, the difference is particularly sensitive to inner core. With many crossing rays, we can map the structure within the inner core.

Seismograms corresponding to (a) an equatorial path ($\zeta = 79.4^\circ$), and (b) a polar path ($\zeta = 22.2^\circ$). The predicted travel times for a radial (1D) velocity model are shown with vertical dashed lines; the measured PKIKP(PKPdf) and PKPbc arrivals are shown with labelled solid vertical lines. Figure from Deuss (2014). Anisotropy can be very complex. Often, we must resort to using simplified models of anisotropy.

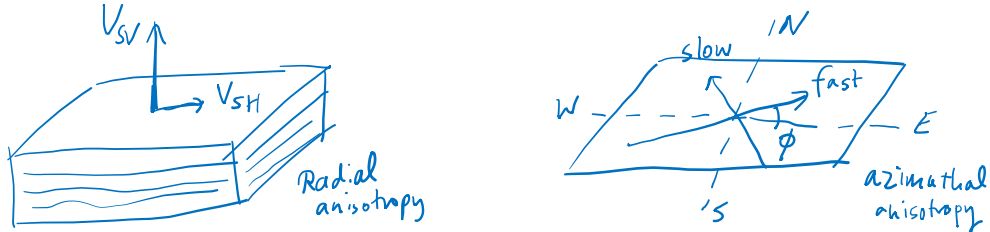


- (d) Describe the geometry of two of these simplified models of anisotropy that are commonly assumed for the mantle. For each, give an example of a seismic observation that helps constrain that type of anisotropy. [10 minutes]

1. Radial anisotropy

This describes differences in the wave speed V_S along the vertical and horizontal direction, i.e. the ratio V_{SV}/V_{SH} , which is mainly due to horizontal layering.

To detect this, seismologists use **body waves** (wavelength of $\lambda \sim 100$ km). Rayleigh waves are sensitive to V_{SV} and Love waves are sensitive to V_{SH} . By looking at their arrival times in earthquakes, we can see the difference in these velocities in the upper mantle (resolution of the order λ)



2. Azimuthal anisotropy

This describes the differences in wave speeds in two directions in the same plane, which constrains flows.

We typically observe this through **SKS splitting**, where S waves split into the fast axis and slow axis (like birefringence), and the direction of the fast axis ϕ can be inferred and the time difference δt can be used to tell us the degree of anisotropy.

(e) How might the geometry of anisotropy differ in the inner core? Explain how the observations in the figure above provide support for this type of anisotropy. [8 minutes]

The inner core shows anisotropy between the N-S direction and the E-W directions, given that the inner core is treated as a spherical object rather than layers in the mantle. This is shown as polar paths (along the N-S direction) arrive faster than the equatorial paths (along the E-W directions), meaning that seismic waves travel faster in the N-S direction compared to the E-W direction in the inner core.

(This anisotropy appears a lot stronger in the western hemisphere than the eastern hemisphere)

(f) Using an approximate inner-core velocity of 11 km/s, and an estimated path length in the inner core of 1000 km, estimate the strength and orientation of anisotropy in the inner core based on the data given in the figure above. [4 minutes]

The time difference is 2 s. Since $t = d/v$, we have

$$\delta t = \frac{d}{v^2} \delta v \Rightarrow \delta v = \frac{11^2}{1000} (2) = 0.24 \text{ km/s}$$

Hence, the anisotropy is about 0.24 km/s, which is around 2.2%. The polar path arrives first, so it shows that the fast axis is aligned with the N-S direction.

(g) What might cause anisotropy in the inner core? [8 minutes]

Thermal convection // non-axisymmetric growth // solidification texturing by outer core flow // deformation due to Maxwell stress caused by the magnetic field

→ alignment of iron crystals, which are shown to display anisotropy at high pressure.

Structure of the Mantle and Core

2021

9. (a) Discuss the geochemical and geophysical evidence that has been used to argue that the lower mantle has a composition similar to that of Bulk Silicate Earth. [25 minutes]

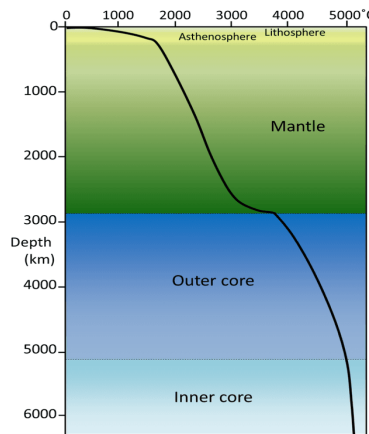
(b) What aspects of the isotope geochemistry of ocean island basalts cannot be accounted for by this model? [20 minutes]

10. (a) What is the composition and structure of the Earth's mantle. Upon what sources of evidence is our knowledge based? [20 minutes]

(b) How might the structure and composition of the mantle have changed over Earth's history? [25 minutes]

2024

7. Drawing from the fields of geodynamics, mineral physics, and seismology, outline the geophysical observations that constrain the geothermal gradient through the mantle and core. Illustrate your answer with a labelled sketch of the geotherm, including approximate absolute values and an indication of any uncertainties. [45 minutes]



Geodynamics

- In the lithosphere, conduction dominates because of the rigidity of the plates, and hence from measuring absolute temperatures in deep mines gives $\sim 20 \text{ K/km}$ (which assumed to extent to mantle).
- In the asthenosphere, the Rayleigh number $\text{Ra} > 10^6$ and therefore shows convection (adiabatic) is dominating. Therefore with knowledge of the mineral physics we get

$$\left(\frac{dT}{dP}\right)_S = \frac{T\alpha}{\rho C_P} \Rightarrow \left(\frac{dT}{dz}\right)_S = \frac{T\alpha g}{C_P}$$

Giving a geothermal gradient of around 0.3-0.6 K/km in the mantle

Mineral physics + Seismology (to determine depth) → Absolute temperatures to infer the gradient

- **Olivine phase transitions** (to wadsleyite, and then ringwoodite to periclase and bridgmanite) are predicted to occur at specific pressures and temperatures, described by a Clapeyron slope $dP/dT = \Delta S/\Delta V$. Observing the depth of a seismic discontinuity related to a phase transition, and converting this depth to a pressure, allows for an estimate of absolute temperature.
 - Susceptible to errors in the observation of the seismic depth, the conversion of depth to pressure, and the errors in determining the Clapeyron slope in mineral physical experiments.
 - At 660 km, $T \approx 1600 - 1800 \text{ K}$
 - D' phase from perovskite to post-perovskite reconstructive transition temperature can be measured accurately with phase equilibrium experiments – see lecture 15.
- Similarly, the absolute temperature at the **ICB (inner core boundary)** could be constrained by measuring the melting temperature of the iron alloy at these pressures.
 - The challenge here lies in the fact that the melting temperature depends on the light elements included in the alloy, and the exact mixture of light elements in the core is largely unknown.
 - Temperature estimates at the ICB are converging towards 5000-6000K.
- A weak constraint for **Core-mantle boundary** comes from the fact that the iron alloy of the outer core needs to be molten at this pressure. Need to also estimate of the temperature jump across the boundary layers next to the CMB (where temperature is transported by conduction) is also needed.
 - This exercise results in estimates of 3800-4500 K

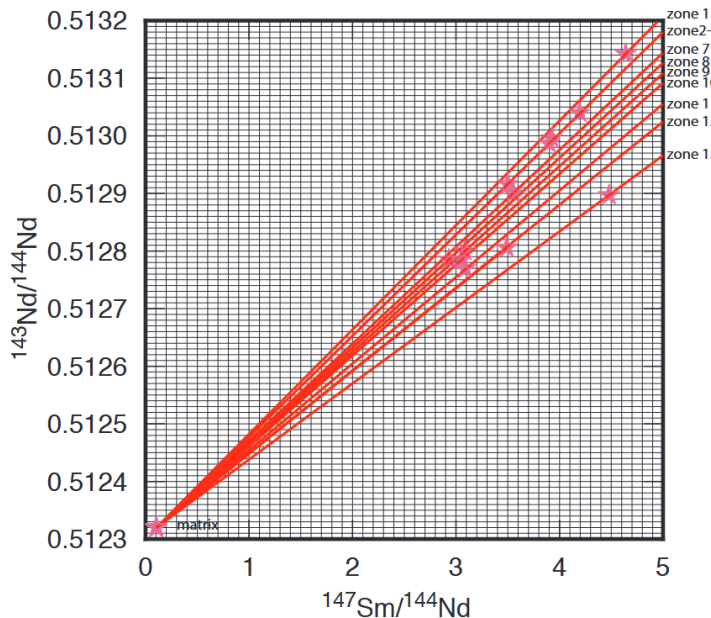
Origins of the Solar System

Isotope Geochemistry

2018

6) Garnet bearing samples were collected from Stillup Tal, a valley in the Tauern Window of the Austrian Alps. $^{147}\text{Sm}/^{144}\text{Nd}$ and $^{143}\text{Nd}/^{144}\text{Nd}$ were collected across different growth zones of a zoned garnet. Fig 1. shows this data. Each line links a different garnet growth zone with the matrix from which the garnet is thought to have grown. Table 1 shows the data from which this figure was constructed, along with the radial distance for each growth zone. Ages have been determined for some but not all of the growth zones.

Fig 1.



Note the decay constant λ for the decay of ^{147}Sm to ^{143}Nd is 6.52×10^{-12} yrs. The formula for $\varepsilon^{143}\text{Nd}$ is:

$$\varepsilon^{143}\text{Nd} = \left(\frac{\left(\frac{^{143}\text{Nd}}{^{144}\text{Nd}} \right)_{\text{sample}}}{\left(\frac{^{143}\text{Nd}}{^{144}\text{Nd}} \right)_{\text{CHUR}}} - 1 \right) \cdot 10^4$$

The formula for a model age (TM) is:

$$T_M = \frac{1}{\lambda} \ln \left\{ \frac{\left(\frac{^{143}\text{Nd}}{^{144}\text{Nd}} \right)_t^{\text{sample}} - \left(\frac{^{143}\text{Nd}}{^{144}\text{Nd}} \right)_t^{\text{CHUR}}}{\left(\frac{^{147}\text{Sm}}{^{144}\text{Nd}} \right)_t^{\text{sample}} - \left(\frac{^{147}\text{Sm}}{^{144}\text{Nd}} \right)_t^{\text{CHUR}}} + 1 \right\}$$

where $(^{147}\text{Sm}/^{144}\text{Nd})_t^{\text{CHUR}}$ has a value of 0.1966 and $(^{143}\text{Nd}/^{144}\text{Nd})_t^{\text{CHUR}}$ has a value of 0.512638, and where CHUR refers to the chondrite uniform reservoir.

Table 1

sample	Radial distance from centre	$^{147}\text{Sm}/^{144}\text{Nd}$	$^{143}\text{Nd}/^{144}\text{Nd}$	Age
	cm			Ma
matrix	0	0.104	0.512320	n/a
Garnet zone 1	0.094	4.639	0.513142	
Garnet zone 2	0.337	4.195	0.513040	26.00
Garnet zone 4	0.884	3.927	0.512996	27.13
Garnet zone 5	1.096	3.899	0.512987	26.94
Garnet zone 6	1.271	3.5	0.512916	26.92
Garnet zone 7	1.484	3.554	0.512900	25.76
Garnet zone 8	1.743	2.93	0.512785	25.20
Garnet zone 9	1.998	3.084	0.512800	24.70
Garnet zone 10	2.175	3.053	0.512785	24.15
Garnet zone 11	2.306	3.089	0.512770	
Garnet zone 12	2.457	3.491	0.512806	
Garnet zone 13	2.646	4.479	0.512897	

a) Calculate $\varepsilon^{143}\text{Nd}$ for the matrix from which the garnet grew. Does this rock have a metabasic or pelitic origin?

The matrix has $^{143}\text{Nd}/^{144}\text{Nd} = 0.51232$, so

$$\varepsilon^{143}\text{ Nd} = \left(\frac{0.512320}{0.512638} - 1 \right) \times 10^4 = -6.20$$

- Hence, the rock is depleted in Nd. Since ^{144}Nd is incompatible, it partitions into the melt which forms the crust, and ^{147}Sm is compatible, it partitions into the mantle, which gives more ^{143}Nd upon radioactive decay, so the crust has a lower $^{143}\text{Nd}/^{144}\text{Nd}$ ratio than the chondritic reservoir.
- Hence, the rock is more likely have a pelitic origin.

b) Calculate the model age for the matrix. How does this model age relate to Alpine metamorphism?

The matrix has a $^{147}\text{Sm}/^{144}\text{Nd}$ ratio of 0.1, so

$$t_M = \frac{1}{6.52 \times 10^{-12}} \ln \left(1 + \frac{0.512320 - 0.512638}{0.104 - 0.1966} \right) = 0.526 \text{ Gyr}$$

This age obviously predates the alpine metamorphism.

c) Write down the isochron equation for the Sm-Nd system.

We have $^{147}\text{Sm} \rightarrow ^{143}\text{Nd}$, so

$$^{143}\text{Nd}|_t = ^{143}\text{Nd}|_0 + (^{147}\text{Sm}|_0 - ^{147}\text{Sm}|_t)$$

And since $^{147}\text{Sm}|_t = ^{147}\text{Sm}|_0 e^{-\lambda t}$, we have

$$^{143}\text{Nd}|_t = ^{143}\text{Nd}|_0 + ^{147}\text{Sm}|_t (e^{-\lambda t} - 1) \Rightarrow \left. \frac{^{143}\text{Nd}}{^{144}\text{Nd}} \right|_t = \left. \frac{^{143}\text{Nd}}{^{144}\text{Nd}} \right|_0 + \left. \frac{^{147}\text{Sm}}{^{144}\text{Nd}} \right|_t (e^{-\lambda t} - 1)$$

d) From Fig 1 and/or Table 1, determine the ages for zones 1, 11, 12 and 13.

The slope of the graph gives $e^{-\lambda t} - 1$, so the age is just $\ln(1 + m)/\lambda$, but due to the poor resolution of the graph I would prefer just using two points in the table, between the matrix and the zone in question. Therefore,

$$t_1 = \frac{1}{6.52 \times 10^{-12}} \ln \left(\frac{0.513142 - 0.512320}{4.639 - 0.104} + 1 \right) = 27.80 \text{ Ma}$$

$$t_{11} = \frac{1}{6.52 \times 10^{-12}} \ln \left(\frac{0.512770 - 0.512320}{3.089 - 0.104} + 1 \right) = 23.12 \text{ Ma}$$

$$t_{12} = \frac{1}{6.52 \times 10^{-12}} \ln \left(\frac{0.512806 - 0.512320}{3.491 - 0.104} + 1 \right) = 22.01 \text{ Ma}$$

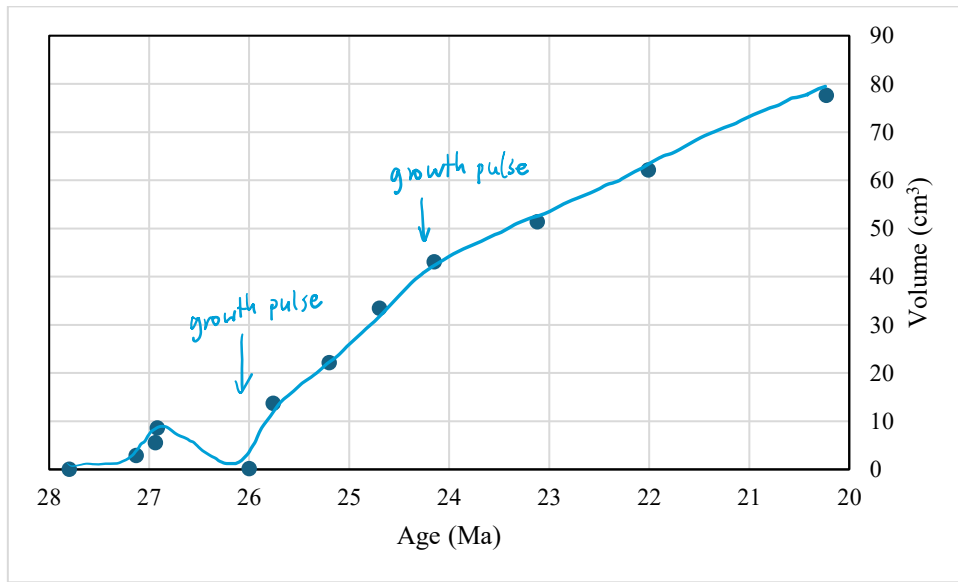
$$t_{13} = \frac{1}{6.52 \times 10^{-12}} \ln \left(\frac{0.512897 - 0.512320}{4.479 - 0.104} + 1 \right) = 20.23 \text{ Ma}$$

e) Assuming that the garnets are spherical, determine the total garnet volume at each growth stage.

If the garnets are spherical, then we the garnet volume at each growth stage is $\frac{4}{3}\pi r^3$. Therefore,

sample	Radial distance from centre (cm)	Volume (cm ³)	Age (Ma)
Garnet zone 1	0.094	0.0035	27.80
Garnet zone 2	0.337	0.1603	26.00
Garnet zone 4	0.884	2.8936	27.13
Garnet zone 5	1.096	5.5147	26.94
Garnet zone 6	1.271	8.6005	26.92
Garnet zone 7	1.484	13.6896	25.76
Garnet zone 8	1.743	22.1810	25.20
Garnet zone 9	1.998	33.4010	24.70
Garnet zone 10	2.175	43.0990	24.15
Garnet zone 11	2.306	51.3650	23.12
Garnet zone 12	2.457	62.1304	22.01
Garnet zone 13	2.646	77.5994	20.23

f) Using the graph paper provided, plot the growth volume (x-axis) vs age (y-axis). Does the data follow a linear trend?



It is not a linear trend – rather the volume does not always increase, meaning that there could be resorption at some stage. The changes in slope could mean that the growth comes in a few pulses.

2020

10. A costal exposure along a 1000m long beach in the northwest of Scotland is composed of a foliated granite that is cut in the centre by a single 100m wide dolerite dyke.

Four rock samples were collected from the granite and analysed for their isotopic composition.

Table 1

Rock Sample	$^{87}\text{Rb}/^{86}\text{Sr}$	$^{87}\text{Sr}/^{86}\text{Sr}$
A	0.21	0.7133
B	0.44	0.7214
C	0.49	0.7232
D	0.72	0.7312

Rock A, which was collected at one end of the beach, far from the dyke, contains minerals with the following isotopic compositions.

Table 2

Mineral	$^{87}\text{Rb}/^{86}\text{Sr}$	$^{87}\text{Sr}/^{86}\text{Sr}$
Muscovite	10.58	1.0765
K-feldspar	0.90	0.7375
Plagioclase	0.13	0.7106

Recall that the decay equation for ^{87}Rb to ^{87}Sr can be rewritten as

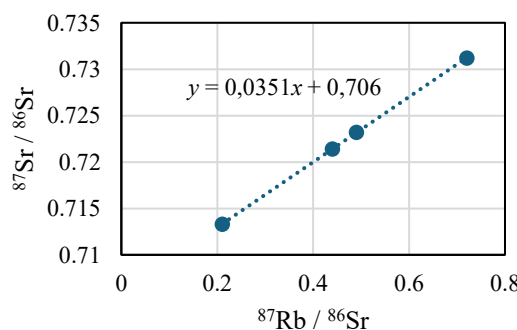
$$\left(\frac{^{87}\text{Sr}}{^{86}\text{Sr}}\right)_t = \left(\frac{^{87}\text{Sr}}{^{86}\text{Sr}}\right)_0 + \left(\frac{^{87}\text{Rb}}{^{86}\text{Sr}}\right)_t [e^{\lambda t} - 1] \quad \text{Equation 1}$$

and that the related decay constant is $\lambda = 1.42 \times 10^{-11} \text{ yr}^{-1}$.

A zircon crystal extracted from the interstitial material in the groundmass of the centre of the dolerite dyke is found to have $^{206}\text{Pb}/^{238}\text{U}$ of 0.0094. The overall decay of ^{238}U to ^{206}Pb via a decay series has a constant of $\lambda_{238} = 1.55 \times 10^{-10} \text{ yr}^{-1}$.

(i) Use the rock data provided in Table 1 to estimate an age and initial $^{87}\text{Sr}/^{86}\text{Sr}$ for the granite. [5 minutes]

From equation 1, if we plot $^{87}\text{Sr}/^{86}\text{Sr}$ against $^{87}\text{Rb}/^{86}\text{Sr}$, then the slope is $e^{\lambda t} - 1$ and the y-intercept is the initial $^{87}\text{Sr}/^{86}\text{Sr}$ of the granite. We can assume the data all lie on a straight line (and then estimate slope using two points), but we can double check by actually plotting:



Hence the initial $^{87}\text{Sr}/^{86}\text{Sr}$ is 0.706 and the age is

$$t = \frac{\ln(m+1)}{\lambda} = \frac{\ln(0.0351+1)}{1.42 \times 10^{-11}} = 2.43 \times 10^9 \text{ yrs}$$

(ii) Is the mineral data in Table 2 consistent with this age estimate? Provide calculations to justify your answer. [3 minutes]

We can just calculate the predicted $^{87}\text{Sr}/^{86}\text{Sr}$ from the straight line fit:

Mineral	$^{87}\text{Rb}/^{86}\text{Sr}$	$^{87}\text{Sr}/^{86}\text{Sr}$ (straight line fit)	$^{87}\text{Sr}/^{86}\text{Sr}$ (actual)
Muscovite	10.58	1.077	1.0765
K-feldspar	0.90	0.74	0.7375
Plagioclase	0.13	0.71	0.7106

Hence, they're all consistent.

(iii) Adapt the decay equation (Equation 1) and use the zircon data to estimate the age of the dolerite dyke. Remember that at time of growth, zircon contains no Pb, only U. [15 minutes]

Since there are no initial $(\text{Pb}^{206})_0$, thus all the Pb^{206} comes from the decay of U^{238} , and thus

$$(\text{Pb}^{206})_t = (\text{U}^{238})_0 - (\text{U}^{238})_t = (\text{U}^{238})_t (e^{\lambda t} - 1) \Rightarrow \left(\frac{\text{Pb}^{206}}{\text{U}^{238}} \right)_t = e^{\lambda t} - 1$$

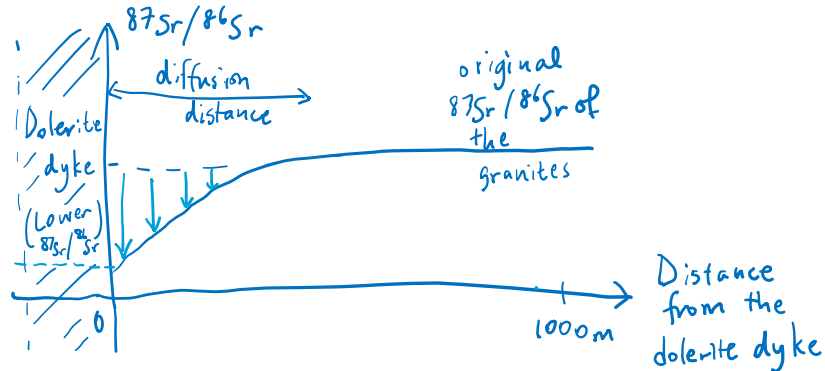
Since we are given the modern ratio $^{206}\text{Pb}/^{238}\text{U}$ of 0.0094, then

$$t = \frac{\ln(0.0094 + 1)}{1.55 \times 10^{-10}} = 6.04 \times 10^7 \text{ yrs}$$

As expected, the dolerite dyke is much younger than the granite, as the intrusion comes after and directly cuts the granite.

(iv) Rock D was collected from the granite immediately adjacent to the dolerite dike. There is no evidence of melting of the granite nor of transfer of matter from the dolerite to the granite. Nevertheless, the present-day $^{87}\text{Sr}/^{86}\text{Sr}$ of the muscovite in Rock D is substantially lower than that seen in Rock A. Speculate on the cause of this difference. Provide calculations as part of the justification for your answer. [12 minutes]

The heat conduction due to the dolerite dyke heated the Rb-Sr system sufficient to surpass the closure temperature. There was sufficient diffusion of the Rb and Sr between the dolerite and the granite (no longer a closed system). Since the dolerite has a lower Rb/Sr ratio, it also has a lower $^{87}\text{Sr}/^{86}\text{Sr}$, so by diffusion.



Estimation of the diffusion distance of the isotopes:

$$t \approx \frac{L^2}{\kappa} \approx \frac{100^2}{10^{-6}} \approx 10^{10} \text{ s} (\approx 300 \text{ yrs})$$

Therefore, the total diffusion distance would be (assuming $D \approx 10^{-14} \text{ m}^2/\text{s}$)

$$d \approx \sqrt{Dt} \approx \sqrt{10^{-14} \times 10^{10}} \approx 10^{-2} \text{ m}$$

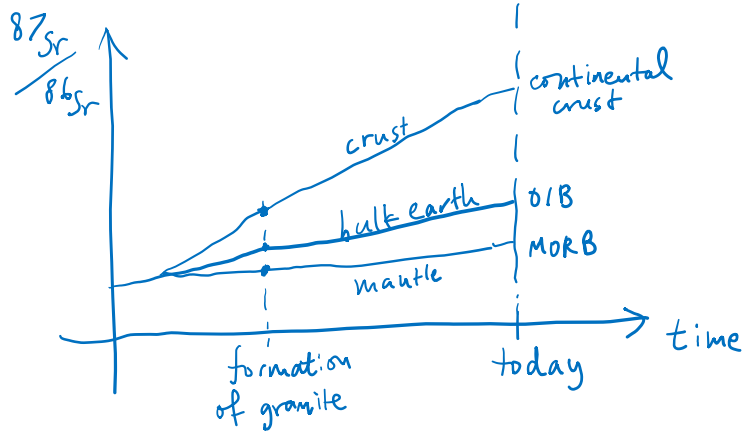
Which is just a few cm, so would not expect this thermal diffusion effect to reach very far, so only rocks just adjacent to the dyke (like rock D) would be affected.

(v) The present-day bulk-silicate Earth (i.e. mantle plus crust) has an $^{87}\text{Sr}/^{86}\text{Sr}$ of 0.705 and $^{87}\text{Rb}/^{86}\text{Sr}$ of 0.091. Use these values and your previous calculations to comment on the likely origin of the granite. [10 minutes]

Let us calculate the BSE isotopic composition at the formation of the granite $t = 2.43 \times 10^9$ yrs:

$$\left(\frac{^{87}\text{Sr}}{^{86}\text{Sr}}\right)_0 = \left(\frac{^{87}\text{Sr}}{^{86}\text{Sr}}\right)_t - \left(\frac{^{87}\text{Rb}}{^{86}\text{Sr}}\right)_t (e^{\lambda t} - 1) = 0.705 - 0.091(e^{1.42 \times 10^{-11} \times 2.43 \times 10^9} - 1) = 0.702$$

Hence, we see from (i) the initial $^{87}\text{Sr}/^{86}\text{Sr}$ of 0.706 in the granite suggests that it is more enriched in $^{87}\text{Sr}/^{86}\text{Sr}$ than the BSE at that time (note $0.706 > 0.702$), so we would see that the continental crust (pre-existing) at that time as an important source of melt of the granite.



2021

6. Radioactive dating using the decay system $^{87}\text{Rb} \rightarrow ^{87}\text{Sr}$ makes use of the relationship

$$\frac{^{87}\text{Sr}}{^{86}\text{Sr}} = \left(\frac{^{87}\text{Sr}}{^{86}\text{Sr}}\right)_0 + \frac{^{87}\text{Rb}}{^{86}\text{Sr}}(e^{\lambda t} - 1)$$

(a) (i) Write an equivalent expression for the system $^{147}\text{Sm} \rightarrow ^{143}\text{Nd}$. The stable isotope of Nd used for a reference is ^{144}Nd in this system. Explain the significance of the terms in this equation.

$$\frac{^{143}\text{Nd}}{^{144}\text{Nd}} = \left(\frac{^{143}\text{Nd}}{^{144}\text{Nd}}\right)_0 + \frac{^{147}\text{Sm}}{^{144}\text{Nd}}(e^{\lambda t} - 1)$$

$\left(\frac{^{143}\text{Nd}}{^{144}\text{Nd}}\right)_0$ gives the initial isotope ratio in the system, which then $\frac{^{147}\text{Sm}}{^{144}\text{Nd}}(e^{\lambda t} - 1)$ represents the addition to the system of daughter isotopes from the decay of ^{147}Sm , which gives the present isotope ratio in the system.

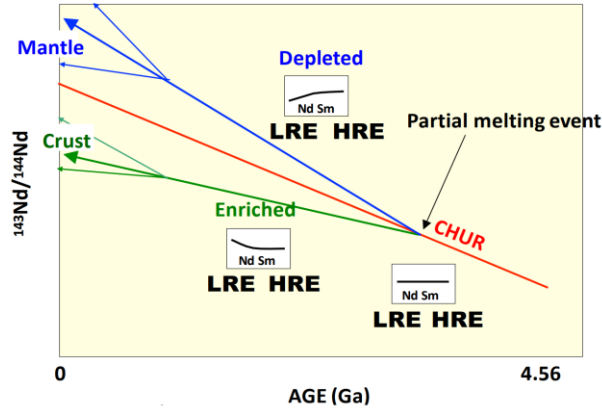
(ii) Outline the principles of $^{147}\text{Sm}-^{143}\text{Nd}$ dating. Explain how the initial Nd-isotopic ratio determined from the analysis of minerals in igneous rocks may be used to understand the chemical evolution of planetary interiors.

[10 minutes]

- Using mass spectrometry obtain the $^{143}\text{Nd}/^{144}\text{Nd}$ and $^{147}\text{Sm}/^{144}\text{Nd}$ ratios from different minerals or rocks (that are assumed to come from the same source).
 - Plot a graph of $^{143}\text{Nd}/^{144}\text{Nd}$ against $^{147}\text{Sm}/^{144}\text{Nd}$ so obtain the slope as $e^{\lambda t} - 1$ and the y-intercept as the initial $^{143}\text{Nd}/^{144}\text{Nd}$ ratio.

Information about chemical evolution of planetary interiors

- During partial melting, Sm (more compatible) tends to stay in the mantle, while Nd (more incompatible) preferentially enters the melt and forms the crust. → The mantle enriched in ^{143}Nd from the decay of ^{147}Sm . This creates distinct Sm/Nd and $^{143}\text{Nd}/^{144}\text{Nd}$ ratios in the mantle and crust
 - Find the timing and extent of mantle-crust differentiation.

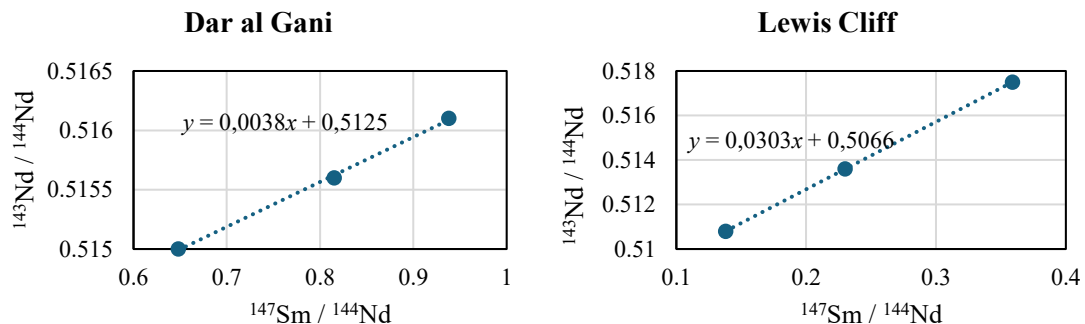


(b) The table below summarises Sm and Nd-isotopic data from minerals separated from two meteorites of basaltic composition, Dar al Gani and Lewis Cliff

	$\left(\frac{^{147}Sm}{^{144}Nd} \right)$	$\left(\frac{^{143}Nd}{^{144}Nd} \right)_t$
<i>Dar al Gani</i>		
Plagioclase	0.815	0.5156
Pyroxene	0.938	0.5161
Olivine	0.648	0.5150
<i>Lewis Cliff</i>		
Olivine	0.359	0.5175
Pyroxene	0.230	0.5136
Plagioclase	0.138	0.5108

(i) Plot the data on an appropriate diagram, and determine the crystallisation ages and initial Nd-isotopic ratios of the two samples. The decay constant for ^{147}Sm , has the value $6.54 \times 10^{-12} \text{ yr}^{-1}$.

We just plot $^{143}\text{Nd}/^{144}\text{Nd}$ against $^{147}\text{Sm}/^{144}\text{Nd}$ according to the equation given at the start of the question:



The initial ratios of Dar al Gani and Lewis Cliff are 0.5125 and 0.5066 respectively. The crystallisation ages are $\ln(m + 1)/\lambda$, giving 0.580 Gyr and 4.6 Gyr respectively.

(ii) Given that basaltic meteorites must have originated from planetary bodies that were once large enough to undergo partial melting, comment on the possible significance of the ages of the two samples. Which meteorite is more likely to have originated from a small planetesimal?

- The one from **Dar al Gani** seems to be more likely, as its age is much younger.
- A larger body (such as Mars-like) compared to a smaller body has more radiogenic heating + heating from impact in accretion and thus can retain heat longer. They have the heating required to melt and crystallise basalt quickly after the start of the Solar system.

- On the other hand, a small body takes more time to accumulate heat and melt less completely, so the rocks crystallise later, giving a younger age.

(iii) Present-day ocean floor basalts on Earth (MORB) have $^{143}\text{Nd}/^{144}\text{Nd} \sim 0.5132$. Comment on the possible significance of the initial Nd-isotopic ratios of the two meteorites.

- Both meteorites have a lower $^{143}\text{Nd}/^{144}\text{Nd}$ than modern-day MORB.
- Therefore the meteorites are less developed than the Earth's mantle, reflects a more primitive mantle in the parent body / or the ancient crust (depleted in $^{143}\text{Nd}/^{144}\text{Nd}$) was recycled and mixed into these mantle rocks. Could also be initial heterogeneity in the solar system.

(iv) You have been asked to determine as precisely as you can the age of the Solar System by further analysis of either of these two meteorites. Comment on how you might do this.

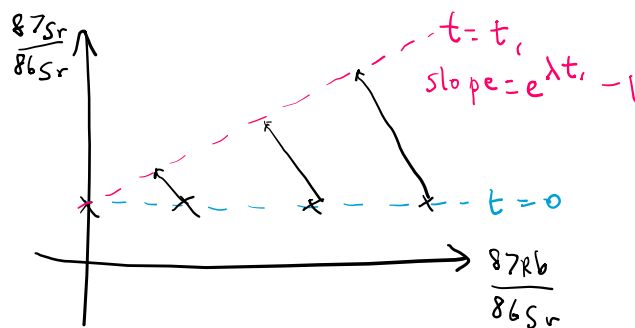
- Analyse the older meteorite (Lewis Cliff)
- Use another radiogenic isotope system (such as Pb-Pb dating, if zircons are found in the meteorites) which has a longer half-life and also a higher closure temperature (less prone to resetting of isotope decays) and thus give more accurate results.
- Oldest age obtained is treated as the time = 0 of the solar system

[35 minutes]

2022

10. (a) Discuss the information which may be deduced from the measurement of radiogenic isotopes in minerals separated from igneous rocks. [15 minutes]

Different minerals have different initial amounts of the parent radioisotope (e.g. ^{87}Rb), and so they also proportionally have more of the daughter radioisotope as time goes on. If we plot the daughter isotope ^{87}Sr against the parent ^{87}Rb (as a ratio with a stable isotope ^{86}Sr), we get a straight line



The equation of the line is:

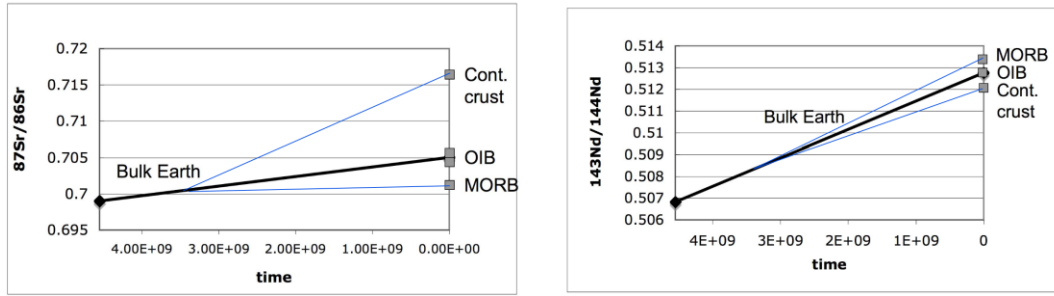
$$\frac{^{87}\text{Sr}}{^{86}\text{Sr}} = \left(\frac{^{87}\text{Sr}}{^{86}\text{Sr}} \right)_0 + \frac{^{87}\text{Rb}}{^{86}\text{Sr}} (e^{\lambda t} - 1)$$

So, the y-intercept gives the initial $^{87}\text{Sr}/^{86}\text{Sr}$ ratio and the slope gives $e^{\lambda t} - 1$, from which we can deduce the age of the rock.

Age

This tells us when the partial melting of the crust/mantle which led to the formation of the rock is, and thus tells us the thermal history of the rock.

Origin of igneous rocks



Rb partitions strongly into melts, and therefore becomes progressively depleted in the upper mantle as melts are extracted. This causes the $^{87}\text{Sr}/^{86}\text{Sr}$ of the upper mantle to decrease with time. In the case of Sm, it tends to remain in the solid residue during melting, causing the $^{143}\text{Nd}/^{144}\text{Nd}$ of the upper mantle to increase with time. Any melts extracted from this region inherit the isotopic signature of the source.

- The lower mantle is thought to be the source of OIBs, which has a more primitive composition (undepleted in Rb and not enriched in Sm), which yields isotopic signatures similar to bulk chondritic Earth.
- The continental crust (e.g. some CFBs) has become enriched in Rb and depleted in Sm with time, resulting in isotopic ratios that show the opposite trend to the depleted upper mantle (MORB)

(b) A granitic complex, intruding a limestone formation, is mainly formed of plagioclase + K-feldspar + biotite + quartz but also contains minor amount of calcite, either as 20 μm -scale euhedral crystals or mm-scale veinlets. Isotopic analyses of whole rock samples of a granite and surrounding limestone, together with mineral separates are available:

	$^{40}\text{K}/^{42}\text{Ca}$	$^{40}\text{Ca}/^{42}\text{Ca}$
Whole rock	0.1224	151.109
Plagioclase	0.0123	151.040
K-feldspar	0.800	151.577
Biotite	1.294	151.941
Calcite, euhedral	9×10^{-6}	151.018
Calcite, veinlet	9×10^{-6}	150.960
Surrounding limestone	nd	150.918

(nd = not detectable)

Given that:

$$\frac{^{40}\text{Ca}}{^{42}\text{Ca}} = \left(\frac{^{40}\text{Ca}}{^{42}\text{Ca}} \right)_{t_0} + \frac{^{40}\text{K}}{^{42}\text{Ca}} \times R \times [e^{\lambda(t-t_0)} - 1]$$

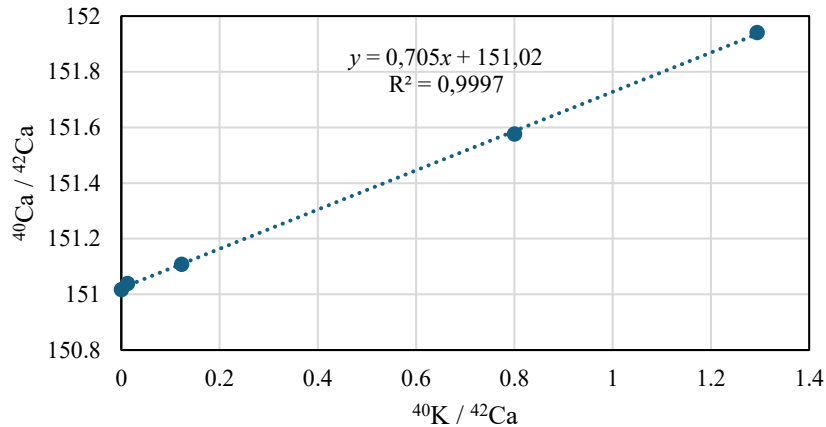
where $R = 0.8952$ and represents the fraction of ^{40}K atoms that decay to ^{40}Ca , and $\lambda = 5.54310 \times 10^{-10} \text{ yr}^{-1}$, t = time and t_0 = time of formation.

Calculate the cooling age of the granite. [20 minutes]

We plot the $^{40}\text{Ca}/^{42}\text{Ca}$ ratio against the $^{40}\text{K}/^{42}\text{Ca}$ ratio to get the following. Note that we have been careful to not use the whole data set, instead only using the whole rock, plagioclase, K-feldspar, Biotite and the euhedral Calcite.

- The euhedral crystals imply a stable equilibrium growth of the calcite (smaller size of crystals probably because of rapid nucleation at high T but not a lot of available carbonate ions) \rightarrow probably the original calcite in the melt?

- The veinlets would probably be a late-stage event (after the granite has cooled) with hydrothermal fluid flow (probably sourced from the limestone) through the cracks and fractures through the granite (could be formed by thermal contraction / tectonic stress), giving a larger scale. → Does not tell us about cooling of granite.



The slope is $R(e^{\lambda\Delta t} - 1)$, so

$$\Delta t = \frac{\ln\left(1 + \frac{m}{R}\right)}{\lambda} = \frac{\ln\left(1 + \frac{0.705}{0.8952}\right)}{5.54310 \times 10^{-10}} = 1.05 \times 10^9 \text{ yrs}$$

Cooling happened at 1.05 Gya.

Discuss the isotopic composition of the two generations of calcite. [10 minutes]

- Both have a low K/Ca ratio – makes sense since there is not a lot of places to substitute in K ions in calcite lattice.
- Euhedral calcite:** Similar Ca/Ca isotope ratio as other minerals in the rock, as seen in the graph where it fits into the st. line quite well → formed at the same time as the granite cooling, the origin of ions likely from the original melt (could also be from reactions with the surrounding limestone releasing some Ca^{2+} ions / metasomatic alteration)
- Veinlet calcite:** Ca/Ca ratio (150.96) obviously different from the others, mid-way (50%/50%) between the granite (151.02) and the surrounding limestone (150.92). Could be a second generation of cooling with fluid from the limestone mixed in. At least we are sure that the liquid should have a different Ca composition from the melt.

2023

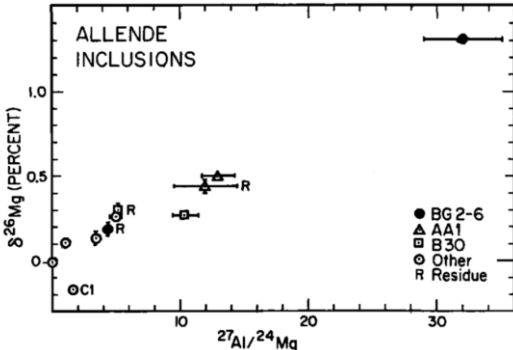
2. (a) What is meant by a radioisotope system being described as ‘short lived’? [2 minutes]

It refers to radioisotope system where the decay of the parent nuclide is too fast in relation to the timescales we want to date. The parent radioisotope is often extinct as of present. The general rule of thumb is that the timescale $T > 5t_{1/2}$, where $t_{1/2}$ is the half-life of a radioisotope.

(b) The graph below shows data from one short-lived radioisotope system, the decay of ${}^{26}\text{Al}$ to ${}^{26}\text{Mg}$, measured in calcium-aluminium-rich inclusions from the Allende meteorite. Recall that $\delta^{26}\text{Mg}$ is a measure of the deviation of ${}^{26}\text{Mg} / {}^{24}\text{Mg}$ from a reference ratio. Describe, without calculation, how these data may evidence live ${}^{26}\text{Al}$ having been present at the birth of the solar system? [8 minutes]

- There is a correlation between the ${}^{27}\text{Al} / {}^{24}\text{Mg}$ and ${}^{26}\text{Mg} / {}^{24}\text{Mg}$.

- If ^{26}Al (which decays to ^{26}Mg) was present when the CAIs formed, then minerals with higher Al/Mg ratios should have incorporated more ^{26}Al relative to stable ^{24}Mg . Decay of ^{26}Al would produce excess $^{26}\text{Mg} \rightarrow$ higher $\delta^{26}\text{Mg}$ values in phases with higher Al/Mg ratios.
- ^{26}Al has short $t_{1/2}$ \rightarrow if it was present in the early solar system, it must have been freshly synthesized and incorporated into solids quickly.



- Cr and Mn are both lithophile (but Cr is less volatile than Mn). Pd and Ag are both siderophile (but Ag is more volatile than Pd).
- These would be sensitive to volatile loss during planet formation (due to their differences in the volatility) and core-mantle differentiation (due to the differences in compatibility between the two sets of isotopes)

(g) Of the processes you have suggested, which accounts for the variation in the data shown in the above figure? Briefly explain your reasoning. [2 minutes]

Loss of volatiles during planet formation seems more likely. The moderately volatile elements have a much lower concentration compared to the less volatile elements. Besides, there doesn't seem to be a difference between siderophile elements and lithophile elements.

(h) The table below gives the Cr and Ag isotope composition of the bulk silicate Earth and details of the Mn-Cr and Pd-Ag decay systems, with the isotopic composition of CI chondrites for reference. What process explains the difference in Cr isotope composition of bulk silicate Earth and CI chondrites?

	$\varepsilon^{53}\text{Cr}$	$\varepsilon^{107}\text{Ag}$
Bulk silicate Earth	0.0	-2.2
CI chondrite	0.3	-2.2
	$^{53}\text{Mn} \rightarrow ^{53}\text{Cr}$	$^{53}\text{Pd} \rightarrow ^{53}\text{Ag}$
Decay constant, λ (yr ⁻¹)	1.87×10^{-7}	1.07×10^{-7}

[2 minutes]

CI chondrites are representative of the bulk elemental composition of the solar system, so it means that the Earth is depleted in volatiles. When the protoplanetary disk condenses and planetesimals, the radiation from the young sun and also the accretion events caused volatiles (i.e. Mn) to be lost from the growing planetesimals (that eventually formed the Earth).

(i) What implication does your answer have for the timing of formation of Earth or its building blocks? Use the rule of thumb that a short-lived radioisotope system is live for approximately 5 half-lives. [7 minutes]

- Half-life of the ^{53}Mn system: $t_{1/2} = (\ln 2)/\lambda = 3.7$ My. This gives the timescale of extinction of this radioisotope system to be about 18.5 My.
- Earth has a lower $\varepsilon^{53}\text{Cr}$ than the CI.
- If Earth was able to trap any of the Mn (as it solidified into the crust it wouldn't be subject to volatile loss anymore) before all of it had gone extinct, then the BSE would have shown signs of having Cr compared to the overall solar nebula composition. This means that the formation of the Earth was later than 18.5 My.

(j) Given your answers above interpreting the Mn-Cr system in terms of the timing and processes occurring during Earth's formation, suggest possible interpretations of the corresponding $\varepsilon^{107}\text{Ag}$ data. [8 minutes]

- Half-life of the ^{107}Pd system: $t = \ln 2 / \lambda = 6.5$ My. So, 5 half-lives correspond to 32.3 My.
- Earth has the same $\varepsilon^{107}\text{Ag}$ as the CI.
- As Ag is volatile, it will likely be lost during the stage of planetesimal accretion, but if the Pd-Ag system is still active during that stage, then Ag will still be continually produced.
- As the Earth was able to trap Ag in its core (which would not be subject to further volatile loss) at the same degree as the CI, this meant that the Earth's formation (and its subsequent core-crust differentiation which partitions the siderophile element into the core) was before this system went extinct → this timing is before 32.3 My (i.e. $18.5 \text{ My} < T < 32.3 \text{ My}$ after the solar system has formed)

2023

5. Data relating to a set of gneisses collected across an area of craton in western Australia are shown in the table below. The biotites are mineral separates from sample A.

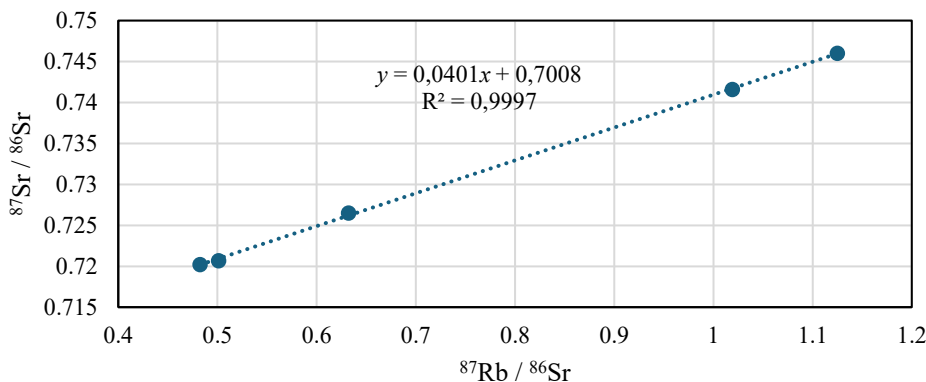
Whole rocks	$^{87}\text{Rb}/^{87}\text{Sr}$	$^{87}\text{Sr}/^{86}\text{Sr}$
A	1.019	0.7416
B	0.5012	0.7207
C	0.4825	0.7202
D	0.6321	0.7265
E	1.125	0.7460
Sample A biotites		
	155.5	2.000
	113.8	1.660
	104.2	1.560
	300.0	3.200

The isochron equation for the Rb-Sr system is given below. The value of λ for this system is $1.42 \times 10^{-11} \text{ a}^{-1}$.

$$\frac{^{87}\text{Sr}}{^{86}\text{Sr}} = \left(\frac{^{87}\text{Sr}}{^{86}\text{Sr}} \right)_0 + \left(\frac{^{87}\text{Rb}}{^{86}\text{Sr}} \right) (e^{\lambda t} - 1)$$

(a) Using the isochron method, use the whole-rock data to calculate the age of the gneisses, and their initial Sr isotope composition. [10 minutes]

From equation 1, if we plot $^{87}\text{Sr}/^{86}\text{Sr}$ against $^{87}\text{Rb}/^{86}\text{Sr}$, then the slope is $e^{\lambda t} - 1$ and the y-intercept is the initial $^{87}\text{Sr}/^{86}\text{Sr}$ of the granite.



The slope is $m = 0.4001$ and the initial $^{87}\text{Sr}/^{86}\text{Sr}$ is 0.7008, so

$$t = \frac{\ln(m+1)}{\lambda} = \frac{\ln(1+0.0401)}{1.42 \times 10^{-11}} = 2.77 \times 10^9 \text{ yrs}$$

(b) If chondritic Earth ($^{87}\text{Sr} / ^{86}\text{Sr}$)₀ is 0.6990 and ($^{87}\text{Rb} / ^{86}\text{Sr}$) is 0.155, calculate the radiogenic Sr isotope composition of bulk Earth at the time the gneisses were formed. [5 minutes]

(Disclaimer: I actually have no idea what the 0 subscript is supposed to mean. I suppose it means the time when the Earth is formed, since this value does look a bit lower than the present day value. Also, it wouldn't make sense to mean the Sr composition when the gneiss is formed since that defeats the purpose of the question. In that case, $\Delta t = 4.5 \text{ Gya} - 2.8 \text{ Gya} = 1.7 \text{ Gy}$.)

Reverse the equation before:

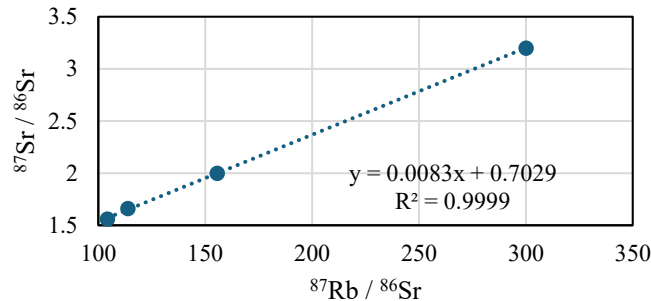
$$\frac{^{87}\text{Sr}}{^{86}\text{Sr}} = \left(\frac{^{87}\text{Sr}}{^{86}\text{Sr}} \right)_0 + \left(\frac{^{87}\text{Rb}}{^{86}\text{Sr}} \right) (e^{\lambda \Delta t} - 1) = 0.6990 + (0.155)[e^{(1.42 \times 10^{-11})(1.7 \times 10^9)} - 1] = 0.703$$

(c) Compare the composition of the gneisses at the time of their formation (from (a)), and the Sr isotope composition of bulk Earth at that time (from b)). What can you say about the mantle source from which the gneisses were derived? [5 minutes]

Since this ratio (0.703) is greater than the initial $^{87}\text{Sr}/^{86}\text{Sr}$ of the gneiss (0.7008), we could say the gneiss is formed in a depleted mantle (just like the MORB). Recall that at the time of differentiation of the crust and mantle (partial melting), since Rb is more incompatible it partitions into the melt, thus the melt (from which the crust is derived) is enriched in Rb and thus the Sr isotope ratio, while the mantle is depleted.

(d) Using only data for sample A, calculate the age recorded by the biotites. [5 minutes]

Plot this graph again (or just use linear regression, since this is supposed to be done in 5 minutes)



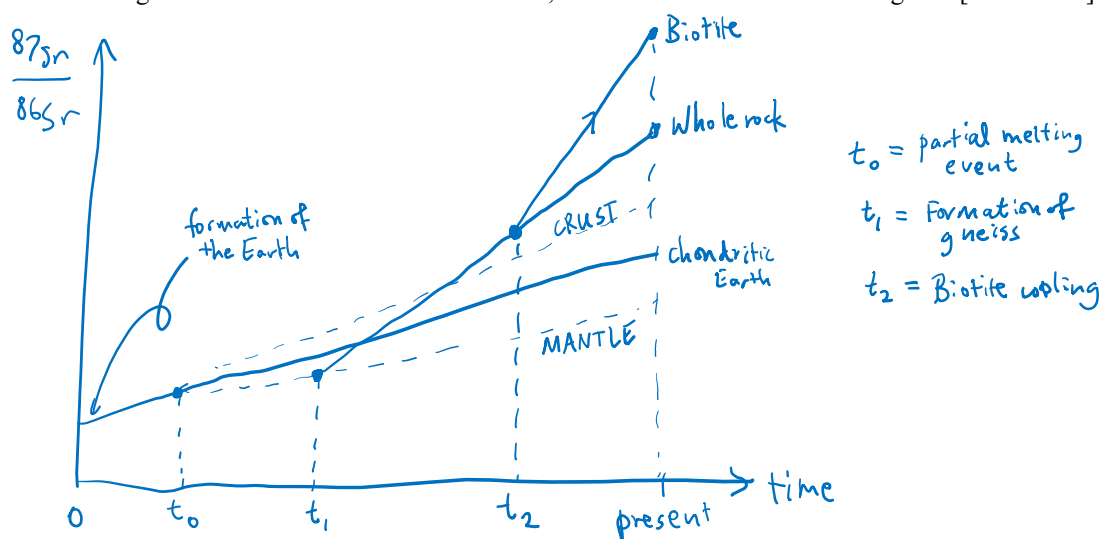
The slope is 0.0083, so

$$t = \frac{\ln(m+1)}{\lambda} = \frac{\ln(1+0.0083)}{1.42 \times 10^{-11}} = 5.8 \times 10^8 \text{ yr}$$

(e) How might the biotite age be interpreted, when compared to the age of the gneisses in (a)? [10 minutes]

- The biotite seems to be much younger than the gneiss.
- The gneiss age obtained probably is when the whole rock is formed from crystallisation, below the closure temperature (beyond which no more diffusion, gain/loss of isotopes) of the overall of the rock.
- However, the biotite age probably represents a later age, probably when the rock is subject to further cooling, by uplift and erosion / subsequent metamorphism. Since the closure T for biotite is lower, could also mean thermal resetting of the isotopes during the formation of the rock.

(f) Sketch an isotope evolution diagram, with $^{87}\text{Sr}/^{86}\text{Sr}$ on the y-axis and time on the x-axis. Show the trends for both the gneisses and their constituent minerals, and chondritic Earth on the diagram. [10 minutes]



2024

2. The amount of any radiogenic daughter isotope (D^*) produced by decay of their parent isotope N (where N = number of parent atoms remaining) over a given time period (t, in years) will be a function of the initial abundance of the radiogenic parent atoms (N_0) and the decay constant (λ), as given below:

$$D^* = N_0 (1 - e^{-\lambda t})$$

The decay constant can also be expressed in terms of the “half life” ($t_{1/2}$) of the radiogenic parent, i.e. the time it takes for one half of a given number of atoms to decay so that when $t = t_{1/2}$, $N = \frac{1}{2} N_0$.

(i) Derive the expression relating half life to λ , showing your working. [5 min]

$$N = N_0 e^{-\lambda t}, \text{ put } t = t_{1/2} \text{ and } N = \frac{1}{2} N_0, \text{ we get}$$

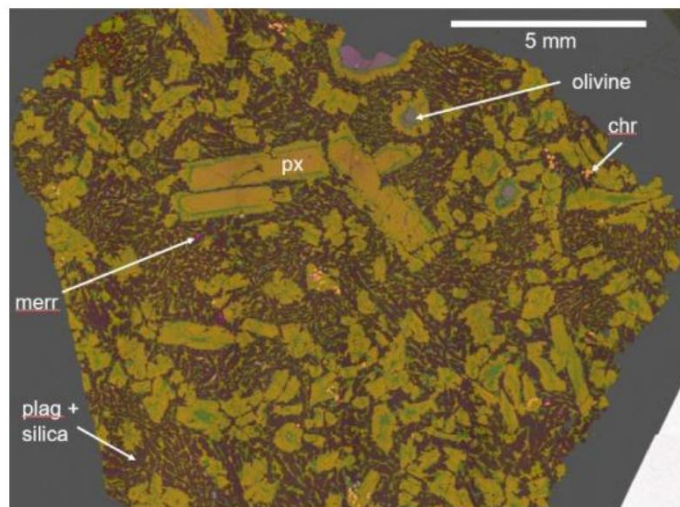
$$\frac{N_0}{2} = N_0 e^{-\lambda t_{1/2}} \Rightarrow -\ln 2 = -\lambda t_{1/2} \Rightarrow t_{1/2} = \frac{\ln 2}{\lambda}$$

The short-lived nuclide ^{146}Sm decays to ^{142}Nd , but controversy surrounds the decay constant of ^{146}Sm , with one study recording a value of $1.0193 \times 10^{-8} \text{ yr}^{-1}$ and another $6.7296 \times 10^{-9} \text{ yr}^{-1}$.

(ii) For these different decay constants, calculate the age of the youngest event that could be dated using ^{146}Sm decay, assuming that the initial age of the solar system is 4568 Ma. [10 min]

The two half-lives are $t_{1/2} = \frac{\ln 2}{1.0193 \times 10^{-8}} = 68 \text{ Mya}$ and $\frac{\ln 2}{6.7296 \times 10^{-9}} = 10 \text{ Mya}$. Since short-lived nuclides are considered extinct in $5t_{1/2}$, we can say at most they can date events that are 340 Mya and 50 Mya after the solar system is formed, i.e. 4228 Ma and 4518 Ma old respectively.

Erg Chech 002 (EC-002) is a unique, silica-rich, coarsely crystalline achondrite recognized as the oldest primordial crust sample discovered to date, with a measured $^{26}\text{Al}-^{26}\text{Mg}$ crystallization age of (1.8 ± 0.01) Ma after the start of the solar system. A coloured backscattered electron (BSE) image of EC-002 is shown below. The BSE image shows large pyroxene (px) megacrysts and rounded olivine crystals surrounded by a groundmass of sodic plagioclase (plag), pigeonite and accessory chromite (chr), merrillite (merr; a calcium phosphate mineral rich in rare-earth elements) and silica polymorphs. A previous study used EC-002 to estimate the half-life of ^{146}Sm .



(i) What aspects of the geochemistry, petrology and age, make EC-002 a suitable sample to estimate the half-life of ^{146}Sm ? [5 min]

- The abundance of coarse crystals of pyroxene and plagioclase in EC 002 makes it possible to separate minerals with fractionated Sm/Nd ratios. Sm is compatible so is more abundant in mafic minerals like pyroxene.

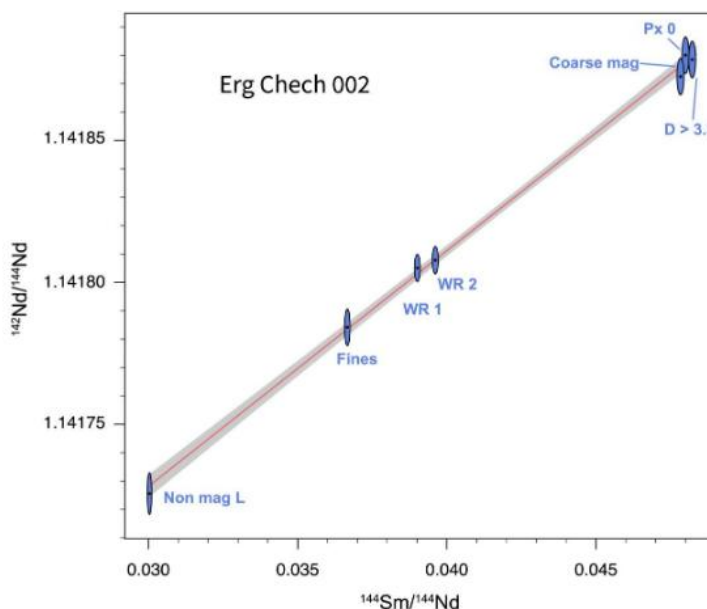
- Given its old reported age, large variations in ^{142}Nd abundances are expected → lower percentage error in $t_{1/2}$

(ii) What assumptions lie behind using the ^{146}Sm - ^{142}Nd and ^{26}Al - ^{26}Mg isotope systems from EC-002 minerals to estimate the half-life of ^{146}Sm ? [5 min]

Assumptions:

- Isochron: all samples come from same parent material.
- Half life of parent isotope is well known and measured.
- Initial abundance of parent isotope and daughter isotope at $t = 0$ is known
- System remains closed (no loss of parent or daughter)

The figure below shows a ^{146}Sm - ^{142}Nd mineral (px = pyroxene; mag = magnetic fractions of minerals separated; fines = non-magnetic fine grain-size crystals) and whole-rock (WR) isochron for EC-002. The slope of the isochron is 0.00830 and the intercept is 1.141479.



(iii) From the isochron diagram and the information above, determine the initial $^{146}\text{Sm}/^{144}\text{Nd}$ and $^{142}\text{Nd}/^{144}\text{Nd}$ ratios of the melt from which EC-002 crystallized, and explain your reasoning. [10 min]

(Question seems to have a typo – should mean $^{146}\text{Sm}/^{144}\text{Sm}$ instead, since it doesn't make sense to ask for $^{146}\text{Sm}/^{144}\text{Nd}$ when the graph shows that this ratio varies between the different minerals and the rock.)

We assume that all of the ^{146}Sm has already been extinct, so we write

$$\frac{^{142}\text{Nd}}{^{144}\text{Nd}} = \frac{^{142}\text{Nd}}{^{144}\text{Nd}}\Big|_0 + \frac{^{146}\text{Sm}}{^{144}\text{Nd}}\Big|_0 = \frac{^{142}\text{Nd}}{^{144}\text{Nd}}\Big|_0 + \left(\frac{^{144}\text{Sm}}{^{144}\text{Nd}}\Big|_0 \right) \left(\frac{^{146}\text{Sm}}{^{144}\text{Sm}}\Big|_0 \right)$$

Therefore, the initial $^{142}\text{Nd}/^{144}\text{Nd}$ of the melt is 1.141479 and the initial $^{146}\text{Sm}/^{144}\text{Sm}$ is 0.00830.

(iv) Assuming that the initial $^{146}\text{Sm}/^{144}\text{Nd}$ of the Solar System is 0.00840, calculate the half-life for ^{146}Sm from the data given above, showing your working. From your calculation, which of the two half-lives proposed for ^{146}Sm is most likely to be correct? [10 min]

Assume radioactive decay:

$$\frac{^{146}\text{Sm}}{^{144}\text{Sm}}\Big|_0 \times e^{-\lambda t} = \frac{^{146}\text{Sm}}{^{144}\text{Sm}}\Big|_t \Rightarrow \lambda = \frac{1}{t} \ln \frac{^{146}\text{Sm}/^{144}\text{Sm}|_0}{^{146}\text{Sm}/^{144}\text{Sm}|_t} = \frac{1}{1.80 \times 10^6} \ln \frac{0.0840}{0.0830} = 6.65 \times 10^{-9}$$

$$t_{\frac{1}{2}} = \frac{\ln 2}{\lambda} = \frac{\ln 2}{6.65 \times 10^{-9}} = 10.4 \text{ Ma}$$

So, it seems that the value of $6.7296 \times 10^{-9} \text{ yr}^{-1}$ (i.e. the shorter half-life) seems to be much more likely to be correct.

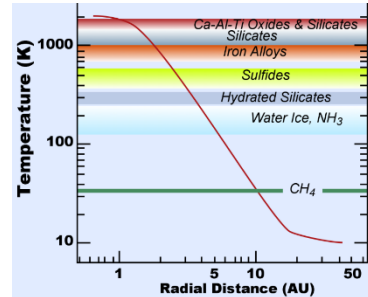
Formation of the Solar System

2018 (Paper 1)

7. How does element volatility control the distribution of elements in undifferentiated meteorites formed in different regions of the solar nebula? Discuss the importance of element volatility and the Goldschmidt classification in the application of the Sm-Nd, Rb-Sr and Hf-W radiogenic isotope systems to dating solar system objects.

Element volatility control distribution of elements

- Some event (e.g. supernova) triggers gravitational collapse of a cloud (nebula) of dust and gas consisting of H, He and other elements to form a spinning disc, GPE released heats centre forming star.
- Temperature of the disk decreases with distance from centre, and as temperature decreases different minerals start to condense.
- Refractory elements have a higher condensation temperature, so condenses first (Platinum group elements, Ca-Al-Ti oxides)



Goldschmidt classification

- Siderophile (Fe-loving): will partition into Fe-Ni metal → Inner core
- Lithophile (Rock-loving): will partition into silicates (e.g. alkali metals with strong affinity for oxygen) → Mantle / crust (BSE)
- Chalcophile (S-loving): will partition into sulphides (e.g. sulphur, copper, lead). → Outer core
- Hydrophile: will partition into (water-rich fluids) and ices - basically soluble elements.
- Atmophile: will partition into gases. (e.g. nitrogen, helium, hydrogen)

Sm-Nd and Rb-Sr isotope systems

- Both systems feature lithophile elements → preferentially partitioned into the mantle and crust during early differentiation.
- Sm-Nd are both refractory elements (not prone to volatile loss) and the ease of accommodation into minerals differ between the two elements. Sm is less incompatible than Nd so Nd tends to be incorporated into melts in crust-mantle segregation. Sm-Nd dating of solar system objects give information as to the timing and extent of differentiation, e.g. on Earth.
- Similar case for Rb-Sr: Rb is more incompatible and goes into the melt; hence rocks from melting the mantle has a lower Sr ratio (this is the reverse of the Sm-Nd system). However, Rb is a fairly volatile element → susceptible to volatile loss, which could be a source of error to the dating method (gives wrong estimate of Rb/Sr at t=0) but could also give a glimpse to volatile loss during planetary formation (e.g. collisions and accretion).
- The way to test this is to know independently the age of the rock (maybe from Pb-Pb?) then backcalculate Rb/Sr and assess the volatile depletion extent.

Hf-W isotope system

- Hf-W system is short-lived and only has 9 Myr half-life. However, notice that Hf is a lithophile, but W is a siderophile, so during core-mantle differentiation, Hf will remain in the mantle, but W will be partitioned into the core. Therefore, if this event is before 5 half-lives, then there would be considerably more W in the BSE than if this event happened after 5 half-lives
- Could be used to date the core formation date of solar system objects, e.g. for Mars dating of shergottite meteorites constrains that it grew to half its current size in just ~2 Myr, establishing its status as a planetary embryo.

8. Core formation is a process that defines the chemical composition of a planet's mantle. Discuss how the elemental abundances and isotopic compositions of terrestrial mantle rocks and meteorites can be used to place constraints on the timing and conditions of core formation on Earth.

The Ni/Co of the bulk Earth is taken to be the same as chondritic meteorites as neither Ni nor Co is particularly volatile and likely to be lost during accretion and impact processes.

Values that match equilibrium between Earth's mantle and core is still relatively low (around 28 GPa - but some studies argue 40).

This is at odds with current pressure of core-mantle boundary (140 GPa).

One theory: 'core-mantle' - equilibrium at base of magma ocean, where metal droplets pooled at the interface between molten silicate rock and solid silicate residue and recorded a chemical signature of equilibrium at this depth, before coagulating together and migrating to the centre of the planet to form the core.

Hf-W system useful for dating metal-silicate segregation. Hf is lithophile and W is siderophile. Trace element partitioning depends on how easily an element can substitute for a major element in a crystal lattice site. This depends on **ionic size and charge: smaller ions are more compatible**.

$$\text{Partition coefficient } p_i = \frac{[i]_{\text{solid (metal)}}}{[i]_{\text{melt (silicate)}}}, \epsilon_i = \frac{\left(\frac{\text{daughter}}{\text{non-radioactive nuclei}}\right)_{\text{sample}} - \left(\frac{\text{daughter}}{\text{non-radioactive nuclei}}\right)_{\text{standard}}}{\left(\frac{\text{daughter}}{\text{non-radioactive nuclei}}\right)_{\text{standard}}} \times 10^4$$

Boundary from short lived radionuclides (SRNs): Rule of thumb, SRNs go completely extinct after 5 half-lives. Hf/W system, $^{182}\text{Hf} \rightarrow ^{182}\text{W}$, $t_{1/2} = 9 \text{ Mya}$. $D_w > 100$, $D_f \sim 0$. Hence:

HYPOTHESIS if core formation < 45 Mya, should see **radiogenic W in Earth's mantle**

$\epsilon^{182}\text{W} = 0$ so negates hypothesis, core formation took longer than 45 Mya.

Results:

Some iron meteorites older than CAIs; hence planetesimals, which had already differentiated, were common in early solar system.

Earth and lunar mantles have similar $^{182}\text{W}/^{184}\text{W}$ ratio; suggests earth and moon equilibrated together much later after the start of the solar system. (what is this bit talking abt lol)

Assumptions:

Isochron: all samples come from same parent material.

Half life of parent isotope is well known and measured.

Initial abundance of parent isotope and daughter isotope at $t=0$

System remains closed (no loss of parent or daughter); no thermal resetting occurred.

9. Evaluate the elemental and isotopic evidence for a chemically and mineralogically heterogeneous mantle on Earth. To what extent can this heterogeneity be linked with geophysical observations?

Isotopic composition of upper mantle and deep mantle are very different. This is because the upper mantle has been depleted in incompatible elements by the formation of continental crust. However, MORB is remarkably uniform globally, while OIBs show variation with location.

TWO-LAYER MANTLE MODEL

Explains the big difference between MORBs and OIB. The two-layer boundary is defined at 660 km with the reaction ringwoodite \rightarrow periclase + bridgmanite. This physical and chemical discontinuity manifests itself in the isotopic differences between these two groups.

UPPER MANTLE: Represented by MORB. Chemically homogeneous. Created by adiabatic decompression melting at shallow depth. Extraction of partial melts to form continental and oceanic crust has depleted the mantle uniformly in incompatible elements (e.g. Rb, Nd, U)

LOWER MANTLE: Represented by OIB. Mix of a common component (PREMA) + special component which varies by location. This variability in special component is attributed to material sampled by plumes at the base of the mantle; the variability is too big for it to arise from differences in degree of partial melting. Reservoirs include HIMU (defined by extremely high Pb anomaly), EMI (high 207Pb/204Pb but low Rb/Sr) and EMII (high 207Pb/204Pb and high Rb/Sr).

Geophysical evidence also shows heterogeneities in density in the lower mantle. At the base lies two LLSVPs, which shape can be deduced using ScS waves which reflect off those structures. Gravitational measurements also result in positive **geoid** anomalies above the theorized locations of LLSVPs. S waves passing through such structures are much slower, representing big piles of high-density material. Theory: primordial remnants of mantle differentiation, or remnants of protoplanet Theia (explains antipodality). ScS waves from other side of Earth can also show vertical structures like mantle plumes

EVIDENCE FOR DISCONTINUITY

Helium-3 primordial, generated during stellar fusion; Helium-4 radiogenic, generated by alpha decay. We can normalize He-3/He-4 ratios in rocks with He-3/He-4 ratio of the atmosphere to get the relative abundances across different rocks. **MORB** show uniformly low ratios (lose primordial He) while **OIB** show a large range (retain primordial He). This shows that the MORB may have been **degassed** during the melting event that created the continental crust.

A paragraph on Rb/Sr and Sm/Nd systems.

Preserved minerals in diamonds. (e.g. The recent discovery of ringwoodite in diamond inclusions from Juina)

Geophysical evidence shows that a big positive change in velocity occurs for both P and S waves at 660 km depth. The discontinuity also results in precursors (faster waves which reflect off the boundary) and triplications. This is thought to be due to differences in chemical phases in upper and lower mantle. Corroborated by chemical experiments involving diamond anvil cells.

EVIDENCE AGAINST 2-LAYER MODEL

Seismic tomography at depth has shown fast anomalies around subducting slabs that extend into the lower mantle. This shows **subducting plates descend into the lower mantle**, and there is some evidence that **mantle plumes may extend to the top of the upper mantle**. This implies that **mass transfer across the boundary** is significant. This corresponds to the otherwise unexplained enrichment of HIMU in 206Pb/204Pb, and EMI/EMII in 207Pb/204Pb. The subducted material may melt and mix into the mantle locally, creating differences in OIB isotopic composition.

Counterarguments...

8. How do the processes of condensation, accretion and differentiation influence the distribution of elements between and within chondrites and the terrestrial planets? How can extinct and long-lived radiogenic isotope dating systems be used to investigate the timescales of these processes? [45 minutes]

CONDENSATION: the **partitioning** of elements from gas into solid phases (e.g. metals, oxides, silicates...) according to their volatility.

Gravitational collapse of nebular gas to form nebular disk; associated with material condensation from gas to solid. Near the Sun, temperatures are higher; only refractory elements are able to condense at this point, therefore the objects near the sun are enriched in refractories.

Condensation order: Platinum group elements -> Ca-Al-Ti oxides (e.g. corundum, perovskite) & silicates -> metallic Fe-Ni -> sulphites -> magnetite -> water & ammonia -> methane... (Think about sequence of planets) Hence, chondrites were the first objects to form, retain primordial compositions with refractory-rich CAIs; terrestrial planets (close to the sun) are enriched in refractories, gas giants are enriched in volatiles. The frost line is the minimum distance from the protostar where temperature is low enough for volatiles (e.g. water) to condense into solid grains. Beyond the frost line: gas & ice giants form. Within it: rocky planets form.

ACCRETION: From dust to planets: the **assembling** of tiny solids into planets

Accretion and coagulation of material -> form undifferentiated meteorites -> form planetesimals -> planets.

Second stage of accretion: **Late Veneer** where primitive material from carbonaceous chondrites were added to bulk silicate Earth after core formed. Evidence: higher amounts of siderophile in the mantle and crust than expected.

DIFFERENTIATION: the **sorting** of homogeneous planet into layers by density / affinity

Heating, from impacts and decay of short-lived isotopes like ^{26}Al , causes melting: denser elements sink into core while silicate forms mantle and crust. Atmosphere may form from gases (volatile) released from liquid silicate magma ocean. Crust may form if planetesimal has long enough to cool between impacts

RADIOGENIC ISOTOPES:

Extinct isotopes can resolve rapid early events (core formation) while long-lived systems show planetary evolution (crust formation, mantle dynamics). Isotope systems that involve **lithophile (Hf)** vs **siderophile (W)** parent / daughter ideal for dating accretion & differentiation; they record timing of **metal-silicate segregation** which reflects **core formation**.

EXTINCT ISOTOPES: Hf/W system.

By assuming the solar system had an equally distributed $^{182}\text{W}/^{184}\text{W}$ distribution and w/ knowledge of the Hf/W decay constant and current abundance of daughter W isotopes, the age of core formation can be determined.

SHORT-LIVED ISOTOPES: Boundary from short lived radionuclides (SRNs): Rule of thumb, SRNs go completely extinct after 5 half-lives. Hf/W system, $^{182}\text{Hf} \rightarrow ^{182}\text{W}$, $t_{1/2} = 9 \text{ Mya}$. $D_w > 100$, $D_f \sim 0$. Hence:

Hypothesis: if core formation < 45 Mya, should see **radiogenic W in Earth's mantle**

$\epsilon^{182}\text{W} = 0$ so negates hypothesis, core formation took longer than 45 Mya. In addition, the figure shows that the extent of differentiation can be estimated from age of core formation as well as the delta Hf/W found in terrestrial and core PB samples.

Can also test **Late Veneer**: as late veneer material has different $^{182}\text{W}/^{184}\text{W}$ ratio to BSE and proportionally more material was added to Earth than the Moon, the BSE and Moon have different ratios. Testing shows the moon has an ^{182}W excess of 27 ppm over BSE, consistent with theory.

LONG-LIVED ISOTOPES: study events that happen for a long time, like the formation of crust and depletion of upper mantle, e.g. Rb/Sr system, relies on Rb being lithophile and Sr being siderophile.

Rb partitions strongly into melts, depleted in upper mantle. In MORB samples $^{87}\text{Sr}/^{86}\text{Sr} < \text{BSE}$ and in crust > BSE. In OIB, $^{87}\text{Sr}/^{86}\text{Sr} \sim \text{BSE}$. Hence upper mantle depleted because of crust, lower mantle not depleted.

STABLE ISOTOPES: Equilibrium stable isotope partitioning learn about Earth's core.

It has been shown from seismic data that the core is not completely Fe/Ni; there are some light elements like Si. Lighter isotopes tend to concentrate in weaker bonding environments with lower oxidation state (the core) Light Si partitions into the core, leaving mantle with heavy Si (relative to chondritic concentrations)

9. Discuss the radiogenic isotope and trace element evidence for a compositionally heterogeneous mantle. What is the radiogenic isotope evidence for: (i) early extraction of the continental crust from the mantle; and (ii) the tectonic recycling of surface material into the mantle? [45 minutes]

i) Proof can be derived from MORB magmas

- More radiogenic Nd isotopes than CHUR (high Sm/Nd \rightarrow compatible vs incompatible)
- Less radiogenic Sr isotopes than CHUR (high Sr/Rb \rightarrow higher compatible vs incompatible)

MORB derived from reservoir that had experienced melt extraction; consistent with trace element evidence for extraction of continental crust from primitive mantle to form depleted mantle. (MORB source)

ii) U, Th are highly incompatible relative to Pb.

Crust: high U/Pb and Th/Pb relative to mantle. Radiogenic Pb isotope signatures ($^{206}\text{Pb} / ^{204}\text{Pb}$) thus high.

Recycled slab material incorporating oceanic crust introduces high U/Pb Th/Pb material into the mantle. These create enriched mantle sources of varying radiogenicity. Lower continental crust (EMI)/ lithospheric mantle has lower $^{206}\text{Pb}/^{204}\text{Pb}$ and $^{207}\text{Pb}/^{204}\text{Pb}$ than upper continental crust (EMII)

HIMU reservoir high U/Pb mantle: very high $^{206}\text{Pb}/^{204}\text{Pb}$ means high U/Pb and took a long time to decay (>1 Ga - ^{238}U Decay) but low Rb/Sr \rightarrow ancient oceanic crust recycled into deep mantle.

However, BSE estimates of U differ by up to a factor of 2 between different papers. This is because they are based on different chondrites.

2022

8. Give a brief account of the early history of the solar system. To what extent have the chemistry, mineralogy and textures of meteorites helped in the process of reconstructing the subsequent evolution of the Earth? [45 minutes]

9. (a) Discuss the application of radiogenic and stable isotopes to understanding the early solar system, including condensation, accretion, volatile depletion and planetary differentiation. [30 minutes]

$$\text{Partition coefficient } p_i = \frac{[i]_{\text{solid (metal)}}}{[i]_{\text{melt (silicate)}}}, \epsilon_i = \frac{\left(\frac{\text{daughter}}{\text{non-radioactive nuclei}}\right)_{\text{sample}} - \left(\frac{\text{daughter}}{\text{non-radioactive nuclei}}\right)_{\text{standard}}}{\left(\frac{\text{daughter}}{\text{non-radioactive nuclei}}\right)_{\text{standard}}}$$

STABLE ISOTOPES

Spectroscopy of the sun and carbonaceous Cl chondrites are assumed to represent the bulk solar composition of elements, which reveals the bulk composition of the solar system.

Knowledge of bulk composition has allowed the creation of models which can predict the order of element condensation as a function of temperature and radial distance.

This can be used to determine how element condensation varied across the early solar system.

The $^{26}\text{Al}/^{26}\text{Mg}$ radiogenic isotope system can reveal how early core formation occurred on planetary bodies (PBs). Since, the earlier it formed, the more ^{26}Al would have been present so the more ^{26}Mg daughter isotopes will be left behind.

However, a larger PB would have had a higher amount of ^{26}Al so the influence of PB size must be considered.

For Mars, its core formation was estimated as <2 Myrs after CAIs (time zero) but accretion simulations predict that at this age, Mars should be a more massive PB.

This could suggest a lack of accretionary material at this radius in the Early solar system- and this kind of simulation could be expanded to estimate relative amounts of accretionary material across the early solar system.

$^{87}\text{Rb}/^{87}\text{Sr}$ radiogenic isotope system can be used to determine the timing of volatile depletion on meteorite PBs.

Rb and Sr are lithophile elements but Rb is more volatile. If age is known, Rb/Sr at time can be calculated and compared with independently determined solar nebula Rb/Sr.

This can reveal whether meteorite PB was formed in volatile-rich (high Rb/Sr) or volatile-depleted (low Rb/Sr) regions of the solar nebula. So whether the PB was formed from volatile-rich precursors which later became depleted or PB was formed with already volatile-poor materials.

This can then be expanded to determine how volatile abundance varies across different areas of the early solar system.

The behaviour of stable isotope Fe can reveal the oxygen fugacity of the area of the early solar system where a PB formed.

In reduced conditions, most iron exists in the metal Fe form in the core= large core/ small mantle PB.

In oxidised conditions, most iron exists as oxide minerals (FeO) in the mantle= small core/large mantle PB.

The figure shows a heliocentric gradient in the Fe contents of the inner solar system could be reflecting how they were formed. Inner solar system is more reduced compared to outer solar system material.

The delta Hf/W of samples can be used to determine the timing and extent of differentiation in a PB.

Hf is lithophile and W is siderophile, and both elements are refractory so that variation in Hf/W in planetary bodies is likely due to metal-silicate segregation- thus core formation.

By assuming the solar system had an equally distributed $^{182}\text{W}/^{184}\text{W}$ distribution and with knowledge of the Hf/W decay constant and current abundance of daughter W isotopes, the age of core formation can be determined.

Boundary from short lived radionuclides (SRNs): Rule of thumb, SRNs go completely extinct after 5 half-lives. Hf/W system, $^{182}\text{Hf} \rightarrow ^{182}\text{W}$, $t_{1/2} = 9 \text{ Mya}$. $D_w > 100$, $D_f \sim 0$. Hence:

HYPOTHESIS if core formation $< 45 \text{ Mya}$, should see **radiogenic W in Earth's mantle**

$\epsilon^{182}\text{W} = 0$ so negates hypothesis, core formation took longer than 45 Mya.

In addition, the figure shows that the extent of differentiation can be estimated from age of core formation as well as the delta Hf/W found in terrestrial and core PB samples.

If delta Hf/W of a PB is similar to that of the original solar nebula, then no differentiation is assumed to have occurred.

(b) How can radiogenic isotopes be used to place precise constraints on the timing of events close to the beginning of the solar system? [15 minutes]

Need to look at **absolute ages** instead of relative ages, define solar system $t = 0$: date **Calcium-Aluminium inclusions** (An, Fo, spinel) in chondrules as they are the first compounds in the condensation sequence.

Get $t = 0$ by dating CAI with Pb-Pb system:

The isotope system must be short-lived/ extinct to enable a high resolution of events close to the start of the solar system. In most cases, both elements must be refractory or of similar volatility in order to prevent the influence of volatility on parent/daughter ratios.

Depending on the event which is measuring the isotope system must have further specific properties:
To date core formation, one isotope must be siderophile and the other lithophile.

To date core differentiation, one isotope must be siderophile and the other chalcophile.

To date volatile depletion, the isotopes must have varying volatility.

To specify the timings further, the Pb-Pb isotope system may be used to determine the absolute age of the event relative to the time zero measured from CAIs.

$$207\text{Pb} = 207\text{Pb}_0 + 235\text{U}(e^{\lambda t} - 1)$$

2023

1. (a) What is the evidence for an episode of late accretion having occurred onto the terrestrial planets? [30 minutes]
- (b) What are the potential causes for the differential signal of late accreted material seen in the basalts of Mars, Earth, and the Moon? [15 minutes]

2024

1. (a) Describe the petrology of the main groups of Martian meteorites, giving the ages of each group. [10 min]
- (b) What lines of evidence point to the origins of these meteorites from: (i) a differentiated planet; and (ii) Mars? [10 min]
- (c) Discuss how the short- and long-lived isotope systematics, and trace element compositions, of Martian meteorites can be used to place constraints on the volatile budgets and accretion history of Mars. [25 min]

5. (a) How can multi-element diagrams normalised to primitive mantle be used to constrain the relative compatibility of different elements in typical mantle minerals (olivine, clinopyroxene, orthopyroxene, spinel, plagioclase, garnet)? [15 minutes]

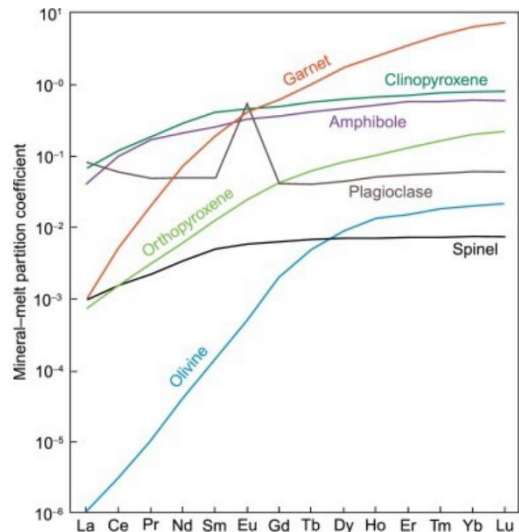
Abundances of elements in minerals are useful in deducing the geologic history of the mineral: can be determined by ICP-MS to produce a diagram of concentration against atomic number. However, this will produce a saw-toothed pattern which is not caused by chemical partitioning but by the basal abundance of nuclei from nucleosynthesis. Therefore to remove this ‘background noise’ to look at the changes in abundance caused by partitioning, we can normalize this diagram by dividing concentrations of all elements by their concentrations in certain reservoirs.

Primitive mantle is often chosen for this task, as it is undifferentiated, so it would represent the concentration of all elements before any partitioning processes happen. With this done, we can draw diagrams, but its form depends on the mineral. Minerals which form from silicate melts are enriched in incompatible elements compared to primitive mantle.

REE become progressively more compatible in silicate minerals with decreasing ionic radius

However there are specific anomalies. For example, plagioclase preferentially incorporates Eu³⁺ due to its similarity in ionic radius with Ca²⁺; this shows up as a positive anomaly in the normalized multi-element diagram. Therefore, if a rock is depleted in Eu³⁺, we can deduce fractional crystallization and removal of plagioclase must have occurred.

Similarly, Garnet has a relatively tight structure, so it is relatively enriched in heavy REEs. Therefore if a rock has positive HREE anomalies, we know that it probably contains a lot of garnet and it didn’t undergo much partial melting.



(b) Using appropriate figures to illustrate your answer, explain how differences in the compatibility of samarium, neodymium, rubidium, and strontium may be reflected in the neodymium and strontium isotope compositions of mid-ocean ridge basalts, the continental crust, and ocean island basalts. [30 minutes]

The compatibility of elements can be predicted using Goldschmidt's laws; they predict element partitioning behaviour based on the ability for an ion to substitute into a particular lattice site. This manifests in 3 ways: 1. The ionic size difference between elements should not be $>15\%$ 2. Ions with smaller size are always preferentially incorporated in lattices 3. Ions with same size but higher charge will be incorporated.

We can apply these principles to Sm/Nd and Rb/Sr. We predict that Sm (element no 62) is more compatible than Nd (60) and Rb (37) more incompatible than Sr (38). Therefore there is a difference in partitioning behaviour: Rb and Nd are lithophiles while Sr and Sm are siderophile (relatively). This means that in a liquid-solid interface, Rb and Nd will partition into the liquid, while Sr and Sm go into the solid. This has been confirmed by experimental studies. From this we may use relative element abundances to deduce the formation processes of the MORB, OIB and crust.

Doing analysis on radiogenic elements reveals MORB to be depleted in Rb & Nd and crust enriched in Rb & Nd compared to OIB.

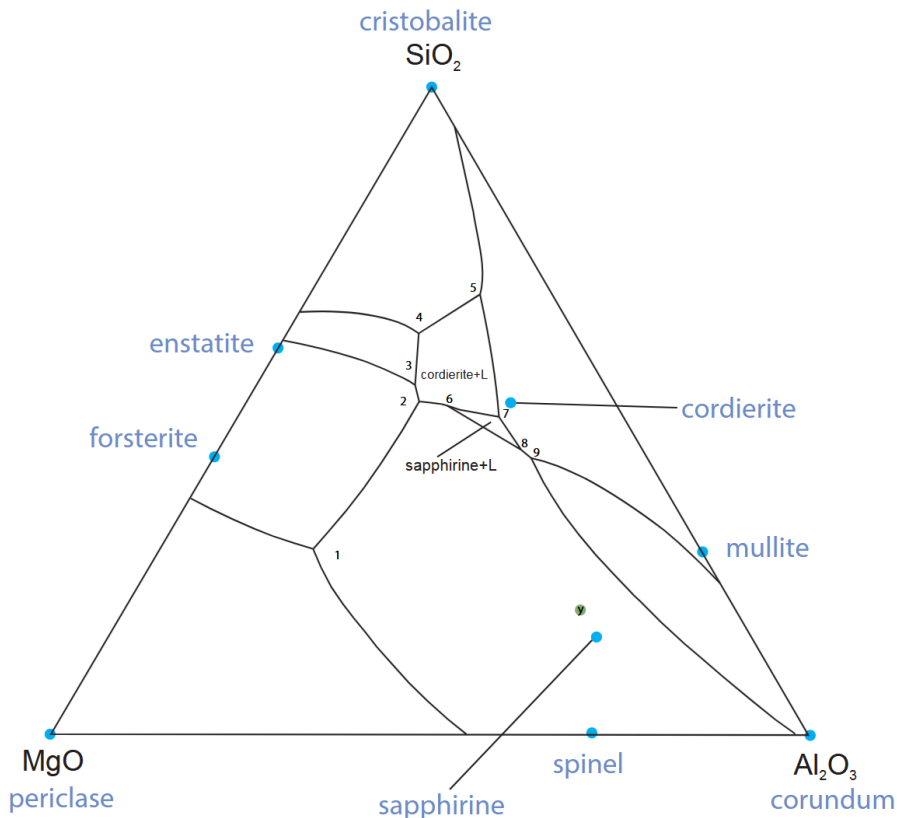
OIB in particular seems to be from a few reservoirs.

Igneous Petrology

Phase Diagrams

2018 (Paper 1)

10. You are provided with a liquidus ternary projection of the system cristobalite, periclase and corundum Fig 2. The dots indicate the location of solid phases. You should detach Fig 2 and include it as part of your answer.



i) Complete the diagram by labelling the liquidus fields (Note the cordierite + L and sapphirine + L fields have been completed for you).

ii) Draw in all stable sub-solidus tie-lines.

For example, spinel + L and forsterite + L are neighbours to each other. Then, we can draw the tie-line between spinel and forsterite. The end result should be all triangles, no quadrilaterals allowed.

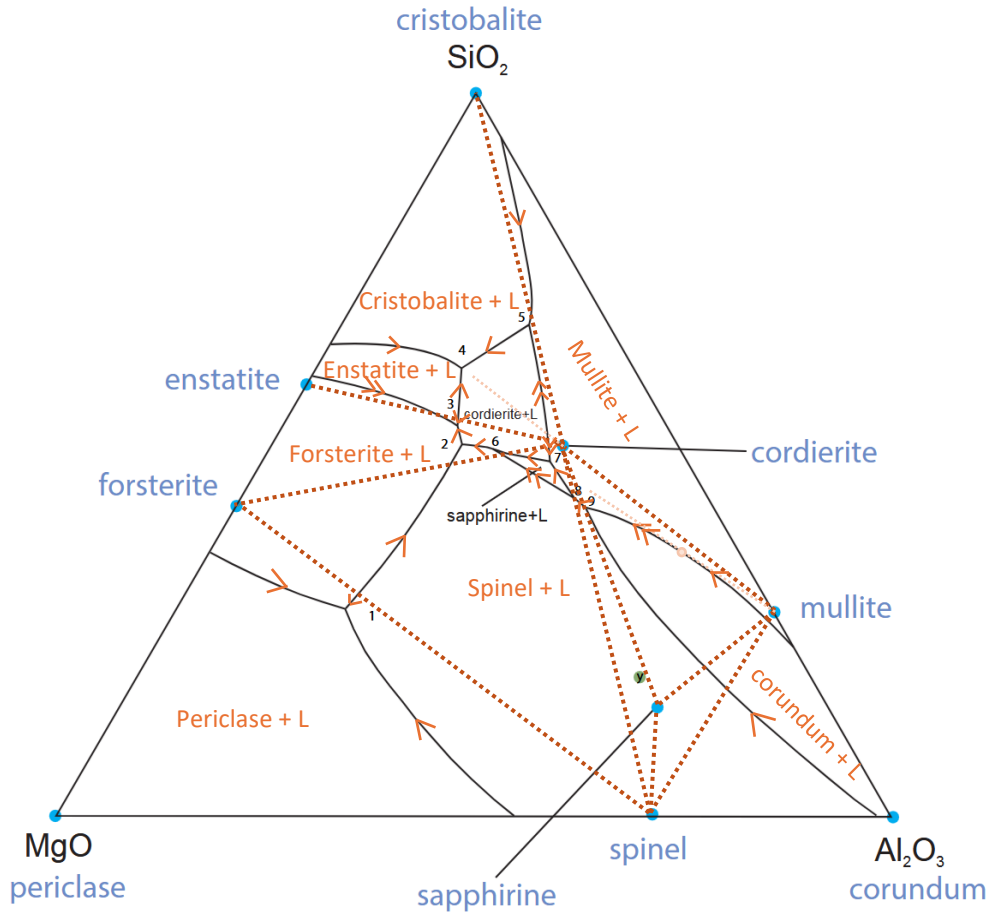
iii) Show with arrows the down-temperature directions on the divariant reaction boundaries. Use double arrows to denote resorptional boundaries.

If two adjacent fields are A+L and B+L, check how the cotectic lines are back projected onto the A-B solid solution line. Down temperature arrows always point away from AB line. If the back tangent doesn't lie on AB line, then it is resorptional.

iv) Write schematic reactions for each of the ternary points labelled 1-9 on the diagram.

- 1: L \rightarrow Periclase + Spinel + Forsterite
- 2: Spinel + L \rightarrow Cordierite + Forsterite
- 3: L \rightarrow Cordierite + Forsterite + Enstatite
- 4: L \rightarrow Enstatite + Cristobalite + Cordierite
- 5: Mullite + L \rightarrow Cristobalite + Cordierite

- 6: Sapphirine + L \rightarrow Cordierite + Spinel
- 7: Mullite + L \rightarrow Sapphirine + Cordierite
- 8: Mullite + Spinel + L \rightarrow Sapphirine
- 9: Corundum + L \rightarrow Spinel + Mullite



v) Describe composition y as a function of its subsolidus mineralogy.

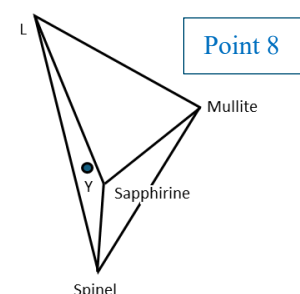
y is in the cordierite-sapphirine-spinel subsolidus triangle, so by lever rule we deduce that it is about 70% sapphirine, 18% cordierite, and 12% spinel.

vi) Discuss the equilibrium crystallisation of composition y . You need only be quantitative where necessary to justify the liquid evolution pathway.

Start by noticing that y is in the spinel + sapphirine + cordierite triangle, so naturally it will end up as the sum of the three, and we notice that the corresponding univariant point is at 6 (notice where the three stability fields touch?).

In the following, I will use **orange** to denote the evolution of liquid composition.

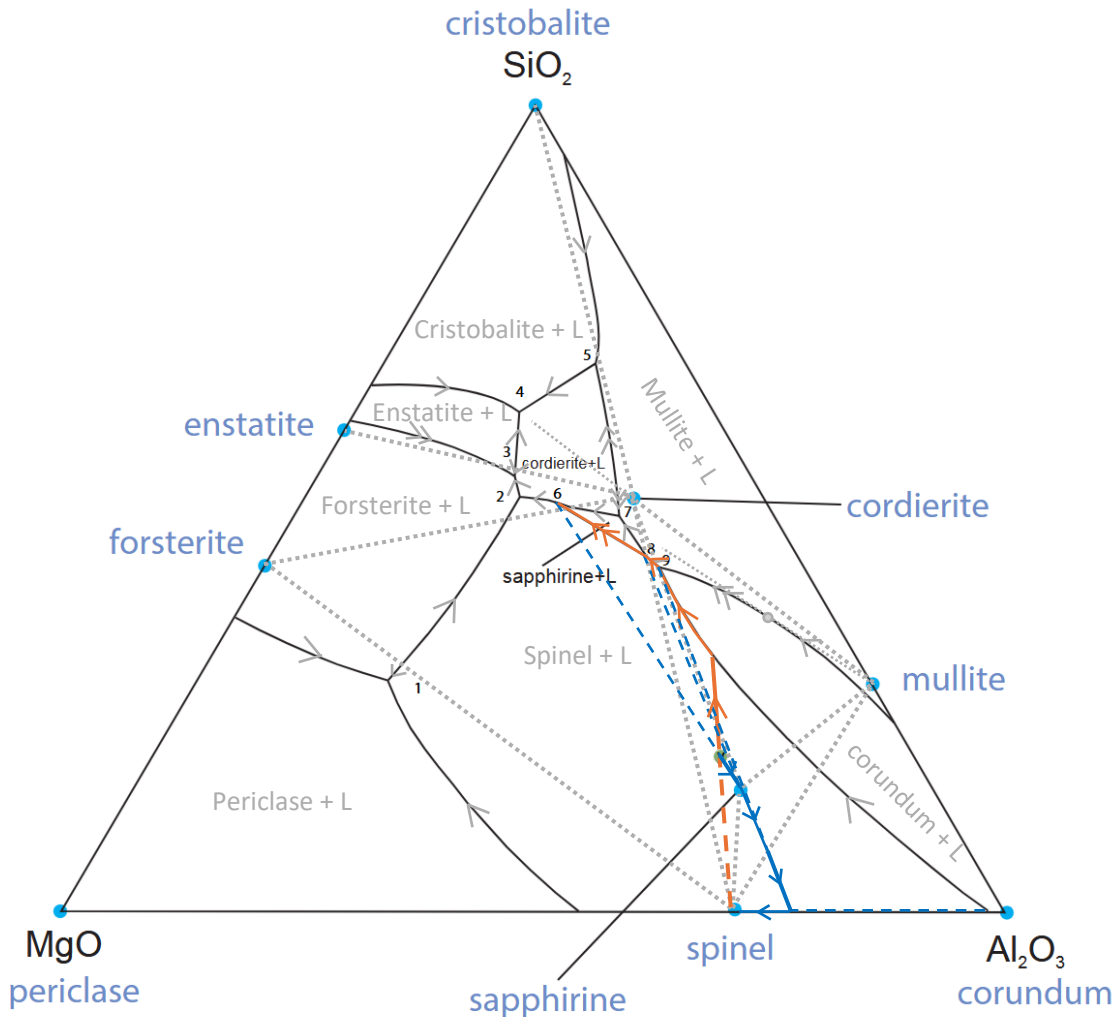
- As y is in the spinel + L stability field, the first to crystallise is spinel. It goes until it intersects the divariant reaction line between spinel and corundum.
- After that, it goes down this reaction line, where $L \rightarrow \text{corundum} + \text{spinel}$. Both corundum and spinel are crystallised, until it reaches point 9.
- At point 9 (univariant reaction), we have $\text{corundum} + L \rightarrow \text{spinel} + \text{mullite}$. We draw the triangles Corundum-spinel-mullite and L-spinel-mullite and find that y lies in the L-spinel-mullite triangle, this means that in the reaction that corundum is consumed first.
- Then continues to go from 9 to 8, where $L \rightarrow \text{mullite} + \text{spinel}$. At 8, we have $\text{mullite} + \text{spinel} + L \rightarrow \text{sapphirine}$. To determine which one goes out first, I would look at this triangle. See that y lies in the L-sapphirine-spinel triangle, so I will believe that Mullite is exhausted first.
- Therefore, with $L + \text{sapphirine} + \text{spinel}$ remaining, the reaction goes along the lower path (instead of the 8 \rightarrow 7 path). This cotectic is resorptional, so we have $\text{spinel} + L \rightarrow \text{sapphirine}$.
- At point 6, we have the final reaction $\text{sapphirine} + L \rightarrow \text{cordierite} + \text{spinel}$. Here L will be all used up and finally the composition is spinel + sapphirine + cordierite in the ratio mentioned in (v).



vii) Discuss the fractional melting of composition y. Your answer does not need to be quantitative.

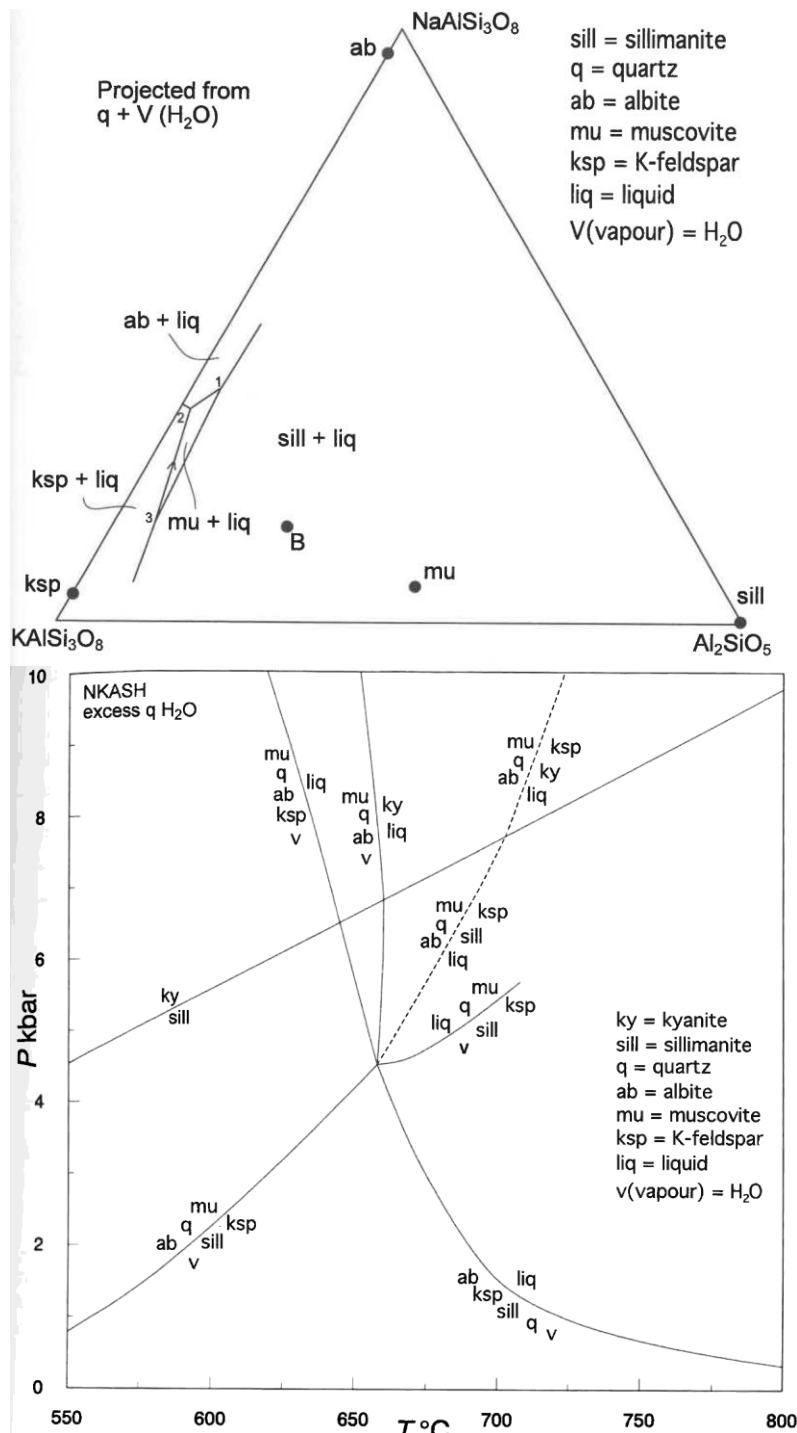
I will use **blue** to denote the evolving (remaining) solid composition.

- Note that melting starts with liquid composition at invariant point 6, and we have sapphirine + spinel + cordierite \rightarrow L. The L is continuously removed. So, the remaining solid composition moves away from point 6, until it reaches into another subsolidus triangle, where now it is mullite + sapphirine + spinel.
- Thus, the melt produced is now of composition 8, and here we have sapphirine \rightarrow mullite + spinel + L, and now we have the composition moving away from 8, until it goes into the spinel + mullite + corundum triangle, and now we have the reaction at point 9: mullite + spinel \rightarrow corundum + L.
- Finally, the solid composition moves on the corundum-spinel line, so now it is just a binary solid solution of these two components. The temperature will increase until it reaches the eutectic point, and then the solid composition is removed of this eutectic melt until it reaches spinel. Spinel is the final crystal to be melted, and we have to wait until the temperature reaches the pure spinel melting point.



2019 (Paper 1)

10. You are provided with a ternary liquidus projection from quartz and H_2O onto the plane $Al_2SiO_5—NaAlSi_3O_8—KAlSi_3O_8$ showing phases sillimanite (sill), K-feldspar (ksp) and albite (ab). Additionally, Figure 4 is a PT projection of the relevant univariant reactions in the system $K_2O—Na_2O—Al_2O_3—SiO_2—H_2O$. The dashed line in the PT diagram is the H_2O -absent reaction and only occurs under H_2O -undersaturated conditions.



- Draw in all stable sub-solidus tie-lines.
- Show with arrows the down-temperature directions on the divariant reaction boundaries. Use double arrows to denote any possible resorptional boundaries.
- Write schematic reactions for each of the ternary points labeled 1-3 on the diagram, explaining how you determined them.

- iv. If ternary point 2 occurs at 655°C, estimate the temperatures of points 1 and 3, and determine the pressure for which the diagram is drawn.
- v. Draw a sketch ternary liquidus diagram for a pressure of 3 kbar. Give your reasons for the topology you show.
- vi. What liquid composition would be expected for initial melting of (a) a mu-ksp-q-sill petite and (b) a ksp-ab-mu-q granite?
- vii. Describe as completely as you can the equilibrium crystallisation of bulk composition B.
- viii. Allowing for the presence of quartz, equilibrium melting of B reaches nearly 50% melt fraction at the point where ksp melts out completely. What is the melt composition at this point? What might the geological significance be of exceeding the so-called critical melt fraction of 40%?
- ix. if, on first melting of a petite at 6 kbar, all H₂O is removed into the liquid, describe what you expect to happen as temperature continues to rise.
- x. Compare and contrast water-saturated and water-undersaturated melting, at pressures around 6 kbar, providing an example of each kind of melting from nature.

2020 (Paper 1)

1. Figure 1 shows a ternary liquidus projection with subsolidus phase compositions shown as dots with labels. The projection is in the system K₂O-Na₂O-Al₂O₃-SiO₂-H₂O under the assumption that a pure H₂O fluid phase and quartz are present. Paragonite is a sodic mica that can accommodate some K in its structure. A rock composition, labelled 'a', is shown as a 4-pointed star.

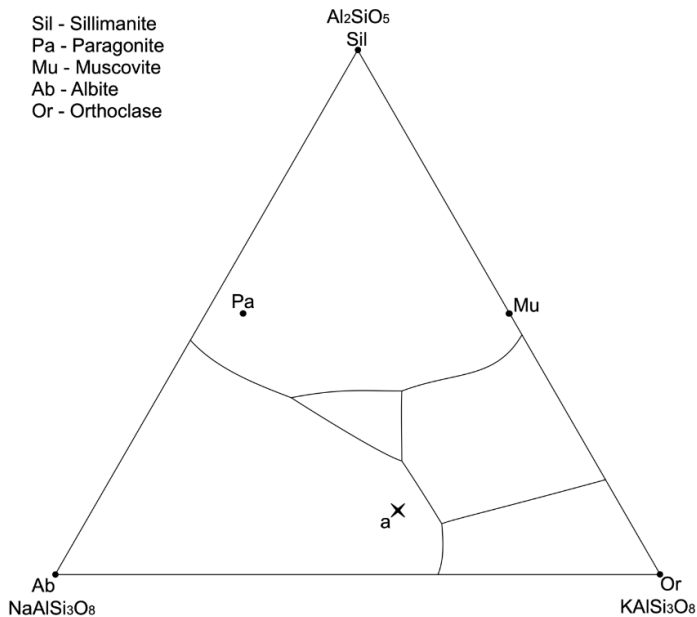


Figure 1. Ternary liquidus projection in the system K₂O-Na₂O-Al₂O₃-SiO₂-H₂O

(i) Label the liquidus fields on Figure 1. (HINT: Sil, Ab and Or undergo congruent melting and Mu is a liquidus phase in the Al₂SiO₅-KAlSi₃O₈ binary subsystem). [2 minutes]

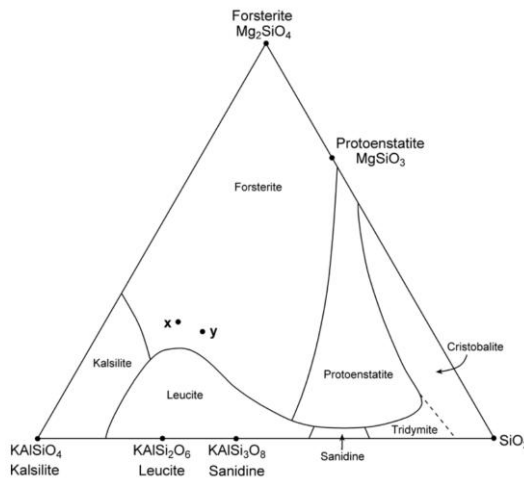
(ii) Draw the Alkemade lines that join the stable sub-solidus assemblages on Figure 1. [3 minutes]

(v) Describe the evolution in liquid and solid compositions during the equilibrium (batch) melting of bulk composition 'a'. Sketch the liquid and solid compositions on a copy of the ternary diagram and provide quantitative estimates of the phase proportions at each point that the melting reaction changes.

[10 minutes]

2021 (Paper 1)

8. (a) You are provided with a slightly modified version of the liquidus phase diagram for the system forsterite (Mg_2SiO_4) – kalsilite ($KAlSiO_4$) – silica (SiO_2) at atmospheric pressure (Fig.1).

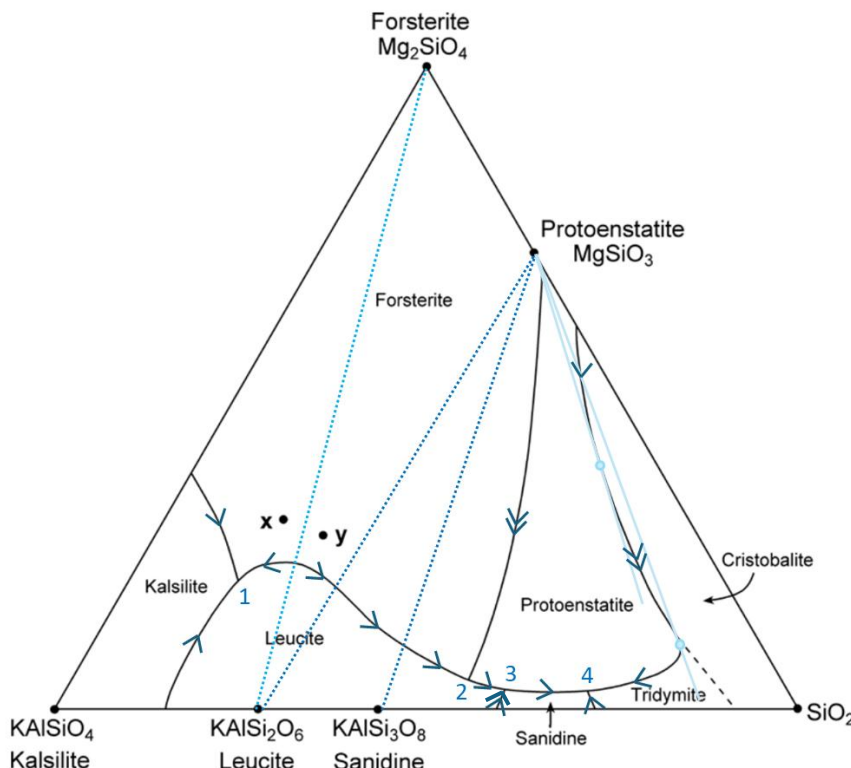


(i) Insert all stable two-phase tie lines (Alkemade lines) and put down-temperature arrows on the univariant boundaries (using single arrowheads for co-precipitational boundaries, and double arrowheads for resorptional boundaries). Locate any thermal divides that might be present.

(ii) Which of the Alkemade lines divides the ternary into silica-saturated and silica-undersaturated compositions? [The forsterite-leucite line](#)

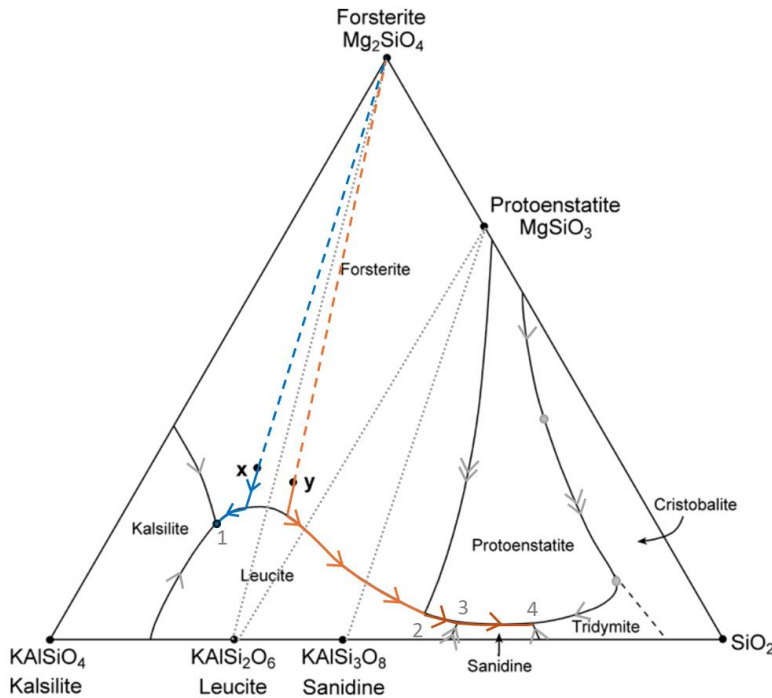
(iii) Write schematic reactions to describe each of the invariant points on the diagram. [10 minutes]

- 1: $L \rightarrow Kalsilite + Forsterite + Leucite$
- 2: $L + Forsterite \rightarrow Protoenstatite + Leucite$
- 3: $L + Leucite \rightarrow Protoenstatite + Sanidine$
- 4: $L \rightarrow Tridymite + Protoenstatite + Sanidine$

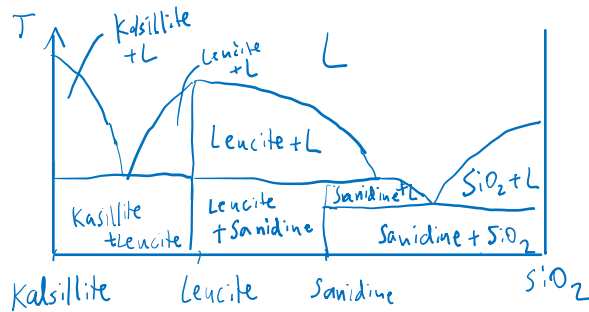


(b) Potassic lavas with bulk compositions that can be approximated by this system occur in the Leucite Hills of Wyoming. Describe the crystallisation sequences of the lavas with (simplified) bulk compositions marked on the phase diagram (labelled x and y) under: (a) equilibrium conditions, and (b) conditions of fractional crystallisation. [5 minutes]

	Equilibrium crystallisation	Fractional crystallisation
x	Path $L \rightarrow$ Forsterite $L \rightarrow$ Forsterite + Leucite $L \rightarrow$ Forsterite + Leucite + Kalsilite	Same
y	Path $L \rightarrow$ Forsterite $L \rightarrow$ Forsterite + Leucite $L +$ Forsterite \rightarrow Leucite + Protoenstatite	Path $L \rightarrow$ Forsterite $L \rightarrow$ Forsterite + Leucite $L \rightarrow$ Protoenstatite + Leucite $L \rightarrow$ Protoenstatite + Sanidine $L \rightarrow$ Protoenstatite + Sanidine + Tridymite

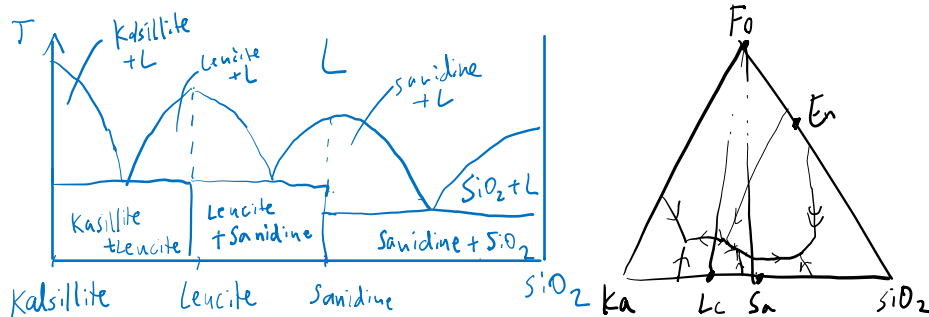


(c) (i) Sketch a possible binary phase diagram for the join kalsilite ($KAlSiO_4$) – silica (SiO_2).



(ii) At pressures above a few kilobars, sanidine ($KAlSi_3O_8$) melts congruently. How will the topology of the kalsilite – silica binary phase diagram change with increasing pressure? Comment on the significance of a line drawn between forsterite (Mg_2SiO_4) and sanidine ($KAlSi_3O_8$) in the forsterite – kalsilite – silica ternary system in relation to the evolution of silica-saturated and silica-undersaturated rocks. [15 minutes]

As pressure increases the peritectic point between Leucite and Sanidine shifts to the left (towards Kalsilite) until it becomes an entirely eutectic point.



In this case, then the Forsterite-Sanidine becomes an effective thermal divide. The rocks will evolve in two directions depending on which side of the thermal divide they are in and produce alkaline rocks or silica rich rocks, just like the divide between alkali basalts and tholeiites.

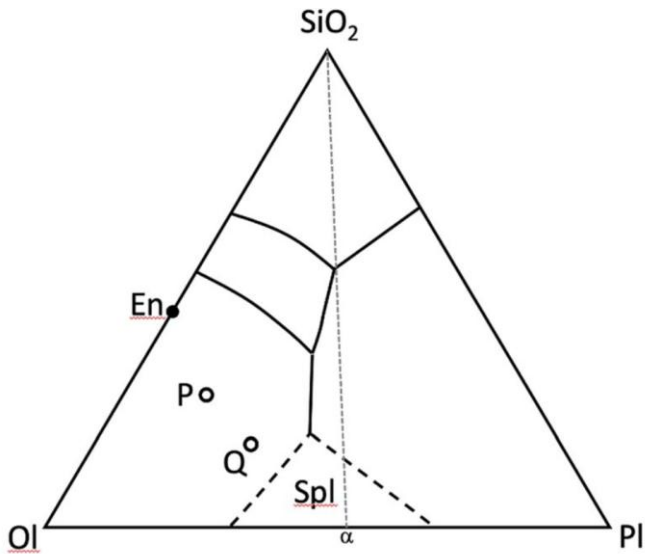
(d) (i) What composition melts would be produced by melting mantle containing a small amount of a K-bearing phase at low pressure?

K₂O is also quite incompatible, so it will be preferentially partitioned into the melt, so the melt have quite a high K content. From the diagram, the invariant point is located near the K-rich vertex. As the rock is likely a forsterite-rich rock, it is likely that Fo is the first phase to enter the melt.

(ii) Given that leucite is not stable at high pressures (reacting to a mixture of kalsilite and sanidine), what can you deduce about the topology of the ternary diagram at high pressures from the compositions of the potassiac lavas of the Leucite Hills? [15 minutes]

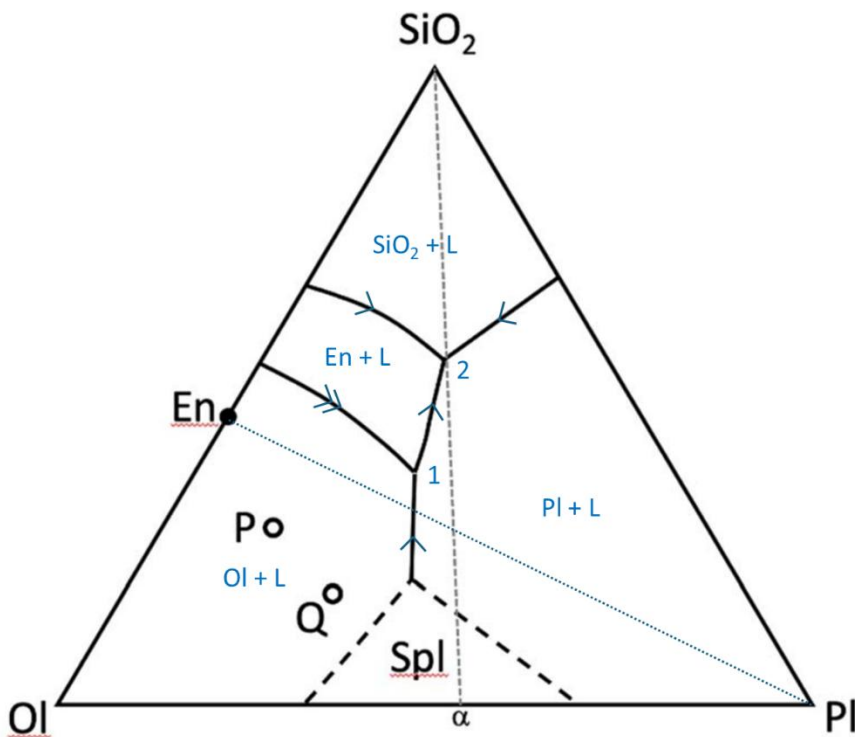
- Leucite Hills lavas probably contain leucite so probably not a high pressure
- Potassiac lavas → invariant points close to the K vertex as pressure increases
- At high pressures Lc will not be a stable phase, and so the Lc + L field will probably disappear, and Ka + L and Sa + L fields will expand as a result.

2022 (Paper 1)



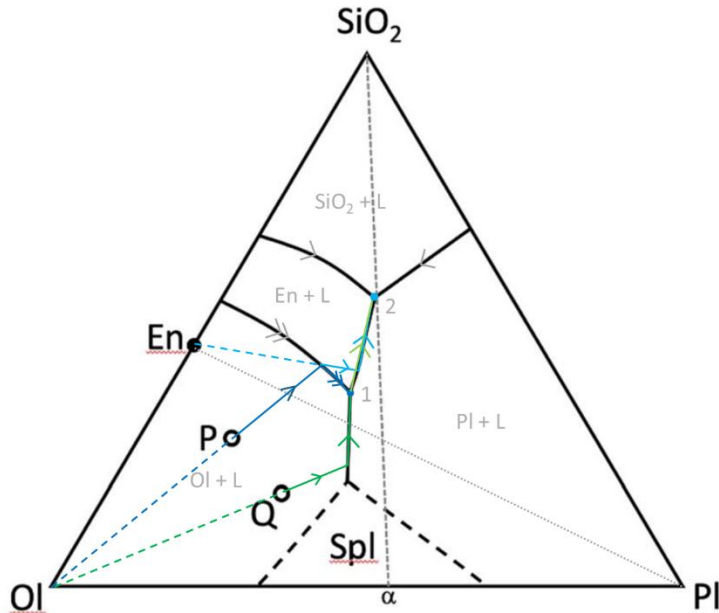
5. The ternary phase diagram provided separately is a liquidus projection from the system $\text{SiO}_2\text{-Ol-Pl}$ at lunar pressures. Volatiles are present but are omitted from the diagram. Abbreviations are SiO_2 - silica, Ol - olivine (MgSiO_4), En - Enstatite ($\text{Mg}_2\text{Si}_2\text{O}_6$), Spl - Spinel (MgAl_2O_4 – projected into the plane of the diagram) and Pl - Plagioclase solid solution containing K-feldspar (KAlSi_3O_8) and anorthite ($\text{CaAl}_2\text{Si}_2\text{O}_8$) endmembers. The stable sub-solidus phase compositions are shown as a filled black dot. Bulk compositions of two lunar parent melts, P and Q, are indicated with open dots, α is the composition of an immiscible melt phase.

- (a) Add all sub-solidus tie lines (Alkemade lines) and down-temperature arrows, distinguishing cotectic from resorptional boundaries and marking the locations of any thermal divides. [5 minutes]
- (b) Write down schematic reactions for the invariant points on the diagram. [5 minutes]

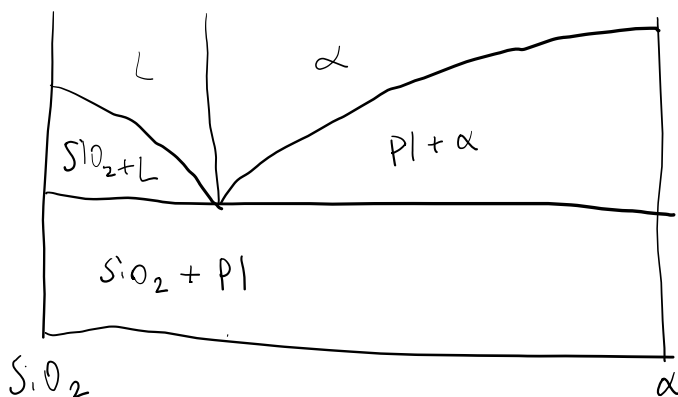


(c) Describe quantitatively the liquid compositions during both fractional and equilibrium crystallisation of bulk compositions P and Q. [15 minutes]

	Equilibrium crystallisation	Fractional crystallisation
P	Path $L \rightarrow Ol$ First phase to be crystallised is Ol, liquid decreases concentration in Ol. $L + Ol \rightarrow En$ Resorptional cotectic, En is crystallised out from the liquid. $Ol + L \rightarrow En + Pl$ Remainder of liquid is crystallised and used up first. Final composition is 60% En, 20% Ol, 20% Pl	Path $L \rightarrow Ol$ First phase to be crystallised is Ol, liquid decreases concentration in Ol. $L \rightarrow En$ Once liquid reaches the resorptional boundary between En and Ol, no more olivine (crossed the thermal divide) and so starts to crystallise En. $L \rightarrow Pl + En$ Finally, $L \rightarrow SiO_2 + En + Pl$ in eutectic proportions
Q	Path $L \rightarrow Ol$ First phase to be crystallised is Ol, until hits the Pl-Ol cotectic $L \rightarrow Pl + Ol$ Pl and Ol are crystallised from the liquid. $Ol + L \rightarrow En + Pl$ Remainder of liquid is crystallised and used up first. Final composition is 40% En, 30% Ol, 30% Pl	Path $L \rightarrow Ol$ First phase to be crystallised is Ol, until hits the Pl-Ol cotectic $L \rightarrow Pl + Ol$ Pl and Ol are crystallised from the liquid. Cannot react at the peritectic as no Ol, so continue with $L \rightarrow En + Pl$ Finally, $L \rightarrow SiO_2 + En + Pl$ in eutectic proportions



(d) Sketch a binary phase diagram for the α -SiO₂ join. [5 minutes]



(e) At the eutectic, the residual melt separates into two immiscible liquids; a volatile-rich, silica phase and an olivine-plagioclase melt, α . Calculate the proportions of these two immiscible liquids and describe the equilibrium crystallisation of the resulting olivine-plagioclase mixture. [10 minutes]

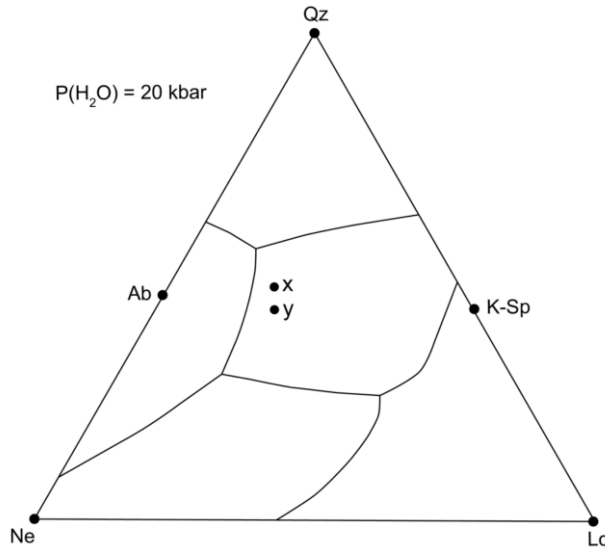
I assume we're talking about the invariant point 2 here, so by lever rule the $\text{SiO}_2 : \alpha$ ratio is about 56% : 44%. The equilibrium crystallisation of the mixture will be a binary system. If we assume no complete solid solution, then as temperature decreases, we first get Pl crystallised. Then at the eutectic temperature, we have $L \rightarrow \text{Pl} + \text{Ol}$ which gives the solid as the intergrowth of plagioclase and olivine.

(f) Consider the slow crystallisation of composition Q in a lunar magma chamber, including the separation of the eutectic melt into two immiscible fractions, and sketch the textures in thin section that you might expect to arise in lunar rocks. [5 minutes]

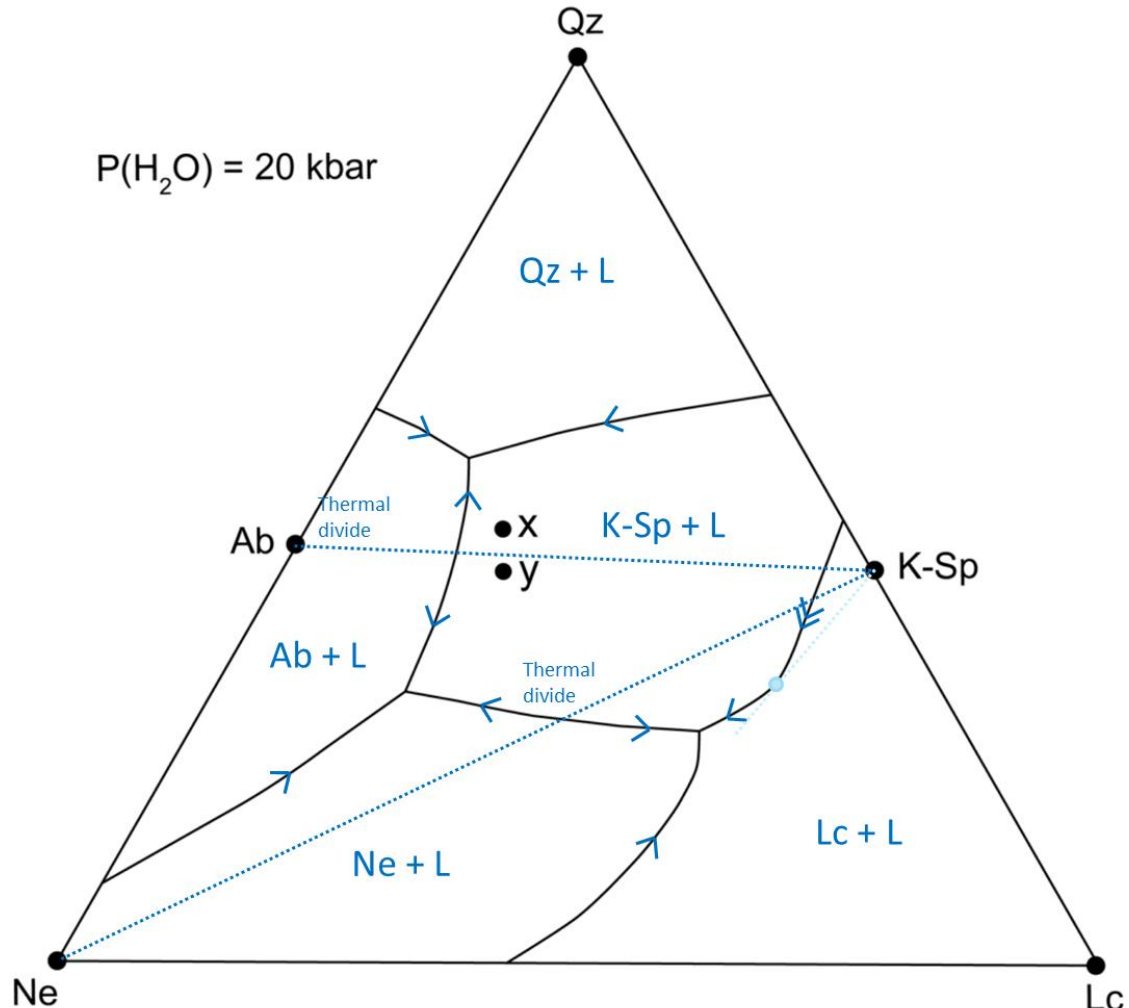
Slow crystallisation in chamber (I would assume it is crystal fractionation), then as the melt evolves it will result finally in two melt sections, one is quartz and the other is a Ol-Pl intergrowths. Since it is slow crystallisation, I would draw **large grains** that are in equilibrium (and **euhedral**), and **separate regions** where Ol-Pl are growing together, and regions where it is full of quartz. No zoning because we have time to allow for diffusion.

2023

4. You are provided with a ternary phase diagram involving the phases quartz (Qz), albite (Ab), orthoclase (K-Sp), nepheline (Ne) and leucite (Lc) for a pressure of 20 kbar under water-saturated conditions.

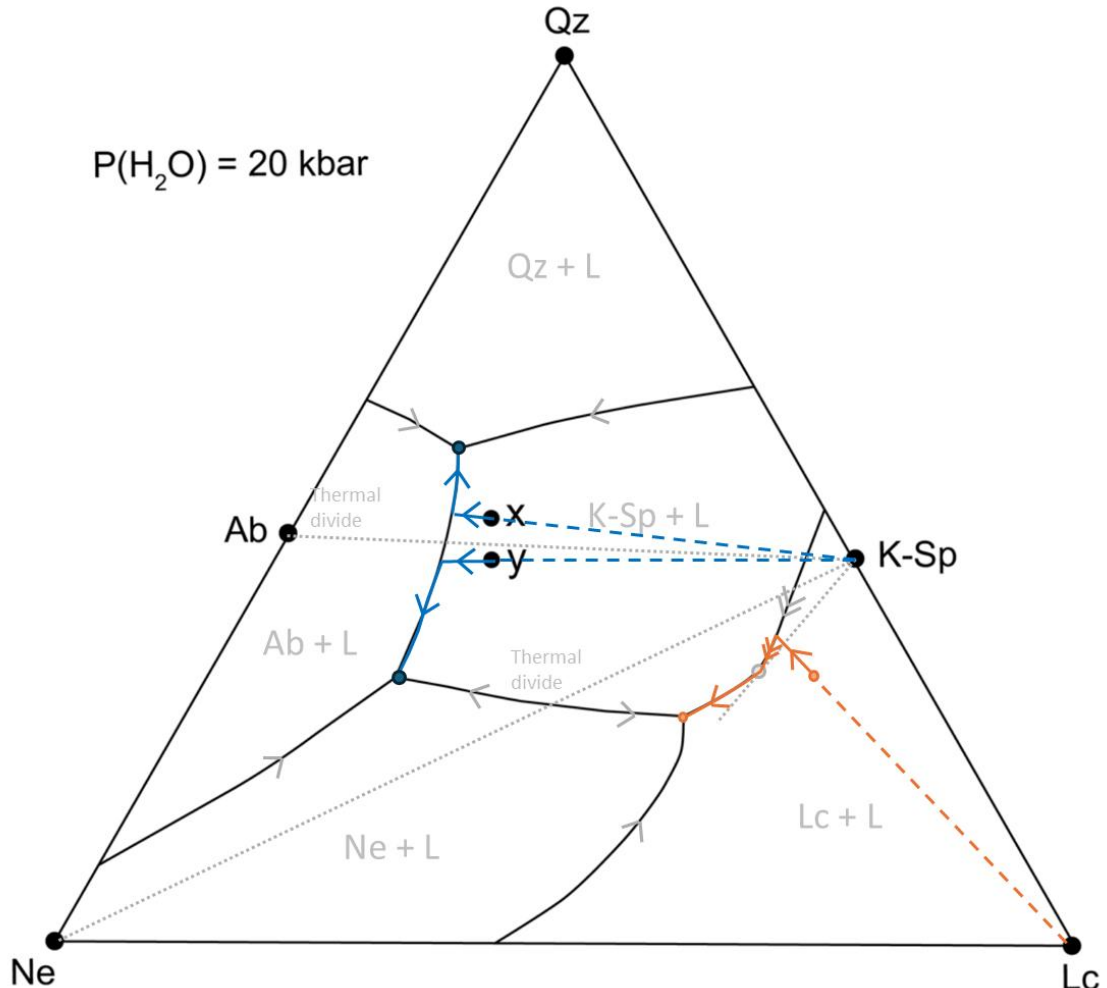


- (a) Draw on the stable sub-solidus tie-lines and label the primary phase fields. [5 minutes]
- (b) Mark down-temperature arrows onto the co-precipitational boundaries. Distinguish cotectics from resorptional boundaries. Mark on any thermal divides that may be present. [5 minutes]



(c) Mark onto the diagram and describe quantitatively the paths taken for liquids x and y during equilibrium crystallisation. [10 minutes]

Liquid x	Liquid y
$L \rightarrow K-sp$ $L \rightarrow K-sp + Ab$ $L \rightarrow Ab + K-sp + Qz$ Finally 8% Qz, 23% K-sp, 69% Ab	$L \rightarrow K-sp$ $L \rightarrow K-sp + Ab$ $L \rightarrow K-sp + Ab + Ne$ Finally 45% Ab, 5% Ne, 40% K-Sp



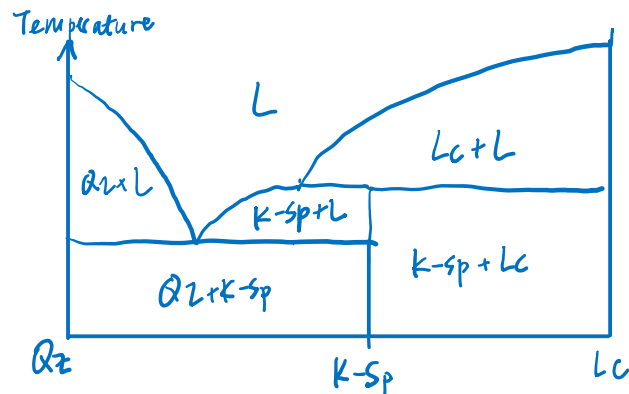
(d) How might the crystallisation paths described in c) differ under dry (water-free) conditions? [5 minutes]

The Ne and Lc fields expand, potentially shifting the Ab-Ksp-Ne invariant point upwards. It could be possible that the Lc+L field covers x and y instead, and so we would crystallise Lc first.

(also if you look at phase diagrams online they merged together K-Sp and Ab, could be that the dry conditions allowed the melting pt of the feldspars to increase and thus allow full solid solution)

Therefore, y could also move past the thermal divide.

(e) Draw the binary phase diagram for the Qz-Lc join. [10 minutes]



(f) A plutonic rock containing 70% K-Sp, 10% Ne and 20% Lc is underplated by basalt in a crustal magma reservoir, which causes heating and partial melting of the rock.

- (i) Plot the rock composition onto the ternary diagram.
- (ii) Describe quantitatively the composition of the partial melt produced, as well as the residual solid, and how they may evolve with continued melting.

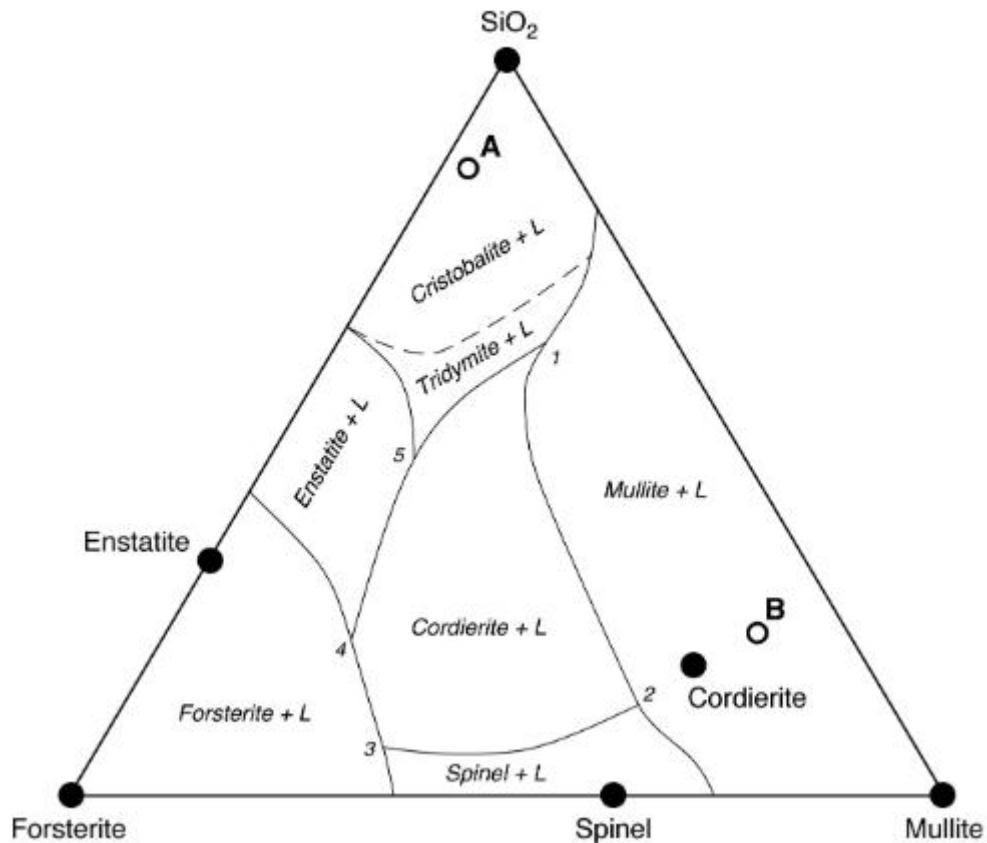


- (iii) In what kind of tectonic setting might this kind of rock be found? [10 minutes]

Given the rock is fairly alkaline and not very silica saturated, would probably say is somewhere in an intraplate setting, such as an ocean island basalt or a continental flood basalt.

2024

4. You are provided with a ternary phase diagram that shows minerals in the system forsterite-silica-mullite, or Mg_2SiO_4 - SiO_2 - Al_2SiO_5 (mullite is closely related to sillimanite, but stable at higher temperatures). The primary phase fields have been labelled and the invariant points numbered 1, 2, 3, 4 and 5.



- (a) What is the likely range of pressures for which this phase diagram is relevant? [2 minutes]

Likely low pressures (e.g. 1 atm) because for instance cordierite is a low-pressure mineral. Cristobalite and tridymite are **high temperature polymorphs** (not high pressure)

(b) Draw all sub-solidus two-phase tie-lines (Alkemade lines) and label the cotectic lines with down-temperature arrows. Identify any thermal divides or resorptional cotectics. [8 minutes]

(c) Write equations for each of the invariant points 1, 2, 3, 4 and 5. [5 minutes]



The compositions of a group of intercalated sandstones and mudstones are shown in the phase diagram. The point labelled A represents the mean sandstone composition, and that labelled B shows the mean mudstone composition. This sedimentary unit has been heated by a dyke, resulting in localised melting of the sandstones and mudstones at the contact.

(d) Identify the composition of the first melts to form from A and B. Determine the proportion of melting that can occur from each of these rock types before one of the phases is exhausted. For both A and B, state which phase is the first to be exhausted. [10 minutes]

- A is in the $\text{SiO}_2 + \text{Enstatite} + \text{Cordierite}$ triangle. This corresponds to the invariant point 5. Then, we will get depletion of 5-composition melt in the solid, so we move A away from point 5. Using lever rule, we see that the extent of melting is 18%, and the first phase to be exhausted is cordierite.
- B is in the $\text{SiO}_2 + \text{Cordierite} + \text{Mullite}$ triangle. This corresponds to the invariant point 1. Then, we will get depletion of 1-composition melt in the solid, so we move B away from point 1. Using lever rule, we see that the extent of melting is 25%, and the first phase to be exhausted is SiO_2 .

(e) In the outer parts of the contact aureole surrounding the dyke, the small amounts of melt formed remained in situ, solidifying rapidly once magma ceased flowing through the dyke. Describe and sketch the likely microstructures that might be seen in rocks of compositions A and B close to the melt-in isograd (mullite crystallises as fine needles). [10 minutes]

- Jagged shape of minerals like quartz ('Restitic' quartz)
- Needle-like mullite
- Quick solidification → zoning due to the lack of diffusion

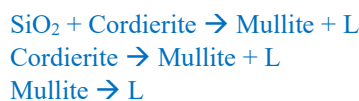
(f) At the contact with the dyke, melting continued beyond the exhaustion of one of the phases. Describe the sequence of melting reactions that occur for both A and B, and state which phase is the last remaining during extensive melting. [10 minutes]

A:

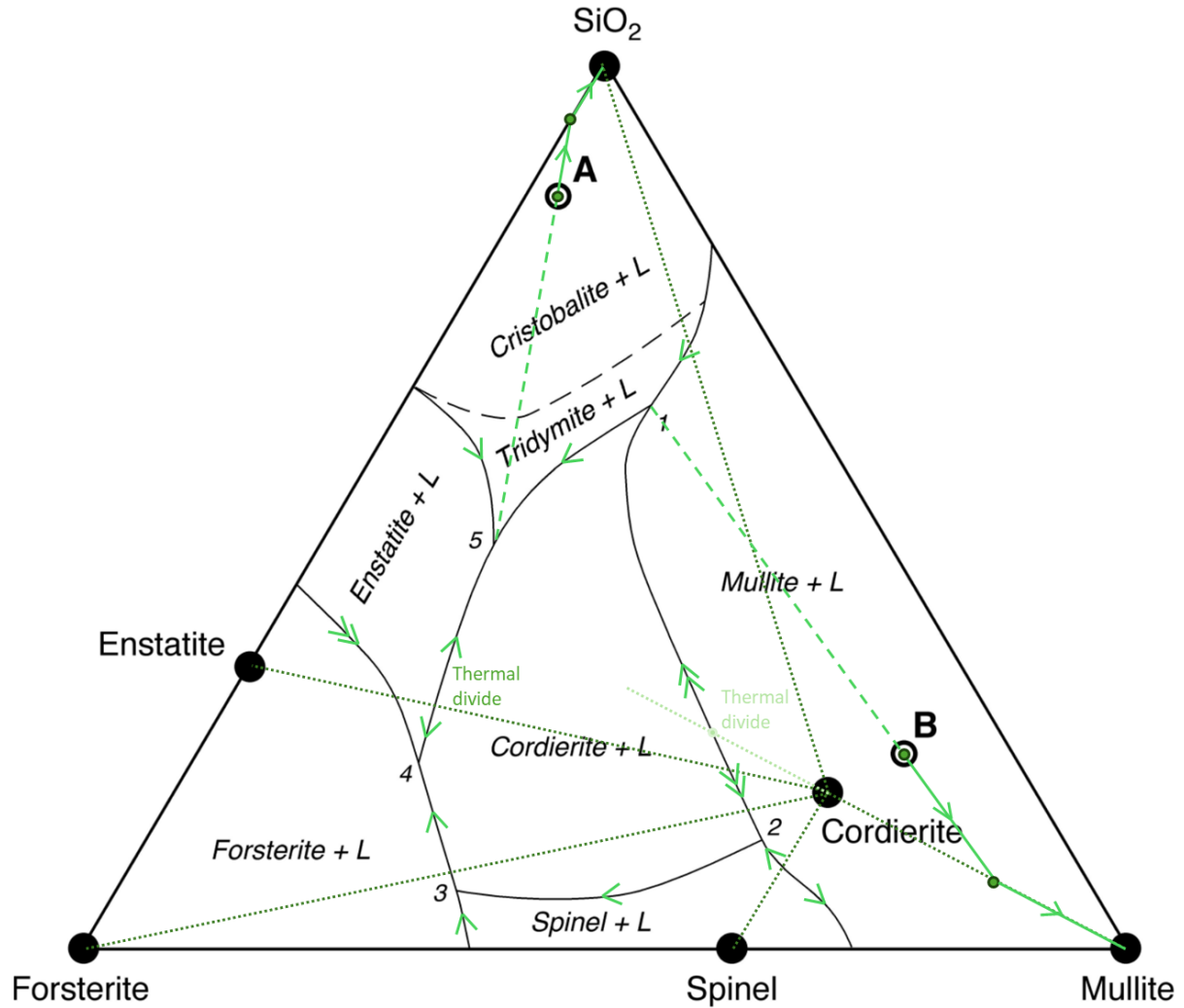


SiO_2 is the last phase standing.

B:



Mullite is the last phase standing.



Mid-Ocean Ridges & Ophiolites

2018 Discuss the techniques that can be used to estimate the composition and lithology of the mantle that rises under mid-ocean ridges. What constraints do ophiolites place on the magmatic processes associated with the formation of mid-ocean ridge basalts (MORB) and are there any caveats to their use?

GEOCHEMICAL CONSTRAINTS

Ophiolites allow us to directly sample MORBs. From there, thin sections reveal distinct characteristics:

- Uniformity in composition worldwide: Low $^{87}\text{Sr}/^{86}\text{Sr}$ ratio and major element ratios (e.g. MgO) are constant across ridges around the globe. Very low alkali content. Most variance comes from seawater
- Low Mg# (60# forsterite in MORB olivines, in comparison to 70# with mantle olivines), hence in disequilibrium with mantle olivine.
- Absence of europium anomaly in REE pattern of MORBs indicate no significant amount of plagioclase has been fractionated. Use LA-ICP-MS
- **Phase diagrams** show compositions lie close to *low-pressure cotectics* so means fractionation must have occurred; typically ‘olivine tholeiites’ with normative Ol + Opx, primary melt must be tholeiitic

If the melt was primary, it should have predictable Mg/Fe ratio in equilibrium with mantle olivine, however it has a low Mg/Fe in disequilibrium. Thus, they are believed to be generated as melt crystallizes at low pressures.

GEOPHYSICAL CONSTRAINTS

Seismic velocity structure of crust has revealed distinct layers of material: sediments -> pillow lavas -> sheeted dykes -> gabbros -> layered gabbros -> layered peridotite -> upper mantle.

Studies of ridges have shown low-velocity zones within the crust (thought to correspond to liquid magma chambers) and strong seismic reflectors (thought to correspond to roof of magma chamber)

However, recent studies debate the extent of magma chambers: velocity is quicker than expected for liquid magma chamber model, suggests ‘mush with interstitial liquid’ instead of ‘crystals in lots of liquid’
Hence, magma reservoirs are small sill-like magma bodies surrounded by larger mush zones.

Caveat: Ocean floor seismic data is not complete (because it is in the ocean),

PETROLOGICAL CONSTRAINTS

- Represents oceanic crust: thickness and order of stratigraphic layers are consistent with seismic data. Thus reveals detailed structure of magmatic system and constrains thickness of layers at MOR.
- Shows direct evidence of melt migration, e.g. dunite channels, pyroxenite dikes.
- MORs consist of presence of multiple magma chambers: in Troodos, less evolved mafic rocks cross cut evolved mafic rocks, implying presence of i) more than 1 magma chamber ii) discontinuous eruption
- Major hydrothermal alteration (Oman)
- Generated by obduction at continental margins or at accretionary prisms.

Caveat: The body of most ophiolites is under the surface, and the exposed rock is only a small fraction of the total structure, so it is difficult to observe ridge structure directly from most ophiolites.

Origin: ophiolites are generated when subduction begins and thus represent fragments of fore-arc lithosphere. Many ophiolites, especially well-preserved ones, are formed in suprasubduction zone (forearc/backarc basins, not purely at MORs). E.g. Troodos (Cyprus), Samail ophiolite (Oman). So not ‘pure’ MOR mantle.

- This results in a **high extent of metamorphism** (greenschist facies)
- **High extent of hydrothermal alteration** (at forearc) – serpentinite / sericite
- **Slab-derived components** can alter chemical signals

However, still worth studying as in-situ evidence for **dominant lithology of upper mantle**, melt transport, etc.

CONCLUSIONS – MOR STRUCTURE:

- Passive upwelling and partial melting of aluminous lherzolite leaves **depleted harzburgite** residue
- Decompression melting generates primary basalt melts which undergo **fractional crystallization**
- Cumulates, and in upper layers, gabbros are formed; the rest is fractionated basalt which is erupted.

2020

1. *With the aid of phase diagrams, show how the results of experiments may be used to constrain processes associated with: (i) mantle melting; and (ii) crystal fractionation beneath mid-ocean ridges. Discuss how the results of experiments on peridotites have been applied to physical models of mantle melting. [45 minutes]*

2022

3. (a) What are the expected compositions of primary melts of Earth's convecting upper mantle? [15 minutes]

alkali b - (nepheline), more na, k, incompatible. ol phenocryst OR groundmass, potential alkali feldspar in groundmass, PLEOCHROIC AUGITE, nepheline as residual glass or in groundmass

tholeiite – defined as basalts containing low-Ca pyroxenes (enstatite or pigeonite) ol / qz. calcic, more sio₂. ol as phenocryst, pyroxene, plag in groundmass., COLORLESS ALBITE, silica as quartz in groundmass.

Nepheline and quartz are chemically separated by the plane of silica undersaturation. melts on silica side evolve to quartz-bearing eutectic (tholeiitic) -> silica saturation, melts on nepheline side evolve to nepheline-bearing eutectic (alkaline) -> nepheline saturation

(b) *Describe the evidence that has been used to determine whether mid-ocean ridge basalts are primary melts. [20 minutes]*

(c) *What are the likely causes of the observed variation in Mg# (i.e. molar Mg/[Mg+Fe]) with depth in the crustal and mantle portions of the Troodos ophiolite? [10 minutes]*

2023

Describe the petrological, geochemical and geophysical evidence that constrains: (a) the structure of oceanic crust, [20 minutes] (b) **how melting occurs at mid-ocean ridges**. [25 minutes]

OBSERVATIONS

- Time between melt generation in mantle and eruption on seafloor is short: < 1000 years. Melt thus moves very quickly upwards.
- Mid Ocean Ridges are only ~2km wide compared to a large area of magma generation in the mantle.
- Thus any model must solve: i) fast movement of melt ii) focusing of melt towards ridge axis

ADIABATIC DECOMPRESSION MELTING

Plate spreading causes underlying mantle to be **drawn upward** to fill gap; causes further **adiabatic decompression** of mantle at shallow levels, lowering the mantle's solidus & triggering partial melting; the thermal structure is dominated by **advection of heat** from below rather than conduction from above.

Amount of melt also controlled by potential temperature, has large impact on % of melt generation; $T_p = 1315\text{ C}$ generates ~7km of crust while $T_p = 1500\text{ C}$ generates ~30 km of crust as seen at Iceland

CORNER FLOW OF MANTLE MELTING MODEL

The corner flow model predicts mantle decompression and melting over a considerable depth range. Melts generated across the broad melting regime migrate **diagonally upward & toward the ridge**, due to pressure gradients.

This allows melts **produced over a range of pressures to mix** to form MORB, explains the homogeneity of melts within the same MOR.

CHANNELISED FLOW OF MELTS

- Dunite channels: formed by reaction between Ol saturated melts and harzburgite residue
- Original orientation perpendicular to MOHO -> shows pathways of deep melts towards the MOHO

2024

3. Describe the processes that link mantle rising under spreading ridges to the layered structure of the igneous crust preserved in ophiolite sequences. Use petrological observations and phase diagrams to support your answer, where appropriate. [45 minutes]

Hot Spot Magmatism (OIB and CFB)

2020 Give an account of how melts are generated in the mantle beneath ocean islands formed at intraplate settings. How do the mantle processes beneath intraplate ocean islands, and also the erupted products, compare with those in continental flood basalt provinces? [45 minutes]

MAGMA GENERATION - OIB

Two distinct magma series: tholeiitic and alkaline, generated in different stages of eruption. Must come from different magma sources and not from fractionation at low P, as compositions divided by thermal divide.

Alkaline melts favoured by **small extent of melting at high pressures**; contains high alkali content and incompatible trace elements. Na, K are less compatible than calcium and are the first elements to partition out when small degree melting of primitive mantle occurs.

Tholeiite melts favoured by **higher extent of melting at low pressures**. The fusible components were extracted in the initial low fraction melts at depth, so remaining mantle is depleted in alkalis and incompatible elements.

PLUME MODEL FOR OIB

Derived by combining the results of **convection models** with **parameterisations of peridotite melting**
Adiabatic decompression melting occurs ~80 km due to a high mantle potential temperature (draw the diagram)
Causes a hot upwelling radially symmetric plume starting at lower mantle, with small % melting at outskirts (due to low T_p) and large % melting in middle (high T_p) – explains the alkaline and tholeiitic basalt distribution.
Complexity: Plumes are isotopically heterogeneous, e.g. Hawaii. Involves more components than pure mantle

PROCESS OF ERUPTION and its products

- **Pre-shield stage:** Alkali basalts (Loihi) from margins of melting region
- **Shield-building stage:** Tholeiitic basalt, directly from central rising column of plume (Mauna Loa)
- **Post-shield stage:** Alkali – Mauna Kea from margins of melting region
- **Post-erosional stage:** *Highly alkaline – nephelinite*. Not directly predicted by plume model, generation may be due to generation of conduction of plume heat into volatile-rich portions of lithosphere, causing very small degree melting. (Haleakala)

Movement of tectonic plate above plume allows us to distinguish between different stages of eruption.

MAGMA GENERATION – CFB

Adiabatic decompression melting again, similarly from plume due to elevated mantle potential temperature. Tholeiitic composition; melts are not primary due to fractionation: proof being picrites (MgO rich rock) are rarely observed. They are found only in sill-shaped magma chambers as they are dense and stall in the crust. Proof of polybaric fractionation: large magma chambers found in Tertiary Skaergaard Intrusion of (opening of the North Atlantic, arrival of the large Icelandic plume)

As basaltic magma ($T \sim 1200C$) enters continental crust ($T \sim 800C$) melting of country rock may occur; xenoliths may also be incorporated. Makes some magma silicic and contributes to both compositional and isotopic (Sr, Nd etc.) variation. Explosive eruptions. Radial dikes from plume head but much larger scale. However most have been adulterated by plate tectonics. One good example is the Mackenzie dike swarm in NT, Canada.

Complexity: Not all CFB origins are from plumes. For example Ontong Java oceanic plateau may instead be the record of a bolide impact, on the grounds that it cannot be linked convincingly to any hot-spot track. This may explain why uplift at the time of eruption – as indicated in other submarine LIPs by the abundance of subaerial lavas in the volcanic sequence – appears to have been minimal: virtually all Ontong Java lavas so far sampled are clearly submarine

DIFFERENCES

CFB: Initial impact of rising mantle plume head, OIB: melting of plume tail

CFB: Crustal contamination, OIB: relatively little

CFB: Very few alkaline basalts (large degree of melting), OIB: alkaline basalts pre/post shield

CFB: short but large volume (e.g. Deccan traps), OIB: long but less volume

CFB: not primary melt OIB: primary melt

5. (a) The life-cycle of Hawaiian volcanoes is often understood in terms of the relative motion of a 90 million year old oceanic plate over a mantle plume. Describe the principal successes and failures of this model in accounting for the observed characteristics of Hawaiian volcanism. [20 minutes]

SUCCESS

Physical: Fixed source with relative plate movement, volcanoes age progressively along the chain. Emperor Seamount 80Myr to Hawaii 0Myr matches concept of plate moving over a fixed melt source.

Chemical: Isotope ratios indicate primitive mantle melted. Also explains alkali vs tholeiite distribution.

FAILURE

Physical: Emperor Bend. Paleomagnetic and plate motion reconstruction suggest bend might require both significant change in plate motion AND plume motion, which contradicts with a fixed source.

Volcanism is not linear: e.g. Honolulu volcanics on Oahu erupted only just 50000 years ago. Hence, secondary magmatic systems can persist.

Asymmetry of the plume: Lava compositions differ systematically between Loa (isotopically enriched – more primitive) and Kea (more depleted) trend volcanoes. Cannot occur with an isotropic plume; suggests chemical zonation within the plume.

Chemical: The presence of the post-erosional highly-alkaline rocks (basanites & nephelinites) is not directly predicted by the plume model. Generation may be due to generation of conduction of plume heat into volatile-rich portions of lithosphere, causing very small degree melting. (Haleakala)

CONCLUSION

The plume model is an excellent first order approximation but requires refinement

(b) Some of the volcanoes of the Emperor Seamount chain were produced when the Hawaiian plume passed beneath young oceanic lithosphere (<10 Myr old). How might the composition and volume of the Emperor Seamounts differ from the Hawaiian Islands? [25 minutes]

VOLUME

- Higher melt production likely: young lithosphere is **thin and thermally hot** so decompression melting occurs at a larger range of depths due to lower pressure.
- Reduced conductive heat loss
- Increased rate of magma ascent, so more magma erupted within same period
- Reduced time spent in shield building stage – less volume of alkali basalts.

COMPOSITION

- Larger extent of melting -> tholeiitic basalts, *less* incompatible elements (and 87Sr/86Sr), higher Mg# (due to less fractional crystallization as rate of ascent is faster)
- Melting is near the lithosphere, so we see more trace element ratios from the depleted mantle. (lower 3He/4He for example)

2022

1. (a) Compare and contrast the processes involved in the generation of melts beneath ocean islands and continental flood basalt provinces. [30 minutes]

- *Intraplate settings ➔ crustal contamination*
- *Decompression melting*
- *Plume activity*
- *Degree of melting*
- *Melt ponding in magma chamber tertiary skaeergard intrusion*

(b) How are these processes manifested in the whole-rock compositions of erupted basalts? [15 minutes]

2024

2. (a) How might the enormous volumes of melt that are preserved in flood-basalt provinces form? [25 minutes]

Impact of plume head onto the base of the lithosphere

Large extent of melting (decompression melting, $T_p = 1500\text{ C}$)

Pre-existing crustal thinning in some rift zones, or due to the action of the flood basalt 'pushing' up the lithosphere → facilitates decompression melting

(b) Discuss the variations in how magma is: (i) stored in the crust; and (ii) erupted, over the life cycle of a flood-basalt province. [20 minutes]

Polybaric fractionation (Skaergaard intrusion Greenland) (opening of the North Atlantic, arrival of the large Icelandic plume)

Subducting Plates & Arc Magmatism

2020

1. Using examples, describe how water influences: (i) melt generation; (ii) crystallisation; and (iii) eruption of magmas at **continental** margins. How would you identify igneous rocks erupted at this tectonic setting in thin section? [45 minutes]

5. How would you use: (i) major elements; (ii) trace elements and (iii) isotopic ratios to distinguish between magmas erupted at “Japan” type and “Andean” type destructive plate margins. Using examples, comment on the role that the crust plays in the generation of these magmas. [45 minutes]

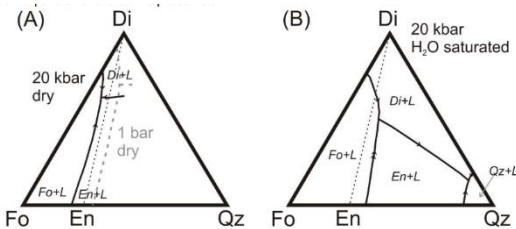
(a) Describe the role of water in the generation of subduction-related magmas. [25 minutes]

Seismic studies have shown the subducting plate and the areas around it are quite cold: cannot melt on its own. Thus require water. Proof of water: presence of amphiboles in some arc basalts, 4% H₂O in Ol melt inclusions

- Hydration of oceanic crust by mid-ocean ridge hydrothermal activity
- Subduction of oceanic lithosphere and breakdown of hydrous minerals to produce hydrous **slab fluid**
- Upwards transport of fluid into cool mantle wedge
- When fluid reaches parts of wedge at T=1100°C or more, silicate melts of peridotite produced: water hydrolyses silica polymer bonds, thus reducing the melting point significantly from 1300 to 800. Water is thus fixed in the structure of hydrous minerals, e.g. amphibole
- Buoyant silicate melts travel upwards towards crust

MAGMATIC COMPOSITIONAL CHANGE

Primitive subduction magmas are **quartz-normative**, contrasting with MORB. This is due to the **expansion of the olivine phase field** in the presence of water.



Tie line thermal divide (dry) – cannot evolve to Qz-normative.

Wet: As ternary point lies outside subsolidus triangle, it is a **peritectic** with reaction $\text{Fo} + \text{L} \rightarrow \text{Di} + \text{En}$.

If liquid does not run out (which does not happen as large degree of melting due to water) \rightarrow Qz is produced.

i.e. This melt can evolve to high silica compositions during crystallization. Case in point: hong kong

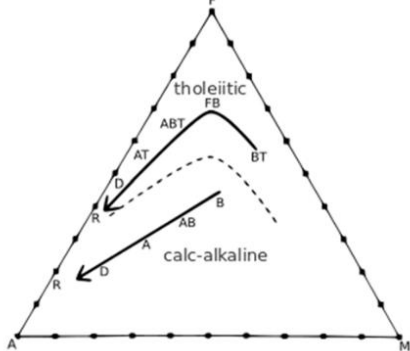
HYDROTHERMAL ALTERATION AND ASSOCIATED METAMORPHISM

Accelerates hydrolysis and metamorphic reactions: forms amphibole, chlorite, serpentine, lawsonite etc. in the overhead mantle. Fluids enrich magmas in **mobile** elements: the **slab fluids** strip LILEs e.g. Rb, K from the slab and bring them into the peridotite. Thus a subduction component to mantle is added.

(b) What are the differences in subduction-related and intraplate volcanic rocks in: (i) The mineral phases that crystallise. (ii) The textural relationships of these minerals. [20 minutes]

2023

1. (a) Describe where calc-alkaline magmas occur, and how they are formed. [30 minutes]

AFM PLOT

$A = \text{Na}_2\text{O} + \text{K}_2\text{O}$, $F = \text{FeO}$ $M = \text{MgO}$. As crystallization occurs, concentration of incompatible trace elements (K and Na) rises; more **evolved** magmas move closer to A.

However, in tholeiitic rocks, **plagioclase** first crystallizes; Fe is particularly incompatible in plagioclase so composition moves to F vertex before moving to A. **Marked Fe enrichment**

In calc-alkaline rocks, not much plagioclase present, so does not move towards Fe. **No Fe enrichment**

JAPAN MARGINS (Ocean-sub-ocean) – Tholeiitic trend, basaltic; IAB.

- Oceanic arcs have depleted mantle wedges and thin overlying crust, leading to high extents of melting of depleted sources.

ANDEAN MARGINS (Ocean-sub-continent) – Calc-alkaline trend, andesitic

- Continental crust is thick; magma undergoes multiple stages of differentiation and produces cumulates. **Arclogites contain garnet and rutile.**
- (b) Why do some arcs transition from tholeiitic compositions to calc-alkaline compositions along-arc? [15 minutes]

CRUSTAL THICKNESS

Tholeiitic series formed on the relatively thin oceanic crust of an immature arc and are therefore mostly low pressure differentiated magmas. Calc-alkaline series formed in a mature arc setting where the crust is thicker and encourages higher pressure crystallisation. E.g. Fiji's Old series (tholeiite) vs young series (calc-alkaline)

CRUSTAL INCORPORATION

Due to incorporation of continental crust into melts: New Zealand vs Tonga, Kermadec AFM plot. New Zealand is a mostly submerged microcontinent.

DPM basalts typically SiO₂ rich,

2024

1. (a) Compare and contrast the mantle and crustal processes that are associated with magmas formed at island arcs and continental arcs. [30 minutes]

Process	IAB	CA
Slab input	Oceanic crust + pelagic sediments	Oceanic crust + some terrigenous sediments from continental margin (accretionary wedge)
Melting	Tholeiitic	Calc-alkaline
Incorporation	Not much change	Xenoliths alter isotopic composition greatly

- (b) Discuss the processes that might give rise to the calc-alkaline trend. [15 minutes]

CRUSTAL THICKNESS**INTRACRUSTAL PROCESSING:**

- Hot basalt melts or incorporates xenoliths of Si-rich Fe-poor continental crust to form rhyolites. This mixes into basalt, forming andesitic Fe-poor calc-alkaline rocks.

SLAB FLUIDS:

- Suppression of plagioclase crystallization. High H₂O content from slab fluids delays plagioclase nucleation, which allows early Fe depletion.
- Stabilization of amphibole in hydrous conditions which may contain Fe, further depleting magma.
- Slab fluids are **oxidized** and so FeO formation is promoted.

Volcanic Eruptions

2018

3. What factors control eruption style? How did the study of the eruption of Mt St Helens in May 1980 further improve our understanding of volcanic hazard and environmental impact in i) local and (ii) global settings?

Viscosity (Si-rich melts have higher viscosity; viscosity decreases with increasing T, water decrease viscosity), gas content;

Eruption in water produces pillow lavas, when molten basalt touches liquid water it generates surtseyan explosions due to conversion of water into steam

Pahoehoe: near vents, surface of lava wrinkled – remained *ductile* while lava still in motion (high T, low strain)
 A'a: far from vents, surface of lava brecciated – became *brittle* (cooler temperature, high strain rate)
 Due to difference in viscosity and temperature

2021

2. How and why do the styles of eruption vary between volcanoes located at continental margins and intraplate settings? Discuss how these different eruption styles are reflected in the products of volcanic eruptions. [45 minutes]

Stratovolcanoes: Andean eruptions, hk

Shield volcanoes: Mauna Kea, Mauna Loa

Temperature, composition affect Density, viscosity, rate of eruption

During the middle Jurassic to the early Cretaceous period, Hong Kong was right at the convergent plate boundary where the Paleo-Pacific oceanic plate subducted beneath the Eurasian continental plate.^[8] The oceanic plate carried sea water into the hot lower crust, which lowered the melting point of the crust.

Hexagonally jointed tuff

2022 (Paper 1)

7. How do magmas ascend through Earth's crust? What dictates the style of a volcanic eruption? [45 minutes]

2023

3. (a) Describe the processes involved in an explosive eruption, from magma reservoir to atmosphere. [25 minutes]

(b) What observations can be made to constrain column height and erupted volume for a particular eruption? [20 minutes]

2022

5. (a) Compare and contrast the style of volcanic activity associated with the eruption of Mt Mazama at 6850 yrs BP with that of the eruption of Mt St Helens in May 1980. [30 minutes]

(b) How did the study of the eruption of Mt St Helens in May 1980 further improve our understanding of volcanic hazard and environmental impact in: i) local and (ii) global settings? [15 minutes]

Mantle Convection

2020

4 Describe the constraints that (i) mineralogy and (ii) noble gases place on the composition and structure of Earth's mantle. How might structures that have been identified at the core-mantle boundary by seismic studies be associated with surface volcanism? [45 minutes]

Isotopic composition of upper mantle and deep mantle are very different. This is because the upper mantle has been depleted in incompatible elements by the formation of continental crust. However, MORB is remarkably uniform globally, while OIBs show variation with location.

TWO-LAYER MANTLE MODEL

Explains the big difference between MORBs and OIB. The two-layer boundary is defined at 660 km with the reaction ringwoodite \rightarrow periclase + bridgmanite. This physical and chemical discontinuity manifests itself in the isotopic differences between these two groups.

UPPER MANTLE: Represented by MORB. Chemically homogeneous. Created by adiabatic decompression melting at shallow depth. Extraction of partial melts to form continental and oceanic crust has depleted the mantle uniformly in incompatible elements (e.g. Rb, Nd, U)

LOWER MANTLE: Represented by OIB. Mix of a common component (PREMA) + special component which varies by location. This variability in special component is attributed to material sampled by plumes at the base of the mantle; the variability is too big for it to arise from differences in degree of partial melting. Reservoirs include HIMU (defined by extremely high Pb anomaly), EMI (high $^{207}\text{Pb}/^{204}\text{Pb}$ but low Rb/Sr) and EMII (high $^{207}\text{Pb}/^{204}\text{Pb}$ and high Rb/Sr).

Geophysical evidence also shows heterogeneities in density in the lower mantle. At the base lies two LLSVPs, which shape can be deduced using ScS waves which reflect off those structures. Gravitational measurements also result in positive geoid anomalies above the theorized locations of LLSVPs. S waves passing through such structures are much slower, representing big piles of high-density material. Theory: primordial remnants of mantle differentiation, or remnants of protoplanet Theia (explains antipodality). ScS waves from other side of Earth can also show vertical structures like mantle plumes

EVIDENCE FOR DISCONTINUITY

Helium-3 primordial, generated during stellar fusion; Helium-4 radiogenic, generated by alpha decay. We can normalize He-3/He-4 ratios in rocks with He-3/He-4 ratio of the atmosphere to get the relative abundances across different rocks. MORB show uniformly low ratios (lose primordial He) while OIB show a large range (retain primordial He). This shows that the MORB may have been degassed during the melting event that created the continental crust.

A paragraph on Rb/Sr and Sm/Nd systems.

Preserved minerals in diamonds. (e.g. The recent discovery of ringwoodite in diamond inclusions from Juina)

Geophysical evidence shows that a big positive change in velocity occurs for both P and S waves at 660 km depth. The discontinuity also results in precursors (faster waves which reflect off the boundary) and triplications. This is thought to be due to differences in chemical phases in upper and lower mantle. Corroborated by chemical experiments involving diamond anvil cells.

EVIDENCE AGAINST 2-LAYER MODEL

Seismic tomography at depth has shown fast anomalies around subducting slabs that extend into the lower mantle. This shows subducting plates descend into the lower mantle, and there is some evidence that mantle plumes may extend to the top of the upper mantle. This implies that mass transfer across the boundary is significant. This corresponds to the otherwise unexplained enrichment of HIMU in $^{206}\text{Pb}/^{204}\text{Pb}$, and EMI/EMII in $^{207}\text{Pb}/^{204}\text{Pb}$. The subducted material may melt and mix into the mantle locally, creating differences in OIB isotopic composition.

2021

1. Compare and contrast the most widely-used models of mantle convection, and discuss the evidence that supports each model. [45 minutes]
4. (a) How are the minerals present in basalts, and the bulk rock major and minor element compositions of these basalts, used to constrain the extent and depth range of mantle melting under (i) ocean islands and (ii) mid-ocean ridges? [25 minutes]
- (b) How might this information be used to investigate the physical causes of mantle convection? [20 minutes]

2022

4. (a) Describe the constraints that the following place on the composition and structure of Earth's mantle:

- (i) Trace elements.
- (ii) Radiogenic isotopes.
- (iii) Noble gases.

[30 minutes]

- (b) How might structures at the core-mantle boundary that have been identified by seismic studies be associated with surface volcanism? [15 minutes]

when the locations of hotspots associated with Large Igneous Provinces are corrected for plate motions they frequently overlie the edges of LLSVPs.

ULVZs lie at the edge of LLSVPs – 30-50% reduction in S wave speed – hypothesized to be partially molten. Provides local source of buoyancy for mantle plume.

Granites

2018

4. Both mafic and felsic igneous rocks are preserved on the island of Skye. How do these rocks help us understand how magmas are emplaced in the Earth's crust and the processes that operate in magma chambers? How might the occurrence of both mafic and felsic intrusions relate to each other and how can they be used to inform on the "granite problem"? [45 minutes]

2021

3. Explain how geochemistry and petrographic observations may be used to infer how granites formed. Describe the role of water in granite crystallisation. [45 minutes]

S-TYPE

Melting of **sedimentary rocks** – peraluminous ($\text{Al} > \text{Ca} + \text{Na} + \text{K}$). Found in eroded cores of fold-thrust mountain belts (Himalayas, Trois Seigneurs, SW England). Strontium isotope > 0.708 suggests crustal origin. Water-rich.

I-TYPE

Melting of **igneous rocks** – metaluminous ($\text{Al} > \text{Na} + \text{K}$). Found along continental margins, and in Himalayas, related to continent-continent collisions. Strontium isotope < 0.708 suggests origin in depleted mantle. Porphyry copper deposits.

A-TYPE

Anorogenic granites – peralkaline ($\text{Al} < \text{Na} + \text{K}$). Related to continental rifts. E.g. Basin and Range Province, US

A granite containing both muscovite and biotite micas is called a binary or two-mica granite. Two-mica granites are typically high in potassium and low in plagioclase, and are usually S-type granites or A-type granites.

Magmatism and Volcanism (Others)

2020 (*Paper I*)

7. *Describe the processes by which differentiation of magma bodies occurs during crustal storage. How might these processes be modelled quantitatively and what are the challenges and uncertainties involved in doing so? [45 minutes]*

2021 (*Paper I*)

7. (a) *Describe the controls on trace element concentrations in minerals when they are in equilibrium with melt. [15 minutes]*

(b) *Using examples, show how measured trace element concentrations in minerals may be used to reconstruct previous melting and crystallisation events. [30 minutes]*

2018 (*Paper I*)

5. *What factors control the nucleation and growth of crystals from a melt? Explain the roles of the Gibbs free energy of the melt and crystalline phase, and the formation of the crystal-melt interface (surface energy) in terms of the kinetics of formation of an ideal spherical nucleus of crystal.*

Pegmatites are characterised by very large crystals. Using examples you have seen in the field, discuss how pegmatites may form and how the minerals they contain may give clues to the conditions of their formation.

Metamorphism

Metamorphic Facies

2018

4. Describe the crystal structures of andalusite, sillimanite, kyanite and mullite. To what extent can the stability of these minerals, with respect to pressure and temperature, be understood in terms of their structures? Under what circumstances might two or three of the minerals be found together in the same rock?

7. With examples explain how fabrics differ between regional and contact metamorphic rocks. What key factors control the development of such fabrics?

structural geology and with high-temperature creep processes

9. Using examples discuss the use of the phase rule for metamorphic reactions in pelitic rocks and AFM assemblages.

$$F + P = C + 2; C = 3 \text{ in AFM.}$$

Invariant point: $F = 0$, 5 phases coexist at fixed P-T.

Univariant reaction: $F = 1$, 4 phases coexist. Reaction curve.

Divariant assemblage: $F = 2$, 3 phases coexist. Field in AFM. Map mineral assemblages. The triangles do not overlap; only one possible assemblage of minerals can form and be under chemical equilibrium at the same time

Remember, based on principles of chemical equilibrium, for rocks under same P, T, different assemblages represent different bulk composition, and for rocks under same bulk composition, different assemblages represent different P, T conditions. We can thus use compositional diagrams to show this.

The diagram in which a phase is plotted is for a certain T and P, leaving only chemical components as variables.

- Components that occur in pure phases (SiO_2 in q) can be ignored, as $\mu_{\text{SiO}_2}^q = \mu_{\text{SiO}_2}$ and this only varies with T and P, which are fixed.
- Components which chemical potentials are controlled externally to the system need not be plotted. E.g. H_2O ; activity commonly controlled by CO_2 but as CO_2 not part of NCKFMASH then it is ‘externally controlled’. $a_{\text{H}_2\text{O}} = \exp\left(\frac{\mu_{\text{H}_2\text{O}} - \mu_{\text{H}_2\text{O}}^*}{RT}\right)$ so activity decreases as water becomes a mixture.
- Components that are not sufficiently abundant to stabilize a mineral can be ignored. Add to component which it usually substitutes for.
- If component occurs in two or more phases, and one phase is common to all assemblages, it is convenient to project composition of all phases with this component from the composition of the common phase to some face of the tetrahedron, reducing 3D to 2D (AFMK \rightarrow AFM by projection from mu)

Activity of water can vary from 1 to 0 in fluid (e.g. if fluid was composed of pure CO_2 it would be 0)

Significance: ‘wet’ granulite melting in charnockites in Tamil Nadu.

Schreinemaker’s analysis in AFM space: predicts reaction types based on variance. Produces petrogenetic grids for a particular activity of H_2O .

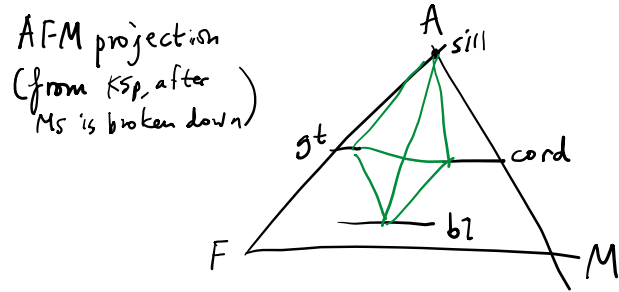
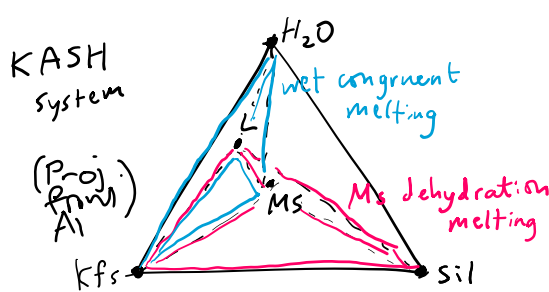
Violations:

- Garnet stability field: more than 3 components should be considered. E.g. Mn expands garnet stability
- H_2O role in dehydration reactions which is not plotted – must use KFMASH system here
- Excess phases assumption: AFM assumes Qz, Ms omnipresent. If Ms consumed (e.g. at high T) then projection fails, and we should switch to projection from Kfs.

2020

6. Discuss the key melt reactions for metapelites, including reference to how these reactions could be distinguished.

At high temperatures, metapelites with appropriate composition and H₂O experiences partial melting, forming **migmatites** where partial melt (leucosome) separates from source (melanosome)



The KASH system is appropriate for modelling these reactions, projecting from Al₂O₃.

Wet melting / solidus: water is present as a **free phase reactant**. Ceases when H₂O runs out (red)
e.g. K-feldspar + muscovite + H₂O + quartz → L

Dehydration melting: water is absent but still involved in the breakdown of **hydrous phases**.
e.g. muscovite + quartz → sillimanite + K-feldspar + L (Subsolidus dehydration seen in Trois-Seigneurs)
e.g. sillimanite + biotite + qtz → garnet + cordierite + L

Tell apart from the peritectic phases produced. E.g. (1) the presence of cordierite in the leucosome would imply that Bt-dehydration has occurred. (2) At Trois Seigneurs, the lack of peritectic phase in the leucosome is consistent with wet congruent melting having occurred.

How would the following factors affect melt production: (a) pressure; (b) water availability; (c) protolith heterogeneity; (d) clockwise versus anticlockwise pressure-temperature-time paths.

PRESSURE affects position on P-T space; stability fields may differ. Melting is favoured for reactions with a negative Clapeyron slope, and vice versa

WATER AVAILABILITY can limit melt production in wet melting reactions (red) but does not affect dehydration reactions, as it is not a reactant.

HETEROGENEITY may affect the stability of certain minerals. E.g. if a portion of the pelite is enriched in Al / Mn / whatever, garnet is stabilized and melt production increases.

DIRECTION OF TEMPERATURE-TIME PATH affects the sequence of melt reactions.

Clockwise melting involves burial → heating → decompression, then exhumation

Additional melting during decompression, the last stage; increased melt production wrt reaction in orange

Anticlockwise melting involves heating → burial → cooling, then exhumation

Melting during heating and burial can undergo back-reactions, melt solidifies, lower preserved melt volume.

7. During what part of a typical pressure-temperature-time path is a metamorphic rock thought to maintain equilibrium, and what are the contributing factors? Which microstructures may indicate a departure from equilibrium? What processes are likely to control this departure from equilibrium? [45 minutes]

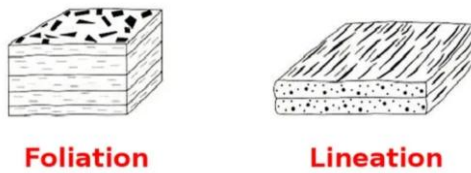
8. Discuss how mineral fabrics develop in response to applied stress. How might mineral textures be used in deciphering the thermal and structural history of an orogenic belt? [45 minutes]

Discuss how mineral fabrics develop in response to applied stress.

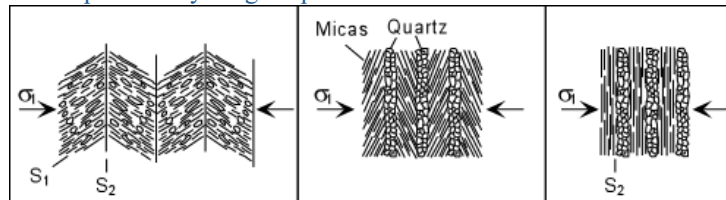
- Lithostatic pressure has no effect on a rock because it is hydrostatic ($P_1 = P_2 = P_3$). Therefore, the keyword here is deviatoric stress (non-hydrostatic).
- Mineral grains have a preferred orientation that reduces the strain as much as possible under applied deviatoric stress, in order to minimise the free energy G of the rock.

Mechanics of developing fabrics

Types of fabrics: foliations and lineations

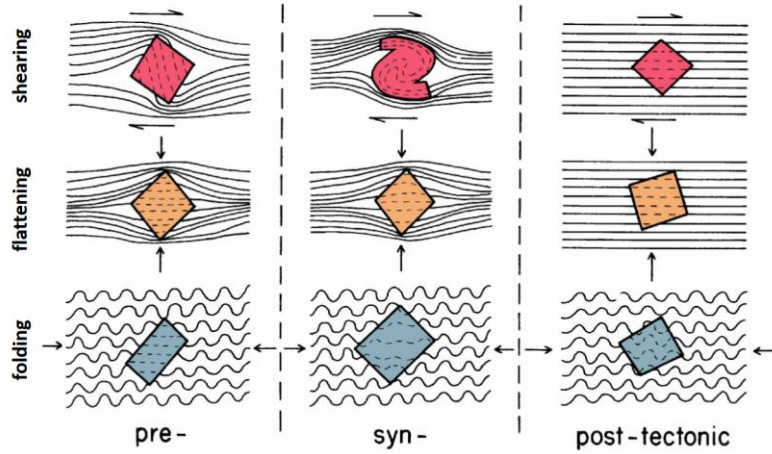


- **Plastic deformation** within crystals. Usually at high T and low strain rate.
 - **Dislocation creep** is the slip and climb of dislocations, and crystals where slip systems can operate tend to reduce strain and more stable. Those which are aligned unfavourably cannot reduce their strain energy and are swallowed by neighbours. → there is a preferred lattice orientation in the rock.
 - Diffusion creep involves diffusion through the lattice (Nabarro-Herring creep) and at boundaries (Coble creep) → change in grain shape (no preferred orientation though), which flattens grains in the direction of maximum compressional stress.
- **Pressure solution:** At low T and low strain rate, minerals where solubility is highly dependent on pressure will dissolve from high P regions to re-precipitate at low P regions, forming **pressure shadows**. E.g. quartz in pressure shadows in garnet porphyroblasts.
e.g. Quartz and feldspars re-precipitate at hinges of folds, and as foliation aligns itself perpendicular to deviatoric stress, we see parallel layering of quartz and micas.



How might mineral textures be used in deciphering the thermal and structural history of an orogenic belt?

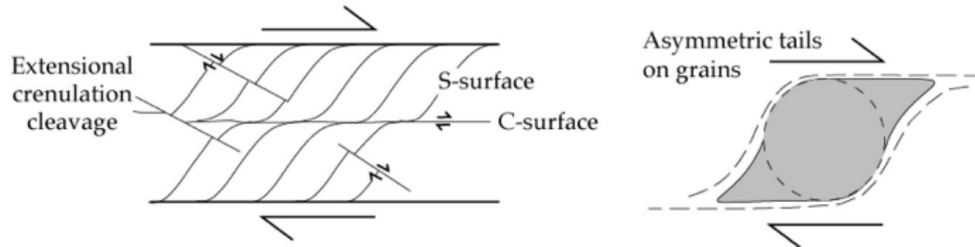
- **Relationship between fabrics and mineral growth:** Porphyroblasts and their inclusion patterns tell us their formation time relative to tectonic activity.
 - Pre-tectonic shows strong deflection of foliation and randomly oriented inclusions.
 - Syn-tectonic shows a continuity in fabric but also evidence of modification during growth. (e.g. Snowball garnets and rotation of the crystal during growth)
 - Post-tectonic shows identical and continuous fabric, as well as a lack of pressure shadows.
- Growth of minerals is closely related to the P-T conditions (due to the metamorphic reactions which produce minerals e.g. garnet isograd, chlorite → garnet + biotite), inform us of the P-T conditions of the belt when deformation happens.



Inferred shear directions

kinematics of deformation — including shear sense and strain intensity

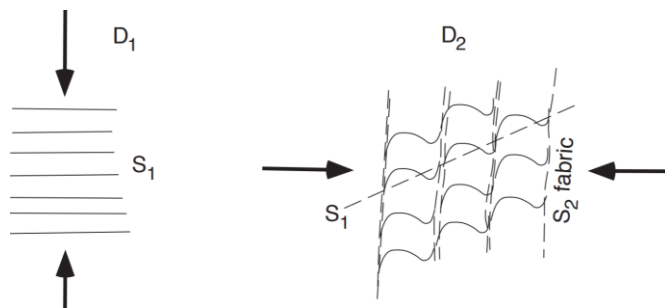
e.g. Sheared gabbros seen at Carrick Luz (Cornwall)



S-C-C' fabrics and mantled porphyroclasts. Based on the orientation of the shear zone and its shear sense → inferred to be an extensional shear zone; relate to Variscan orogeny

Multiple phases of shearing

The effects of overprinting deformation events can include: (1) foliations that are not planar; (2) lineations or fold axes that are curved; (3) ‘refolded folds’(parasitic folds with the wrong ‘sense of vergence’); and (4) complex map patterns called interference structures.



e.g. Trois Seigneurs

Examples: Jessup et 2008

DIFFERENT DEFORMATION REGIMES CAN INFER TEMPERATURE.

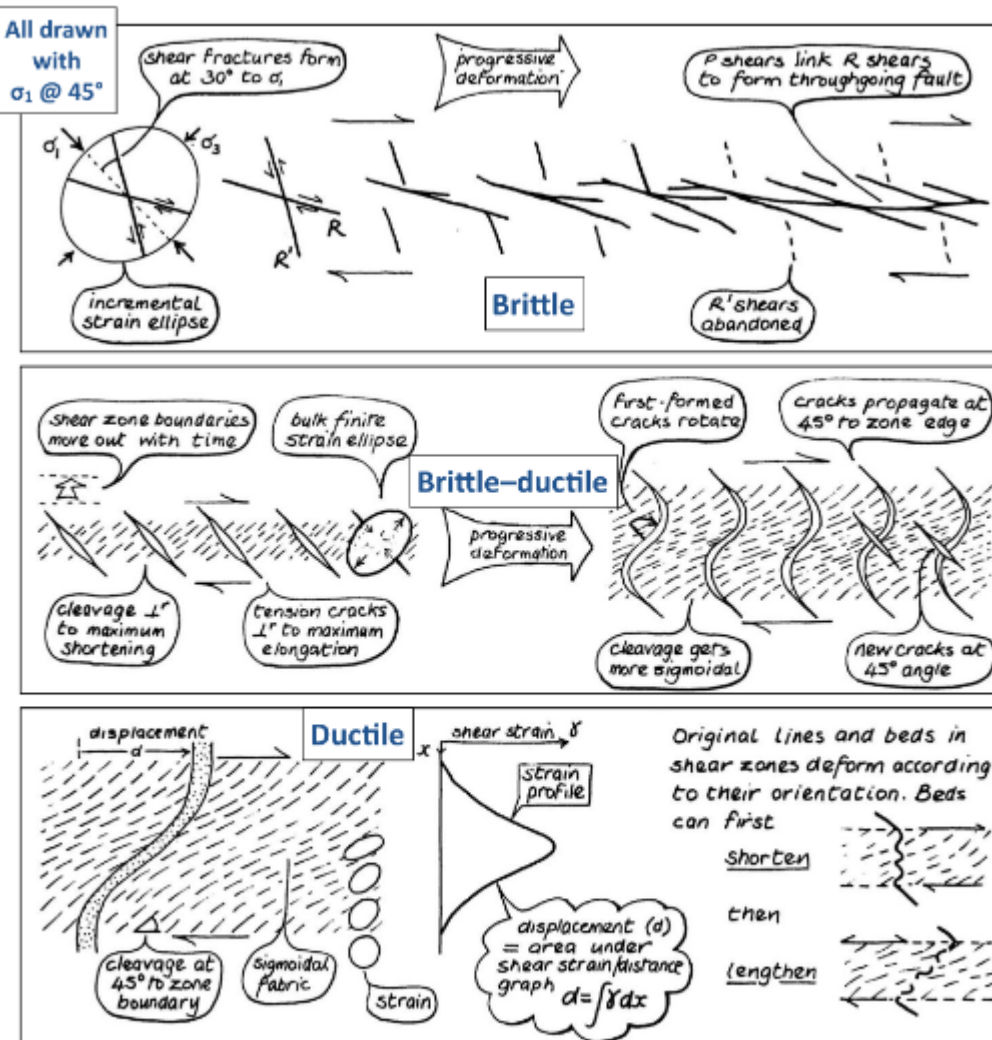
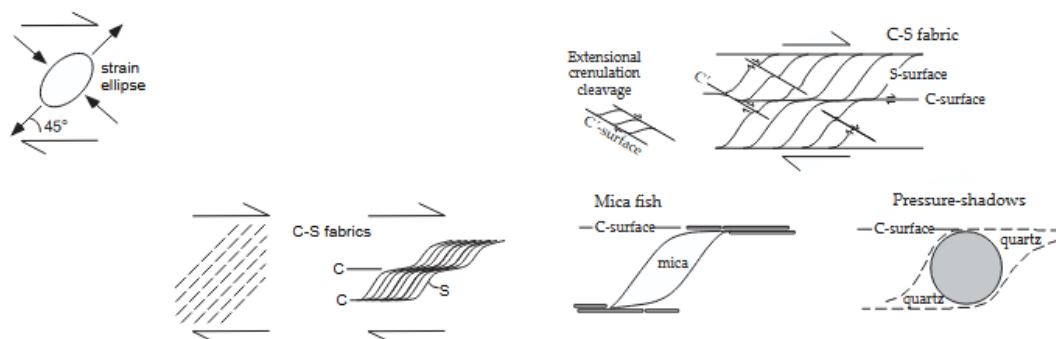


Figure 30: A reminder of the different shear structures formed during brittle, brittle-ductile and ductile deformation.

- Simple shear kinematic indicators include C-S-(C') fabrics, which vary in expression as a function of total strain (e.g. typically C' only at higher finite strain) and protolith (e.g. different minerals have different strengths, monomineralic rocks won't develop composite fabrics as readily):



7. Briefly describe the concept of a “metamorphic facies”. How useful is this concept in decoding the detailed P-T evolution of a geological terrane, and what other lithologies and/or techniques can be used to circumvent any perceived shortcomings? [45 minutes]

9. Define the term “isograd”. Illustrating your answer with examples from pelitic rocks, describe the roles played by bulk composition and temperature in controlling isograds. What features make for a useful isograd? [45 minutes]

Define the term “isograd”.

Lines of a map separating rocks of different grades, usually distinguished by new *index mineral* appearing. (e.g. in Barrow’s zones, chlorite zone → biotite zone → garnet zone → staurolite zone → kyanite zone → sillimanite zone)

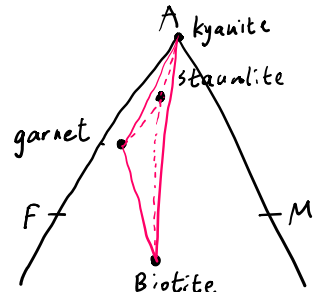
Illustrating your answer with examples from pelitic rocks, describe the roles played by bulk composition and temperature in controlling isograds.

Isograds represent a reaction for the formation of a new index mineral, and therefore the reactions that occur depend on the bulk composition and temperature.

Isograd separation depends on the heat budgets of each region

Whether the rock in a suite will actually ‘see’ the reaction depends also on the bulk composition.

e.g. Kyanite isograd:



e.g. in the garnet isograd, the triangle garnet-chlorite-biotite migrates towards M in the AFM diagram.

e.g. The chloritoid isograd is seldom mapped in metamorphic terranes because chloritoid is relatively rare, only forming in especially Fe-rich pelites.

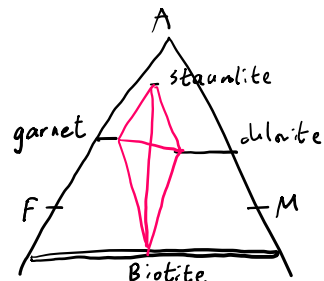
What features make for a useful isograd?

Clear-cut transition in mineral appearance: univariant reactions + discontinuous reactions
(according to Gibb’s phase rule $p + f = c + 2$, if we have $f = 1$ then only one degree of freedom \Rightarrow line on P-T projection)

e.g. Staurolite isograd:



In AFM diagrams, appear as cross tie-line reaction. [here we have four components Al_2O_3 , FeO , MgO , K_2O , and five phases (ignore quartz and H_2O as they are saturated), so $f + 5 = 4 + 2 \Rightarrow f = 1$]



2022

9. (a) Discuss the factors that control the extent of retrogression during the exhumation of a metamorphic rock. Use examples in your answer. [30 minutes]

Speed of exhumation: alps slow -> eclogite to amphibolite, while kokshetau massif eclogites still contain diamonds due to fast exhumation

Fluid availability: drives hydration reactions e.g. granulite to amphibolite. Alps eclogites show amphibole rinds where fluids penetrated shear zones.

Deformation: Creates heterogeneous strain surfaces where energy is higher -> ΔE_a lower.

Grain size: Coarse grains **restrict fluid access** and **less strain surfaces**.

(b) Comment on the way in which retrogressed assemblages may still retain information about peak metamorphism. [15 minutes]

Not completely reacted minerals, inclusions in minerals, partial and full pseudomorphs,

Stonehaven coast → low field metamorphic gradient and therefore goes below the Al_2SiO_5 invariant point and we see andalusite.

2023

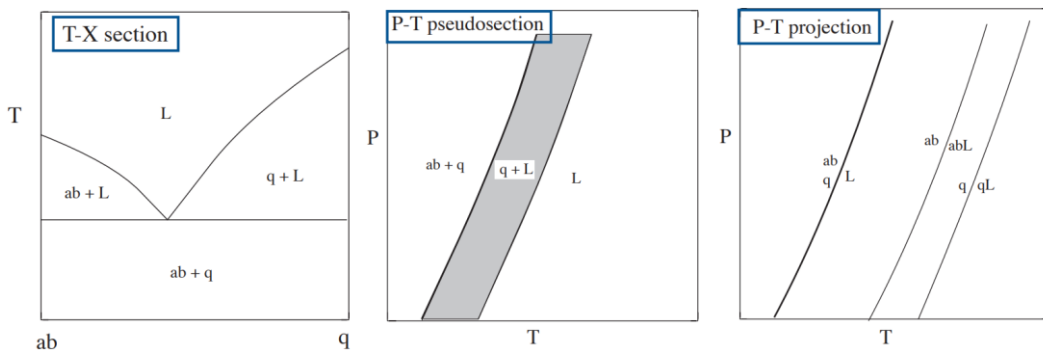
5. (a) Typical pelites are composed of at least 11 different major oxides, yielding a total phase diagram featuring at least 12 dimensions. What approaches can be used to overcome the problem of visualising such a phase diagram, and what are the advantages and disadvantages of each approach? [30 minutes]

Need 10 axes for the composition and 1 for P and 1 for T \rightarrow 12 dimensions in total.

In each approach, we reduce the number of dimensions in various ways, but in any case, we are always bound to lose some information about the system.

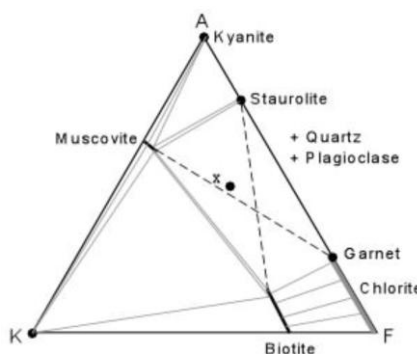
Approach 1: Graphical analysis

- **T-X section:** a section through space at a constant P and thus loss of P information. Equivalent P-X sections are also possible, with consequent loss of T information.
- **P-T pseudosection,** section at constant bulk composition \rightarrow loss of information about all other possible bulk compositions.
- **P-T projection,** which involves projecting all invariant points and univariant equilibria (including those in subsystems) for all compositions onto a P-T plane. Only discontinuous reactions are shown on these kinds of diagrams, so information about continuous reactions is lost.



Approach 2: Model systems / Reduction of system

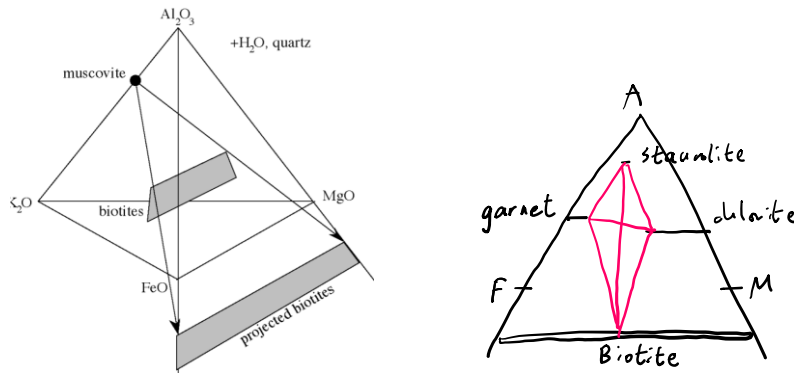
- Ignore minor oxides (e.g. CaO and Na₂O) \rightarrow KFMASH for metapelites (K₂O, FeO, MgO, Al₂O₃, SiO₂, H₂O). Treat some phases as being in excess, such as SiO₂ (quartz) and H₂O. Makes a compatibility diagram (tetrahedron for now) where stable phases are joined by tie lines.
- Combine system components (e.g. FeO and MgO because they have similar size and same charge). \rightarrow AKF diagram. A = Al₂O₃, K = K₂O, F = FeO + MgO. (We use CaO instead of K₂O for metabasites)
 - Problem: Mg/Fe sometimes behaves independently, and therefore we may have the phase rule violated (because really $c = 4$). E.g. in the following, x composition is in a 4-phase field, while divariant equilibrium requires $c = 3$.



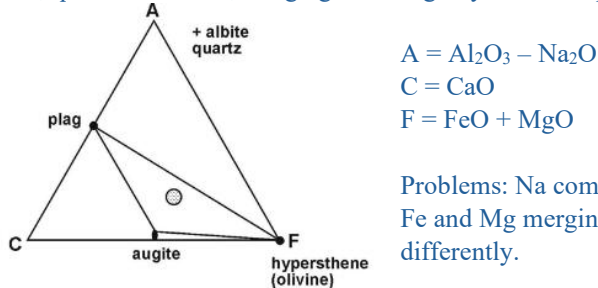
- Project from excess muscovite \rightarrow Thomson AFM diagram. A = Al₂O₃ – 3 K₂O, F = FeO, M = MgO. Each diagram is drawn at a specific P and T condition but contains all composition. By comparing

between the diagrams (e.g. in different Barrow zones) can infer reactions in changing P, T conditions by inferring the rearrangement of tie lines (e.g. Staurolite isograd).

- Problems: K-feldspar is $-\infty$ from A. At high temperatures, muscovite is replaced by K-feldspar + quartz + Al_2SiO_5 . Then cannot project from muscovite anymore.



- Similarly, can use NCFMASH system for metabasites. We can reduce dimensions by projecting from albite, quartz and water, merging Fe & Mg to yield 3 component system



Problems: Na components in other phases not represented, and Fe and Mg merging ignores the fact that Fe and Mg partition differently.

- (b) Phase diagrams represent an equilibrium state. To what extent does this assumption apply to metapelites, and what petrographic observations can be used to distinguish possible disequilibrium features in samples? [15 minutes]

KINETIC BARRIERS to equilibrium

Incomplete diffusion \rightarrow chemical zoning. - Garnet

Arrested retrograde reactions during rapid exhumation. – Preservation of metastable phases, symplectites

FLUIDS

Metabasites & Blueschists (L39 & 40)

2018

8. Why are blueschists regarded as indicators of fossil subduction zones when the eclogites that are frequently found with blueschists are not? Explain how and why these two rock types are commonly found together.

Blueschists are formed under high pressures, which is only found usually in a subduction accretionary wedge, because we need the following reaction (piercing plane)



We need to raise the pressures high without increasing the temperatures, i.e. quick subduction. However, eclogites are typically formed in any scenarios as long as the pressure is high enough, and many P-T paths can cover that part, such as in intense mountain-building events, (e.g. today's Himalayas, western alps), or it can be found in most lower crust settings with amphibolites and granulites (e.g. Glen Elg), or even just as a mantle xenolith (e.g. Kimberly in South Africa). Therefore, blueschists are more indicative of the setting.

These two phases are found together in subduction zones (e.g. Franciscan complex) because of the **high pressure**. Continued subduction of blueschist facies oceanic crust will produce eclogite facies assemblages in metamorphosed basalt, by the piercing plane reaction:



Alternatively, in retrograde metamorphism the blueschist metamorphism is overprinted over the eclogite facies metamorphism, resulting in these two found together

They could also be found together because variations in the original composition of the rocks, such as the amount of CaO (calcium oxide), can influence whether a blueschist or eclogite assemblage develops, even under similar pressure-temperature conditions. For example, higher CaO content favours eclogite formation, while lower CaO content may lead to blueschist formation

2020

9. Compare and contrast the metamorphic and tectonic development of blueschists and granulites. [45 minutes]

Metamorphism from greenschists: Blueschists tend to be formed from greenschists through conversion of actinolite into glaucophane. This is a piercing plane reaction:



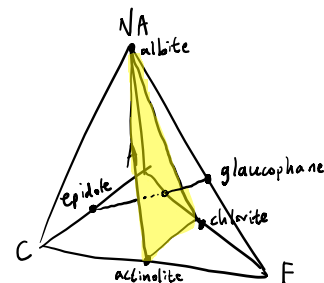
(This is a dehydration reaction, common in subduction zones)

Fairly low temperature reaction as evidenced from the fine grained textures, and the maintenance of original schistosity of the greenschists.

Granulites are typically formed from increasing pressures / temperatures from amphibolite facies, (which feature mainly oligoclase + hornblende), through the breakdown of hornblende:



This reaction can only happen if H₂O activity is low (as this reaction is H₂O producing). Granulite facies therefore requires dry conditions, i.e. H₂O is usually removed from earlier partial melting. This happens a lot in continental collisions where wet melting drives water away. (Only in exceptional circumstances, such as the observations of charnockite in Indian quarries do we see presence of CO₂ reducing water activity)



Tectonic settings: Blueschists are formed at high-pressure, low-temperature settings (common in subduction zones, like the Franciscan complex), whereas granulites are formed at high temperature, high pressure regimes (typically in thick crusts and heavy orogenic activities, found in many of the oldest cratonic roots today). Examples include the granulite xenoliths found in adakitic (derived from melting the lower crust) and shoshonitic (derived from melting the upper mantle) dykes in the Himalayas, where 80 km-thick crust allowed for very high pressures and temperatures allowed high grade metamorphism.

2021

8. What controls the microstructure of metamorphic rocks? How and why does the microstructure typical of a granulite differ from that typical of a blueschist? [45 minutes]

Controls to microstructure

Many factors: Protolith, pressure-temperature conditions, fluids, time, deformation & stresses

Mineral assemblage: Controlled by the original rock composition, the P-T conditions and presence/absence of fluids determine the reactions that happen → control the final mineral assemblage.

Differences between granulite and blueschist

High temperatures and low temperatures comparison → difference in grain size, and textural equilibration (interlocking grains / granoblastic texture)

Reaction rates, reaction textures

Time → Ostwald ripening into larger grain sizes, metastable states

Foliation

2022

7. (a) Compare and contrast the metamorphism of pelitic versus metabasic protoliths. [25 minutes]

- Metapelites show marked changes across P, T in terms of mineralogical changes (Barrow zones); metabasite facies correspond to multiple Barrow zones, less index minerals
- Metabasites exhibit a range of solid solutions due to the structural flexibility of amphiboles: can construct many geothermometers, contrast to mostly Fe/Mg exchange in pelites
- Metabasites are good for preserving high P processes.

Having both pelitic and basaltic protoliths gives multiple compositions to determine PTX relations to deduce tectonic processes.

(b) Discuss how protolith heterogeneity, water content and grain size may influence the fabrics and assemblages developed at a range of pressures and temperatures. [20 minutes]

Wet melting affected by water content

Wet melting / solidus: water is present as a **free phase reactant**. Ceases when H₂O runs out (red)

e.g. K-feldspar + muscovite + H₂O + quartz → L

e.g. possible to retain unmodified basaltic assemblage under greenschist P-T conditions if rock is dry

Dehydration reactions and wet melting affected by protolith chemical heterogeneity

Dehydration melting: water is absent but still involved in the breakdown of **hydrous phases**.

e.g. muscovite + quartz → H₂O + sillimanite + K-feldspar + L (Subsolidus dehydration seen in Trois-Seigneurs)

e.g. sillimanite + biotite + qtz → garnet + cordierite + L

Wet melting:

Anorthite + hypersthene + H₂O → actinolite + chlorite

Augite + chlorite + H₂O → actinolite + epidote

Possible to find relict igneous minerals in greenschists because fluid infiltration is non-pervasive (hence heterogeneous)

Protolith physical heterogeneity also enhances fluid flow facilitating wet melting

Grain size probably affects surface area of reaction

Therefore facies boundaries are fuzzy

2023

6. (a) Describe the mineralogical and microstructural changes that typically occur during the metamorphism of a basalt through the greenschist, amphibolite and granulite facies. [35 minutes]

Greenschist Facies

- Mineralogy:
 - Chlorite, albite, epidote, actinolite, (sometimes titanite, and calcite)
 - Anorthite + Hypersthene + H₂O → **Actinolite + Chlorite**
 - Augite + Chlorite + H₂O → Actinolite + **Epidote** (or clinzoisite in reducing conditions)
 - Secondary reactions: ilmenite -> titanite and actinolite + epidote -> calcite and chlorite
- Microstructural changes (dominated by reactions as T low)
 - Reactions involve hydration of basaltic minerals → igneous minerals remaining as fluid may not permeate through whole rock. However, pseudomorphs of pyroxene replaced amphibole etc.
 - Fine-grained textures (from recrystallisation)
 - Deformation fabrics (e.g. alignment of platy minerals) indicating fluid flow that aid reactions.

Amphibolite Facies

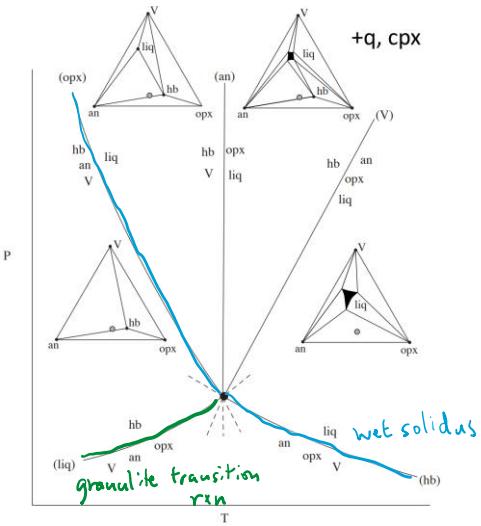
- Mineralogy:
 - Hornblende, garnet, oligoclase (calcic plagioclase), and residual chlorite.
 - Actinolite → Hornblende (requires Al, via Tschermak substitution MgSi-AlAl and edenite exchange Si-NaAl).
 - Albite → Oligoclase
 - Excess chlorite forms garnet.
 - High P: amphibole transition first, low P: Plag reacts first
- Microstructure
 - The green chlorite and actinolite of the greenschist facies are replaced by darker minerals, giving rocks a darker appearance.
 - Coarser grain size compared to greenschist facies.
 - Approach towards textural equilibrium, plus no water needed in these reactions → deformation not necessary

Granulite Facies

- Mineralogy:
 - Orthopyroxene, clinopyroxene, plagioclase
 - Granulites form only under dry conditions (low water activity).
- Microstructure (high T → dominated by textural equilibrium)
 - Granoblastic texture of equigranular interlocking grains, often forming 120° triple junctions which minimises surface energy → no fabrics
 - Gneissic / magmatic texture → Banding may occur as segregation of minerals (allowed through diffusion of minerals which tend to group together to reduce surface energy)
 - Melting may occur

(b) Why and how does the ACF projection need to be modified to model the higher temperature evolution? [10 minutes]

- In amphibolite to granulite transition, water is a variable, as water leads to wet melting in amphibolites (cannot see granulites). The ACF is projected from water, albite and quartz, so the ACF projection needs to be modified.
- The ACF projection is modified by projecting all of the phases from cpx onto the anorthite-orthopyroxene sub-system binary (because cpx is present in all assemblages). Then H₂O can be added as a component to return the system to three effective components → CA-V-FM plot
- The invariant point is shifted up as H₂O content decreases, and so the granulite phase field is shifted up, showing the dependence on water content – explain the occurrence of granulites in orogens, where partial melting in crustal thickening drives water away into the melt and melt is removed.



2024

7. (a) Compare and contrast the mineralogical and textural evolution of a greenschist converting into: (i) a blueschist; and (ii) an amphibolite. [30 minutes]

Greenschist → amphibolite (increase in T)

- (i) actinolite gains Al from chlorite and albite by Tschermak substitution ($Mg + Si \rightarrow Al + Al$) + edenite exchange ($\square Si = NaAl$, where \square represents an A-site vacancy in the amphibole structure) and becomes hornblende (a continuous reaction involving the sliding of actinolite)
- (ii) plagioclase gradually increases in anorthite content at the expense of epidote (albite \rightarrow oligoclase)
- (iii) any excess chlorite is used to form garnet.

Textures: (1) Coarser grain size compared to greenschist facies. (2) The green chlorite and actinolite of the greenschist facies are replaced by darker minerals, giving rocks a darker appearance. (3) Approach towards textural equilibrium (due to thermodynamic considerations, entropy becomes an important factor) \rightarrow not much fabrics

Greenschist → blueschist (increase in P)

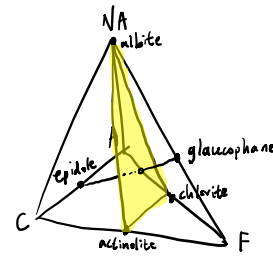
Reaction is actinolite + albite + chlorite \rightarrow glaucophane + epidote (dehydration reaction). A piercing plane reaction, hence univariant and discontinuous.

Low temperature + subduction zone \rightarrow (1) commonly fine-grained and (2) feature reaction textures. For instance, in the practical we have seen chlorite replacing garnet (pseudomorphs), or glaucophane forming rims on green amphiboles. (3) Due to low temperatures it is also not rare to find growth zoning preserved.

(4) Also can find deformation textures, retaining the schistosity from greenschist, and glaucophane will show alignment.

(b) Both the blueschist and amphibolite facies span a wide range of pressures. For each facies, suggest what mineralogical criteria you could apply to determine whether a sample was metamorphosed at relatively low or high pressures. [15 minutes]

All reactions in the above are essentially divariant and occur at a range of temperatures despite being depicted as univariant – this is because if we add in more phases, this guarantees the increase in degrees of freedom. Therefore, the different minerals could indicate the completion of (transitional) reactions.



	Low P	High P
Amphibolite	Chlorite / epidote, oligoclase	Garnet, Kyanite
Blueschist	Epidote, albite	Jadeite, Lawsonite, white micas, aragonite (from calcite)

Trois Seigneurs, Barrow Zones, Himalayas

2018

6. At the highest grades metamorphism culminates in the formation of granites by partial melting. Using appropriate examples such as the Himalaya discuss the role of water in the development of large granite bodies and the production of anhydrous assemblages in the deep crust.

2020

10. With reference to the Himalaya discuss why the typical Barrovian isograd sequence can be more complex than the type locality from the Highland Boundary Fault in Scotland. [45 minutes]

2021

6. Give a brief account of the inverted metamorphic gradient observed in the Himalayas. Discuss the evidence both for, and against, the different hypotheses suggested to explain this inverted gradient. What further information is required to settle the controversy? [45 minutes]

10. High-grade metamorphism commonly culminates in the formation of a melt. Discuss the different reactions resulting in melting of a pelite, and how they might be identified in thin section. Illustrate your answer with examples from Trois Seigneurs and the Himalayas. [45 minutes]

2022

8. (a) Compare and contrast the metamorphic field gradient developed in the Barrow Zones of Scotland versus the Trois Seigneurs region of the Pyrenees. [15 minutes]

(b) What were the key factors controlling any identified differences in the metamorphism of the two regions? [15 minutes]

(c) Discuss how and why the Variscan metamorphism observed on the Cornwall field trip differs from these two case studies. [15 minutes]

10. (a) Give an account of the relationships between tectonic structure and metamorphic grade in the Himalayas. [25 minutes]

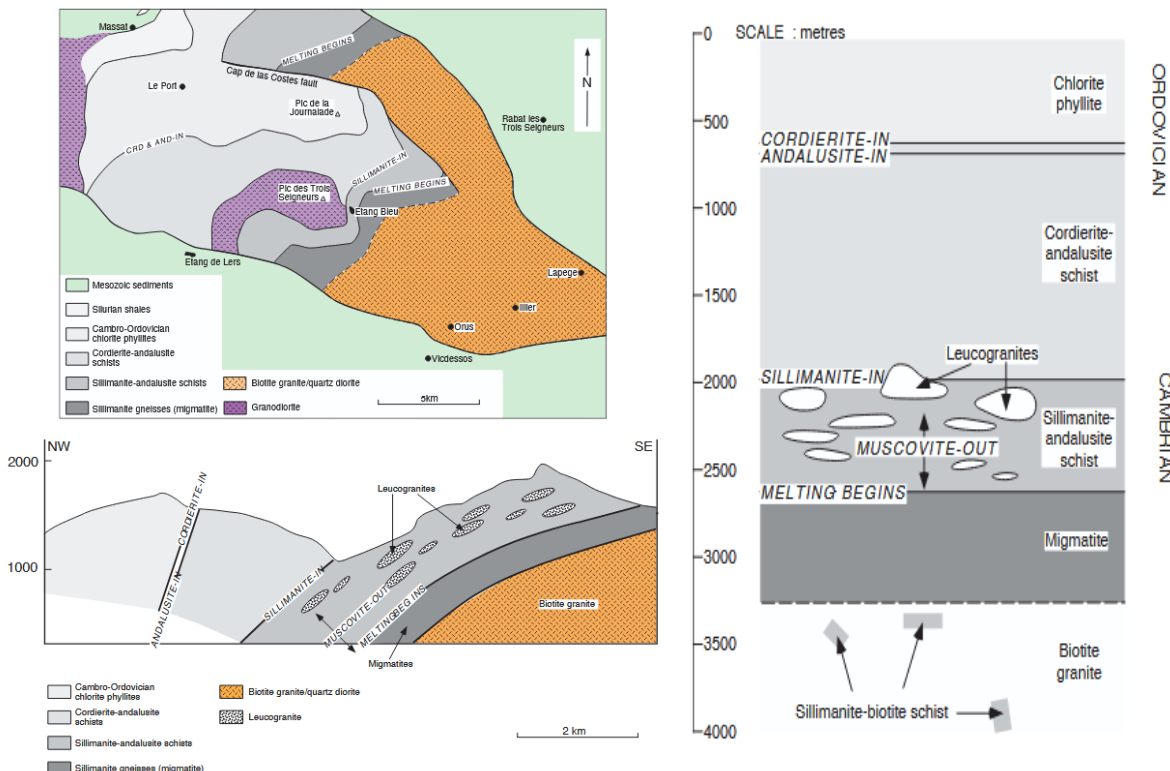
(b) What information does this provide about the mechanisms by which the Himalayas formed? [20 minutes]

2023

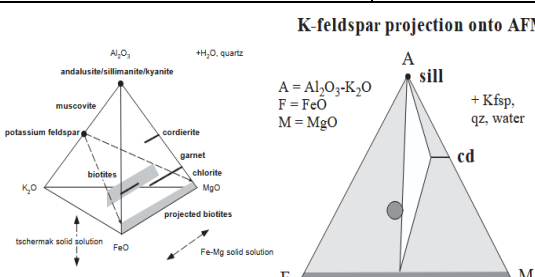
7. (a) What melt reactions can occur in metapelites? What factors control how much melt is produced for each of these reactions, and how may the reactions be differentiated in the field? [20 minutes]
 (b) Compare and contrast the timescales and dominant reactions involved in partial melting in the Trois Seigneurs and the Himalayas. [25 minutes]

Use **mineral assemblages** in metapelites to constrain mineral reactions that took place to determine PT gradient

TROIS-SEIGNEURS: Formed during Variscan orogeny, total time scale of 60 Mya.

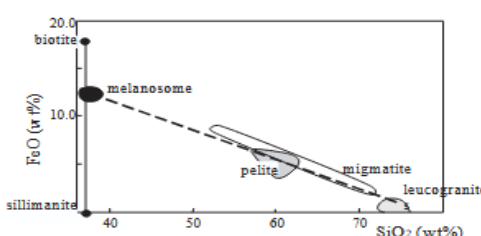


Lower grade (X out)	Higher grade (Y in)	Isograd reaction
Chlorite phyllite: Chl + bi	Cordierite schist: cd + chl + bi, cd + bi	Chl \rightarrow cd + bi; Continuous (intermediate assemblage shown)
Cordierite schist: Cd + bi	Andalusite-cordierite schist: Cd + bi + and, bi + and	Cd \rightarrow and + bi; continuous
Andalusite-cordierite schist: bi + and	Sillimanite-andalusite schist: bi + si	And \rightarrow sill: discontinuous as c = 1, p = 2, so f = 1



At higher temperatures, muscovite reacts out:
 $mu + qz \rightarrow ksp + sill + H_2O$

This invalidates AFM projection from mu; mu was always assumed to be inert, but now it is reacting. We hence project from another point (ksp), giving us A'FM projection. Note coordinates of A are generated by $Al_2O_3 - K_2O$ (instead of $-3K_2O$) and biotite is inside the triangle.



At higher temperatures still, **melting begins**:

bi + sill \rightarrow liq. Lenses of felsic material are rimmed by edges of bi + sill. This suggests the pelite has **segregated into two parts** because of melting reaction: leucosome = melt. It is now a **migmatite**. Further evidence of melting: some leucogranites are seen in upper layers, interpreted as melt which intruded into higher structural levels.

At even higher temperatures, migmatites grade into biotite granite. Evidence that granite comes from melting and not from emplacement:

- Proportion of leucosomes in migmatite get higher the closer they are to granite
- Contains xenoliths of biotite-sillimanite melanosome.
- Biotite granite contains up to 40% biotite; highly peraluminous, S-type.

Melting is only possible at this PT with water – generated as mu reacts out.

The gradient $\frac{dT}{dz} = 100^\circ\text{C}/\text{km}$ – this heat flow is high.

Tectonic conclusion: High heat flow, extensional fabrics suggest tectonic setting which involves stretching of lithosphere and upwelling of hot asthenosphere. Hence, extensional faulting in a rift zone.

8. (a) Discuss what reactions make for an ideal isograd. [10 minutes]

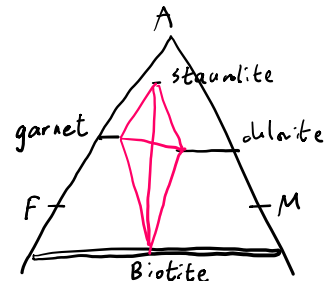
Clear-cut transition in mineral appearance: univariant reactions + discontinuous reactions (according to Gibb's phase rule $p + f = c + 2$, if we have $f = 1$ then only one degree of freedom \rightarrow line on $P-T$ projection)

e.g. Staurolite isograd:

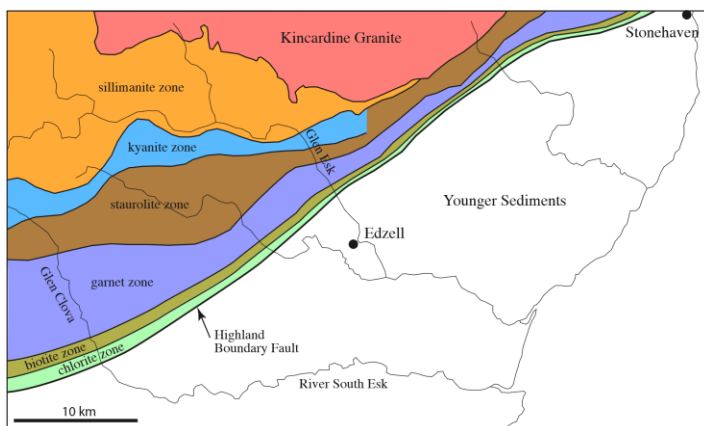


In AFM diagrams, appear as cross tie-line reaction. [here we have four components Al_2O_3 , FeO , MgO , K_2O , and five phases (ignore quartz and H_2O as they are saturated), so $f + 5 = 4 + 2 \rightarrow f = 1$]

Also, minerals should be easily recognizable and abundant for a certain composition. E.g. chloritoid only found in Fe-rich rocks specifically so not often mapped



(b) Describe and account for the mineralogical changes that occur in the Barrow Zones of Scotland. What factors may be contributing to the observed along-strike variation in isograd sequences and widths? [30 minutes]

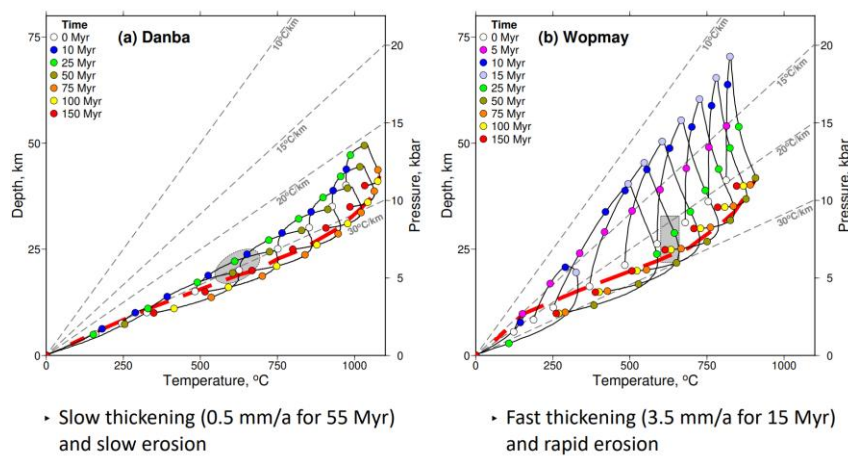


- **Chlorite Zone:** (simple greenschist facies).
- **Biotite Zone:** + biotite (continuous)
 $\text{chlorite} + \text{K-feldspar} \rightarrow \text{muscovite} + \text{biotite}$
- **Garnet Zone:** + garnet (continuous)
 $\text{chlorite} \rightarrow \text{biotite} + \text{garnet}$

- **Staurolite Zone:** + staurolite – chlorite
chlorite + garnet → biotite + staurolite (discontinuous)
- **Kyanite Zone:** + kyanite
chlorite + staurolite → biotite + kyanite (discontinuous)
- **Sillimanite Zone:** + sillimanite – kyanite (discontinuous)
kyanite → sillimanite

Along-strike variation in isograd sequences and widths

- Physical conditions varying along the strike: different crust-building rates, radiogenic heat flows
 - e.g. lower rate of heat flow, could lead to wider isograd spacing
 - e.g. Andalusite-bearing zone in the east of the Scottish Highlands (Buchan zone) due to the lower pressure conditions.



- Deformation post-metamorphic peak condensing the isograds (e.g. in a wide ductile shear zone), plus erosion rates exposing different grades of the metamorphic rocks
- Also contact metamorphism (e.g. Glen Clova in Scotland)

(c) What are the potential pitfalls involved in interpreting isograd maps? [5 minutes]

- **Composition variations:** Isograd maps have to be considered not with the view that the protolith composition is constant across the region; variability in this bulk composition could vary the isograd, i.e. cause the same isograd-forming mineral to appear at different conditions, complicating the interpretation.
- **Overstepping in metamorphic reactions:** Reactions occur after their equilibrium P, T conditions are surpassed (in non-equilibrium conditions), due to kinetic effects → shifts the isograds from their true equilibrium position, inference e.g. appearance of Garnet
- **Structural Complexity:** Folding, faulting, and deformation can displace isograds, making it difficult to reconstruct the original metamorphic sequence. E.g. In the Himalayas we see inverted isograds but they could be just because of a fold, and the isograds lie in the inverted limbs of the fold.

2024

6. (a) What are the principles and assumptions of the AFM projection as applied to metapelites? [10 minutes]

(b) How and why is the AFM projection changed to model metapelites in the amphibolite and granulite facies? [5 minutes]

(c) Discuss how AFM projections can be used to understand the reactions controlling the sequence of mineral assemblages observed in the Barrow zones of Scotland. [30 minutes]

Geochronology and Thermobarometry

2022

6. (a) Discuss methods by which the timescales of metamorphism can be determined. [15 minutes]

DIRECT DATING: $D_t = D_0 + N(e^{\lambda t} - 1); t_{1/2} = \ln(2) / \lambda$

Geochronology gives **absolute age** of mineral formation. requires determination of **isotopic ratio**:

- ID-TIMS (isotope dilution – thermal ionisation): most precise but slow, loses petrographic context, mixes domains – best for igneous crystallisation ages and not for metamorphism
- SIMS (secondary ion): non-destructive but can only analyse small amounts at a time
- LA-ICP-MS (laser ablation): fast but destroys sample. But an advantage is that it can collect isotopic and trace element data at the same time.

The latter two methods are best for metamorphism as they are **accurate**

Decay equations can then be solved if concentrations of U, Th, Pb determined along with isotopic composition.

We can use the Uranium, Actinium and Thorium decay series (which produce different Pb isotopes) and reference it against non-radiogenic ^{204}Pb to get 3 ages: in an ideal closed system, the ages should be concordant

TRACE ELEMENT ANALYSIS

Petrological constraints can reveal **relative timing of mineral growth**. additional trace element data may be useful in determining the **meaning** of PTt dates, attaching time periods to specific metamorphic events.

e.g. absence of Eu anomaly in eclogite means corresponding age occurred beyond stability of feldspar (as feldspar preferentially incorporates Eu) – and means it was during peak metamorphism)

e.g. HREE fractionation indicates co-crystallisation with garnet-bearing assemblage (as garnet eats up HREEs)

(b) What are the challenges associated with this task, and how can they be overcome? [15 minutes]

Assumes system has remained **closed**: sometimes system resets due to heating or fluids.

Assumes decay constants are known **accurately** (good assumption as decay takes place in nucleus which is independent of chemical environment)

Assumes **initial concentration of daughter isotope** is known

Will only get one age if mineral is homogeneous – cannot determine PTt path but time of only one point

Analytical limitations: ICP-MS requires a decently sized sample which sometimes may not be available

Solutions: Use SIMS, and date multiple minerals with contrasting closure temperatures to get a good picture of PTt path

(c) What features make for an ideal geochronometer. [15 minutes]

The closure temperature is the temperature at which system is closed wrt daughter isotope (no longer diffuses)

- High closure temperature is best for dating peak metamorphism / events at high temperatures. Zircon and monazite are good for this.
- Low closure temperatures are best for dating retrograde metamorphism, as the system closes later. Good minerals for this are rutile and apatite.
- Low concentration of daughter isotope at $t = 0$: very important
- Minerals with crystal lattices that permit tetravalent ions (U^{4+}) but do not allow bivalent ions (Pb^{2+}) are suitable, as this means they contain very little Pb when they form
- High chemical and mechanical resilience
- Bonus: one mineral can serve as a geochronometer in different points in PTt space if it grows at multiple points during prograde and retrograde metamorphism. (Zircon, monazite – zoning evident)
- U-Pb decay scheme best for geochronology when hosted by zircon and monazite

2024

5. (a) Explain why measuring U-Pb isotopic ratios in zircon crystals is one of the most widely used geochronological techniques. [20 minutes]

- **Closure temperature:** High closure temperatures ($>700^{\circ}\text{C}$), diffusion no longer occurs below this temperature, so the isotope clock faithfully records the date at which the rock is formed. Less likely to be reset by metamorphic events, which may bring the rock to higher temperatures and potentially resetting some chronometers (e.g. Rb-Sr biotite)
- **U-Pb Half-life:** Long half life, not likely to be extinct, and can date up till the start of the Earth history (e.g. 4.4 Ga zircon in Jack Hills, Australia)
- **Zircon abundance:** Zircon is a common accessory mineral in rocks. It has a high mechanical and chemical resilience, so it is preserved in high-grade and polymetamorphosed rocks.
- **Zircon lattice:** Permit tetravalent ions with moderate octahedral radius (U^{4+}) but not larger bivalent ions (Pb^{2+}). When they form, very little initial Pb, and hence large ratios of U/Pb for analysis.

(b) What are the challenges of dating the timing of metamorphic events, and how can these challenges be overcome? [25 minutes]

8. (a) Discuss the advantages and disadvantages of four different thermobarometric methods. [20 minutes]

*All methods require equilibrium to be attained at peak metamorphism + require precise calibration

	Advantages	Disadvantages
Exchange reaction thermobarometry	<ul style="list-style-type: none"> • Gives both P and T • Inclusions in zoned crystals can provide P-T paths • Can use different reactions to together constrain (good thermometer + good barometer) • Garnet is very often available 	<ul style="list-style-type: none"> • Assumes compositions of minerals analysed are same as that at peak metamorphic conditions • Zoned crystals: crystal heterogeneous and entire composition not representative of peak PT condition
Solvus thermometer (e.g. Ca-Mg exchange between clino, orthopyroxene)	<ul style="list-style-type: none"> • Can be very precise if exsolution is evident in the system. 	<ul style="list-style-type: none"> • We need this system to be present, i.e. usually only basic protoliths and high grades • Cannot tell pressures (need to know pressure first)
Petrogenic grids	<ul style="list-style-type: none"> • Wide range of P-T available, covers essentially all metamorphic facies 	<ul style="list-style-type: none"> • Only rough estimates → only the grid it is in • Choice of chemical elements / phases might be too simplified at times
Single phase thermobarometry	<ul style="list-style-type: none"> • Can also determine zoning in porphyroblasts and the P-T path 	<ul style="list-style-type: none"> • Can be sensitive to other phases, and not always can give both P and T

(b) Explain why garnet-bearing samples are typically chosen for thermobarometry. [10 minutes]

- **Dense structure:** In reactions can produce large ΔV , such as in the GASP geobarometer, which utilises the reaction

$$\text{grossular} + \text{kyanite} + \text{quartz} \rightarrow \text{anorthite},$$
 which has a large ΔV . As the slope of isopleths in P-T space is dependent on $(\Delta S - RT \ln K)/\Delta V$, this gives a flatter slope which makes the lines more sensitive to changes in P.
- **Preference of Fe over Mg:** At lower T, Fe is preferentially partitioned into garnet (rather than biotite), and at high T, there is no more preference. This contrast in behaviour allows for high sensitivity in garnet-biotite geothermometry, which depends on

$$K = \left[\frac{(\text{Mg}/\text{Fe})_{gt}}{(\text{Mg}/\text{Fe})_{bi}} \right]^3$$

- **Slow lattice diffusion:** Small values of D , so diffusion length $x \sim \sqrt{Dt}$ is short, and so it can preserve successive stages of equilibrium and record stages of metamorphism.
- **Poikiloblastic form:** It traps many minerals which are from previous assemblages and **preserves different P-T conditions** (inclusions are isolated from physiochemical change affecting rocks during metamorphism) thus allows reaction thermobarometry to be done effectively.

(c) How might information be extracted from metamorphic samples about pressure-temperature paths? In what metamorphic facies are pressure-temperature paths likely to be most faithfully recorded? [15 minutes]

MINERAL ASSEMBLAGES AND STABILITY FIELDS

CHEMICAL ZONING

REACTION TEXTURES AND MICROSTRUCTURES

Granulite facies: Long duration metamorphism at high T. Exhibit granular microstructures.

Eclogite facies: Short duration metamorphism at low T. Fine grained microstructures, less texturally equilibrated

GEOTHERMOBAROMETRY

Two things:

- Short duration of peak metamorphism also means **prograde zoning** is preserved and not homogenized.
- Fast exhumation means better preservation of peak conditions and no retrograde metamorphism occurs.
- **BLUESCHIST and ECLOGITES** are created at subduction zones. They are often exhumed quickly to the surface and hence time spent at retrogression temperature is short. Able to preserve delicate high pressure minerals, like lawsonite or omphacite.
- **GRANULITES** are bad for this reason: often held at high T for long times, diffusion is able to occur, wiping out chemical zoning.
- **GREENSCHIST** often experience slower protracted cooling and hence have time to re-equilibrate or be replaced. However, this gives information on retrograde PTt: rim compositions and textures mean a certain amount of time must have been spent during cooling.

10. The reaction grossular + aluminosilicate + quartz = anorthite is a commonly used geobarometer, where the chemical formula of grossular is $\text{Ca}_3\text{Al}_2\text{Si}_3\text{O}_{12}$, and anorthite is $\text{CaAl}_2\text{Si}_2\text{O}_8$.

With entropy (ΔS) and volume (ΔV) approximately constant for a solid-solid reaction the formula:

$$\Delta G^0_{P,T} \approx \Delta H^0_{1\text{bar}} - T \Delta S^0_{1\text{bar}} + P \Delta V^0 \quad (\text{Eqn 1})$$

describes the relationship between the Gibbs free energy G, the enthalpy, H, pressure P and temperature T. Recall that chemical potential μ , is related to the Gibbs free energy, equilibrium constant K and the molar gas constant R by the relationship:

$$\Delta \mu = 0 = \Delta G^0 + RT \ln K \quad (\text{Eqn 2})$$

For the reaction grossular + aluminosilicate + quartz = anorthite:

$$\Delta H_{1\text{bar}} = 50.8 \text{ kJ mol}^{-1} \quad \Delta S_{1\text{bar}} = 0.1546 \text{ kJ K}^{-1} \text{ mol}^{-1}$$

$$\Delta V = 6.62 \text{ kJ kbar}^{-1} \text{ mol}^{-1} \quad R = 0.0083145 \text{ kJ mol}^{-1} \text{ K}^{-1}$$

Two rock samples (A and B) containing calcium bearing garnet, kyanite, quartz and plagioclase were collected from the Main Central Thrust region of the Himalaya from Central Nepal. The regional fabric in the vicinity of the samples is near vertical, and the samples have a stratigraphic separation of 5km from each other.

The plagioclase and garnet compositions were determined as follows:

Sample A

Plagioclase $\text{Na}_{0.85}\text{Ca}_{0.15}\text{Al}_{1.15}\text{Si}_{2.85}\text{O}_8$

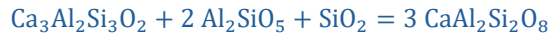
Garnet $(\text{Ca}_{0.06}\text{Fe}_{2.38}\text{Mg}_{0.56})\text{Al}_2\text{Si}_3\text{O}_{12}$

Sample B

Plagioclase $\text{Na}_{0.90}\text{Ca}_{0.10}\text{Al}_{1.10}\text{Si}_{2.90}\text{O}_8$

Garnet $(\text{Ca}_{0.12}\text{Fe}_{2.1}\text{Mg}_{0.78})\text{Al}_2\text{Si}_3\text{O}_{12}$

Write a balanced chemical reaction for: grossular + aluminosilicate + quartz = anorthite



ii) Write down an expression for the equilibrium constant, K, as a function of the activities of grossular, aluminosilicate, quartz and anorthite.

$$K = \frac{(a_{an})^3}{(a_{gr})(a_{al})^2(a_q)}$$

iii) Assume that the activity of anorthite is equal to the mole fraction of anorthite (X_{an}). For garnet, recall that the ideal formula contains 3 Ca ions, so that the activity of grossular is equivalent to $(X_{gr})^3$, where X_{gr} is the mole fraction of grossular in garnet. Calculate the equilibrium constants for sample A and sample B.

Where mixing is ideal, activity equals molar fraction $a_i = X_i$

For molecular mixing (coupled substitutions) the activity is the probability of encountering a CaAl pair (an). For ideal ionic mixing the activity is given by the probability of finding randomly distributed atoms in the right sites to form the correct endmember.

For sample a, $a_{an} = 0.15$, $a_{gr} = \left(\frac{0.06}{3}\right)^3 = 0.000008$, other activities are unity, $K = 421.875$

For sample b, $a_{an} = 0.10$, $a_{gr} = \left(\frac{0.12}{3}\right)^3 = 0.000016$, $K = 15.625$

iv) Based on equations 1 and 2 derive a relationship describing pressure as a function of temperature.

$$\frac{-RT \ln K = \Delta H - T\Delta S + P\Delta V}{\frac{-R \ln K + \Delta S}{\Delta V}} = \frac{dP}{dT}$$

v) On the graph provided (fig. 1) plot pressure as a function of temperature for rock A and rock B. Note that these isopleths are straight lines. Take care with units.

Just plot based on the figures, remember geobarometers should be pretty much horizontal

vi) Fig. 1 also shows lines plotted for you for the garnet-biotite thermometer, labeled gt-bt for each sample. Suggest a pressure and temperature of equilibration for each sample.

vii) Given the stratigraphic separation comment on the apparent pressure gradient witnessed by these samples.

